POLITECNICO DI MILANO

Practical Optimization Strategies In Cantilever Launching Method Of Arch Bridges

Thesis in Civil Structural Engineering

Author:
Claudio Ieva

Supervisor:
Prof. Antonio Capsoni

25 july 2014

Academic Year 2013/14

To My Family

Riassunto in Italiano Questa tesi si propone come obiettivo lo studio di varie strategie di ottimizzazione nella messa in opera di ponti arco in calcestruzzo armato.

Durante la posa in opera dei segmenti dell'emiarco collocando gli stralli in opportuni punti e tensionando le pre-tensioni da affibbiare agli stessi con valori "smart" è possibile generare una configurazione di chiusura in chiave d'arco vantaggiosa. Il sostanziale vantaggio sta nel non dover modificare durante l'intera messa in opera delle sezioni del ponte le pre-tensioni degli stralli, tale miglioramento comporta conseguenti benefici sia pratici che economici.

E' dunque importante, non solo assicurare che per ogni stage di lavorazione l'arco sia stabile, ma anche che gli sforzi durante l'intero processo siano all'interno di un range di valori, in particolare il Momento Flettente agente lungo l'intero processo dovrà essere inferiore al Momento Resistente ammissibile.

Valutando il processo di "back destruction" è stato possibile ricavare quelli che sono i momenti massimi negativi e positivi ai quali l'emiarco è sottoposto lungo l'intera messa in opera.

L'obbiettivo di questo elaborato è di proporre una serie di strategie generali che permetta di minimizzare l'utilizzo di materiali, quindi costi.

Parole Chiave: strategie di ottimizzazione, ponti arco in calcestruzzo, pre-tensioni, stralli, back destruction.

Abstract This thesis proposes as its objective the study of various optimization strategies in the implementation of reinforced concrete arch bridges.

During the installation of the segments of the rib placing the tiebacks at appropriate points and tensioning the pre-tensions to tie to the same smart values it is possible to generate a advantageous closed configuration in middspan. The substantial advantage is not having to change during the entire implementation of the sections of the bridge the pre-tension of the stays, this improvement involves consequent benefits, both practical and economic.

It is therefore important, not only to ensure that each stage of processing the arch is stable, but also that the efforts during the entire process are within a range of values, in particular the bending moment acting along the entire process must be less than the allowable moment.

Evaluating the process of "back-destruction" could be deduced maximum positive and negative moments at which the emiarch is submitted through the entire installation.

The goal of this paper is to propose a set of general strategies that allow to minimize the use of materials, and so costs.

Keywords: Optimization strategies, concrete arch bridges, pre-tensions, tiebacks, back destruction.

Acknowledgements I would like to express my gratitude for all who contributed in a way or another in the accomplishment of this work.
Most importantly, i would like to thank my supervisor, Pr. Antonio Capsoni. His helpful advises, comments, suggestions and contributions regarding all the critical aspects of my thesis have been very profitable over the last year. Many thanks to my family, that made it possible, supporting me in all situations.

Contents

1 Introduction **12**
- 1.1 General Introduction . . . 13
- 1.2 Cost of Cantilever Launching Method in Arch Bridges . . . 13

2 Literature Review and Background Information **14**
- 2.1 Historical Evolution of Concrete Arch Bridges . . . 14
- 2.2 Methods of Construction for Concrete Arch Bridges Structures 14

3 Design Of Concrete Arch Bridges **16**
- 3.1 Layout and Cross-Section . . . 16
  - 3.1.1 Wanxian Bridge . . . 16
  - 3.1.2 Krk Bridge . . . 19
  - 3.1.3 Hoover Dam Bridge . . . 22
  - 3.1.4 Infante Henrique . . . 24
  - 3.1.5 Bloukrans Bridge . . . 26
  - 3.1.6 Contreras Bridge . . . 28
  - 3.1.7 Los Tilos Bridge . . . 30
  - 3.1.8 Almonte Bridge . . . 32
  - 3.1.9 Traneberg Bridge . . . 35
  - 3.1.10 Ulla Bridge . . . 36
  - 3.1.11 Burguillo Bridge . . . 38
  - 3.1.12 Cieza Bridge . . . 40
- 3.2 Statistical Analysis . . . 42
  - 3.2.1 Upper and Lower Bounds of Arch Cross Section . . . 45
  - 3.2.2 Standard Deviation . . . 45

4 Contreras Arch Bridge Like a Sample **50**
- 4.1 Construction Process . . . 50

5 Previously Approximate Evaluations To The Calibration Of The TOA Method **54**
- 5.1 Beam on Elastic Supports - Winkler foundation . . . 54

6 Optimization Of The Construction Process **58**
- 6.1 Tiebacks' Optimization Algorithms TOA . . . 58
  - 6.1.1 Value of T Optimizing The Static Response . . . 60
  - 6.1.2 Pretensions Applied to Tiebacks . . . 62
- 6.2 Sample TOA Bridge Application . . . 63

6.2.1 Application Of The Optimizing Alghorithms to The Sample Case 65
6.2.2 Variable Distribution - VD 98
6.2.3 Moment's Redistribution 156
6.3 Resultant Tieback 160
6.4 Anchorage's Volume 161

7 Conclusions and Future Developments **163**
7.1 Variation Of The Height Of The Tower 163
7.2 Conclusions 164

List of Figures

1 Wanxian Span . . . 17
2 Wanxian Section . . . 17
3 Krk Span . . . 20
4 Krk Section . . . 20
5 Krk Deck . . . 21
6 Hoover Section . . . 23
7 Infante Henrique Span . . . 24
8 Bloukrans Span . . . 26
9 Bloukrans Section . . . 27
10 Contreras Span . . . 29
11 Contreras Section . . . 29
12 Los Tilos Span . . . 31
13 Almonte Span . . . 32
14 Almonte Section . . . 33
15 Traneberg Span . . . 35
16 Ulla Span . . . 37
17 Ulla Section . . . 37
18 Maximum Area . . . 43
19 Median Area . . . 44
20 Minimum Area . . . 44
21 SD Area on Supports . . . 47
22 SD Area in The Center of The Rib . . . 48
23 SD Area in Midspan . . . 49
24 Contreras' Temporary Supporting System . . . 50
25 Free Cantilever Construction of The Arch With Temporary cable-staying from the pier at the springs . . . 51
26 Cantilever construction between de Arch and the Deck . . . 51
27 Centering Supported on the Ground . . . 52
28 Emiarch And Tieback Lenght L_t . . . 54
29 Emiarch Compared to a Winkler Beam . . . 55
30 Winkler foundation . . . 55
31 Before Crown Closing . . . 59
32 Sample Bridge . . . 63
33 Unit Force T1 . . . 65
34 Decompose Force T1 . . . 65
35 Coefficients Product From Force T1 . . . 66
36 Unit Force T2 . . . 66
37 Decompose Force T2 . . . 67

38 Coefficients Product From Force T2 67
39 Unit Force T3 68
40 Decompose Force T3 68
41 Coefficients Product From Force T3 69
42 Unit Force T4 69
43 Decompose Force T4 70
44 Coefficients Product From Force T4 70
45 Unit Force T5 71
46 Decompose Force T5 71
47 Coefficients Product From Force T5 72
48 Unit Force T6 72
49 Decompose Force T6 73
50 Coefficients Product From Force T6 73
51 Unit Force T7 74
52 Decompose Force T7 74
53 Coefficients Product From Force T7 75
54 Self Weight Bending Moment' s Contribution 75
55 Influence Coefficients' Matrix A 76
56 Bending Moment' s Contribution 76
57 Optimized T 77
58 Unitary Pretension Applied into the Tieback 1 78
59 Coefficients Given by Tieback 1 78
60 Unitary Pretension Applied into the Tieback 2 79
61 Unitary Pretension Applied into the Tieback 3 79
62 Unitary Pretension Applied into the Tieback 4 80
63 Unitary Pretension Applied into the Tieback 5 80
64 Unitary Pretension Applied into the Tieback 6 81
65 Unitary Pretension Applied into the Tieback 7 81
66 Matrix D 82
67 Vector T-Ng 83
68 Pretensions N^o 83
69 Closing Arch Configuration 84
70 Section 8 Deleted 85
71 Tieback 7 Deleted 86
72 Section 7 Deleted 87
73 Tieback 6 Deleted 88
74 Section 6 Deleted 89
75 Tieback 5 Deleted 90
76 Section 5 Deleted 91
77 Tieback 4 Deleted 92

78 Section 4 Deleted 93
79 Tieback 3 Deleted 94
80 Section 3 Deleted 95
81 Tieback 2 Deleted 96
82 Section 2 Deleted 97
83 Angle Decreasing 98
84 N=8 $\alpha = 1, 2$ 100
85 Influence Coefficients' Matrix in VD case $\alpha = 1, 2$ 101
86 Self Weight Bending Moment' s Contribution in VD case $\alpha = 1, 2$ 101
87 Optimized T in VD case $\alpha = 1, 2$ 102
88 Matrix D in VD case $\alpha = 1, 2$ 102
89 Vector T-Ng in VD case $\alpha = 1, 2$ 103
90 Pretensions N^o in VD case $\alpha = 1, 2$ 103
91 Closing Arch Configuration in VD case $\alpha = 1, 2$ 104
92 Section 8 Deleted in VD case $\alpha = 1, 2$ 106
93 Tieback 7 Deleted in VD case $\alpha = 1, 2$ 107
94 Section 7 Deleted in VD case $\alpha = 1, 2$ 107
95 Tieback 6 Deleted in VD case $\alpha = 1, 2$ 108
96 Section 6 Deleted in VD case $\alpha = 1, 2$ 109
97 Tieback 5 Deleted in VD case $\alpha = 1, 2$ 110
98 Section 5 Deleted in VD case $\alpha = 1, 2$ 111
99 Tieback 4 Deleted in VD case $\alpha = 1, 2$ 112
100 Section 4 Deleted in VD case $\alpha = 1, 2$ 113
101 Tieback 3 Deleted in VD case $\alpha = 1, 2$ 114
102 Section 3 Deleted in VD case $\alpha = 1, 2$ 115
103 Tieback 2 Deleted in VD case $\alpha = 1, 2$ 116
104 Section 2 Deleted in VD case $\alpha = 1, 2$ 117
105 N=8 $\alpha = 1, 5$ 118
106 Influence Coefficients' Matrix in VD case $\alpha = 1, 5$ 119
107 Self Weight Bending Moment' s Contribution in VD case $\alpha = 1, 5$ 119
108 Optimized T in VD case $\alpha = 1, 5$ 120
109 Matrix D in VD case $\alpha = 1, 5$ 120
110 Vector T-Ng in VD case $\alpha = 1, 5$ 121
111 Pretensions N^o in VD case $\alpha = 1, 5$ 121
112 Closing Arch Configuration in VD case $\alpha = 1, 5$ 122
113 Section 8 Deleted in VD case $\alpha = 1, 5$ 124
114 Tieback 7 Deleted in VD case $\alpha = 1, 5$ 125
115 Section 7 Deleted in VD case $\alpha = 1, 5$ 125

116 Tieback 6 Deleted in VD case $\alpha = 1, 5$ 126
117 Section 6 Deleted in VD case $\alpha = 1, 5$ 127
118 Tieback 5 Deleted in VD case $\alpha = 1, 5$ 128
119 Section 5 Deleted in VD case $\alpha = 1, 5$ 129
120 Tieback 4 Deleted in VD case $\alpha = 1, 5$ 130
121 Section 4 Deleted in VD case $\alpha = 1, 5$ 131
122 Tieback 3 Deleted in VD case $\alpha = 1, 5$ 132
123 Section 3 Deleted in VD case $\alpha = 1, 5$ 133
124 Tieback 2 Deleted in VD case $\alpha = 1, 5$ 134
125 Section 2 Deleted in VD case $\alpha = 1, 5$ 135
126 N=8 $\alpha = 1, 8$ 136
127 Influence Coefficients' Matrix in VD case $\alpha = 1, 8$ 137
128 Self Weight Bending Moment' s Contribution in VD case $\alpha = 1, 8$ 137
129 Optimized T in VD case $\alpha = 1, 8$ 138
130 Matrix D in VD case $\alpha = 1, 8$ 138
131 Vector T-Ng in VD case $\alpha = 1, 8$ 139
132 Pretensions N^o in VD case $\alpha = 1, 8$ 139
133 Closing Arch Configuration in VD case $\alpha = 1, 8$ 140
134 Section 8 Deleted in VD case $\alpha = 1, 8$ 142
135 Tieback 7 Deleted in VD case $\alpha = 1, 8$ 143
136 Section 7 Deleted in VD case $\alpha = 1, 8$ 144
137 Tieback 6 Deleted in VD case $\alpha = 1, 8$ 145
138 Section 6 Deleted in VD case $\alpha = 1, 8$ 146
139 Tieback 5 Deleted in VD case $\alpha = 1, 8$ 147
140 Section 5 Deleted in VD case $\alpha = 1, 8$ 148
141 Tieback 4 Deleted in VD case $\alpha = 1, 8$ 149
142 Section 4 Deleted in VD case $\alpha = 1, 8$ 150
143 Tieback 3 Deleted in VD case $\alpha = 1, 8$ 151
144 Section 3 Deleted in VD case $\alpha = 1, 8$ 152
145 Tieback 2 Deleted in VD case $\alpha = 1, 8$ 153
146 Section 2 Deleted in VD case $\alpha = 1, 8$ 154
147 Sample of a Bending Moment Diagram in an Middlearch . . . 156
148 Arch's Section 158
149 Tieback Resultant 160
150 Anchorage System 161
151 Anchorage's Optimum Slope 162
152 Variation Of The Height Of The Provisional Tower 163

List of Tables

1 Areas Bridge's Summary 42
2 Characteristics of λ and the tiebacks in A_t Variation 57
3 Sample Bridge' Characteristics 63
4 Static Axial Forces in Tiebacks 82
5 Optimization Results' Summary 83
6 Maximum Moments 97
7 Static Axial Forces in Tiebacks in AF case $\alpha = 1, 2$ 103
8 Optimization Results' Summary in VD case $\alpha = 1, 2$ 104
9 Maximum Moments in VD case $\alpha = 1, 2$ Closing Arch Configuration 105
10 Maximum Moments Through the Back Destruction case $\alpha = 1, 2$ 117
11 Static Axial Forces in Tiebacks in VD case $\alpha = 1, 5$ 120
12 Optimization Results' Summary in VD case $\alpha = 1, 5$ 122
13 Maximum Moments in VD case $\alpha = 1, 5$ Closing Arch Configuration 123
14 Maximum Moments Through the Back Destruction 135
15 Static Axial Forces in Tiebacks in VD case $\alpha = 1, 8$ 138
16 Optimization Results' Summary in VD case $\alpha = 1, 8$ 140
17 Maximum Moments in VD case $\alpha = 1, 8$ Closing Arch Configuration 141
18 Maximum Moments Through the Back Destruction case $\alpha = 1, 8$ 154
19 Comparison Among 3 different α in VD case 155
20 Moment's Redistribution Summary 159

Practical Optimization Strategies In Cantilever Launching Method Of Arch Bridges

Friday 25 July 2014

1 Introduction

The primary advantage of an arch bridge is that compression is the dominant stress induced in the arch under uniform loading. Materials such as stone and concrete, with low cost and high compressive strength, are well suited to the arch form. These heavy material arch bridges have historically been used in small and medium spans and were constructed using a full shoring system. Advances in the use of high strength concrete, steel, and concrete-steel composites in recent years have significantly reduced the weight of the structure and have extended the limits of arch bridges to longer spans.
From the 1998 no arch concrete bridge longer than 420 m (Wanxian, China 1998) has been designed; they didn't cross limits like cable-stayed bridge or suspension bridge.

1.1 General Introduction

The height of the pylons, in a cable-stayed bridge, influences the amount of cable-stay steel material and the longitudinal compressive forces in the bridge deck. Leonhardt [5] has developed a relationship for suspension and cable-stayed bridges in which the amount of cable steel required for a given cable force is considered to be a function of the ratio of the tower height to the center span. The effect of the weight of the cable and any load concentrations are neglected. The equation for the resulting weight of the cable required to support a given tensile force is

$$W = \frac{q\lambda L^2}{\sigma} \tag{1}$$

Where:
W = weight of steel in cables in lbs
q = total load (dead load plus live load)
λ = specific weightof cable steel
σ = allowable cable stress in psi
L = lenght of main span in ft
C = dimensionless coefficient depending on bridge type

1.2 Cost of Cantilever Launching Method in Arch Bridges

In the same way has been done for cable-stayed bridge is possible to evaluate the weight of steel in cables for an arch bridge construction; in particular is possible to calculate the weight of steel in cables using the cable-stayed free cantilever launching method.
In fact, one of the three most important components in the cost of anrch bridge constructed by the cable-stayed free cantilever launching method is the weight of the cables. If we call $C1$ the cost of the cables, $C2$ the cost of the foundations to anchor the cables and $C3$ the cost of the provisional tower the total cost C_{tot} of the construction is based on the sum of these three components

$$C_{tot} = C1 + C2 + C3 \tag{2}$$

2 Literature Review and Background Information

2.1 Historical Evolution of Concrete Arch Bridges

Thanks to the greater compression strenght of concrete, it is reasonable to use it in arch bridge because arch works essentially in compression.
The first concrete arch bridge spanning more than 100m, the Risorgimento Bridge in Rome, was built 100 years ago.
Along with the rapid development of construction technology and improvement of structural materials, the span record of concrete arch bridges has been refreshing continually. In 1979, the completion of Krk I Bridge in Croatia with the main span of 390m made a miracle at that time in concrete arch bridge. This bridge was constructed by temporary truss method. However, the lengthening cantilever of arch ring undoubtedly increases the difficulty of construction. Currently the Krk arch bridge still ranks as the world's longest arch bridge erected by cantilever-contruction method.
Now Wanxian Yangtze River Bridge with span of 420m in China is the longest concrete arch bridge in the world. It was built by embedded formwork comprising a latticework structure of concrete-filled steel tubes (CFST). The scaffolding was erected by cantilever cable-stayed method (Yan and Yang 1997). The concrete was cast in situ ring by ring transversally and sectin by section longitudinally to avoid overloading of the formwork and hence also very labor consuming. Therefore, these construction methods are only suitable for the countries with very cheap labor costs. Theoretical studies show that limit spans for concrete arches will not exceed those already built (Wanxian-Yangtze, Krk I).

2.2 Methods of Construction for Concrete Arch Bridges Structures

For long-span arch bridge construction, it is often difficult and costly to erect a temporary shoring system, especially for bridges across deep water channels. Construction methods developed to reduce and even eliminate the requirement for shoring include the cantilever launching method as well as the horizontal and vertical swing methods. The cantilever launching method uses main and auxiliary cables to maintain stability and balance during construc- tion. The horizontal swing method begins with prefabricating a complete half-leaf of an arch rib parallel to the river on both banks with their ends supported on spherical hinges at the abutments. With the help of balance weights and hydraulic jacking equipment, the two prefabricated ribs can be rotated horizontally to the closure position. Using the vertical swing

method, two half-leaves of arch ribs are fabricated at ground level to save shoring cost, and then rotated to the closure position. The combined use of horizontal and vertical swing techniques is also feasible for lightweight arch bridges. Construction methods to maintain balance and stability become more difficult as the span increases and as the arch weight increases.

3 Design Of Concrete Arch Bridges

3.1 Layout and Cross-Section

A parametric study was made analyzing 12 different concrete arch bridges. It is been necessary to analyze plan's bridges one by one to calculate the values of the area all over the archs, so the selfweight and the value of tensions in correspondence of the abutments.
It will be necessary to estimate the weight of the deck, piles, transversal beam if is present and so on with all the components of the bridge.
Here is a list of equation will be used to calculate all these components taken in count in the line before.

$$P_f = sB\gamma \tag{3}$$

$$P_{pv} = B\gamma^I \tag{4}$$

$$P_{tb} = \frac{B^I s^I B\gamma}{i} \tag{5}$$

$$P_l = mB \tag{6}$$

$$P_a = A\gamma \tag{7}$$

Where:
s is the thickness of the flange,
B is the width of bridge's deck,
γ is the specific weight of the concrete,
γ^I is the specific weight of the pavement,
B^I is the width of the transversal beam,
s^I is the thickness of the transversal beam,
i is the center to center distance,
m is the distributed weight per m^2, present in EN 1991-2,
A is the area of the arch section.

Liveload Details Concern to the $5\frac{kN}{m^2}$ used to calculate the liveload on the bridges, it is necessary to specify that was used the Crowd Loading Method to evaluate it, present in [1] in section LOAD MODEL 4.

3.1.1 Wanxian Bridge

The Wanxian Yangtze River Bridge [6] (Yan and Yang 1997) is a record-breaking design for a reinforced concrete arch bridge with a main arch span of 420 m and an 84 m rise. It was completed in July 1997 figure 1. The

total length of the bridge is 856 meters. The north approach consists of eight simple spans of 30,7 m and the south approach consists of five simple spans of 30,7 m. The bridge carries four-lane traffic and two pedestrian sidewalks. The arch is a catenary with a rise-to-span ratio of $\frac{1}{5}$.
The deck is 24 m wide, accomodating dual 7,5 m wide lanes for vehicle traffic and dual 3,0 m lanes for pedestrians. A 16,0m wide and 7,0m deep three-cell reinforced concrete box section was selected for the arch rib [figure 2].

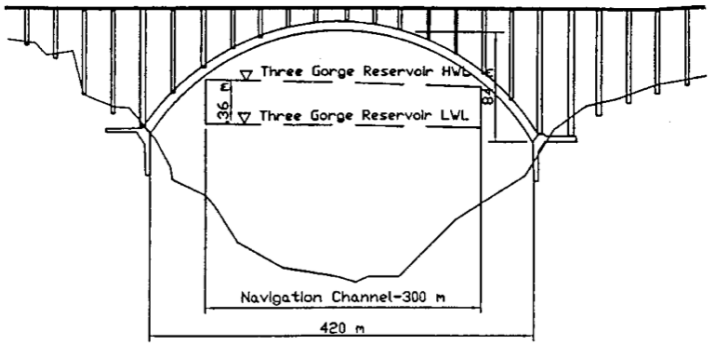

Figure 1: Wanxian Span

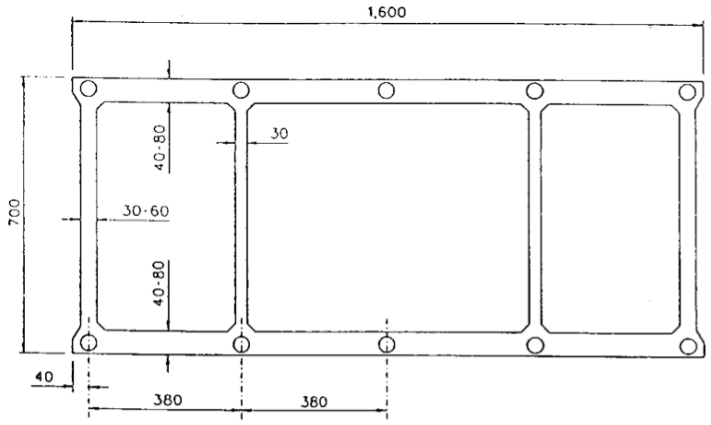

Figure 2: Wanxian Section

If the conventional cantilever launching method were used, crane lifting capacity as well as number of precasted units would be very high. In addition, a very large temporary balance tower system would be required to maintain the balance and stability of the massive cantilever arch rib. For

these reasons, construction cost of the arch would be much higher than that for other design alternatives. To reduce the cost and complexity of construction, a new self-shoring construction method was developed. The method uses a truss frame fabricated with steel tubes by the conventional canti- lever launching technique. This steel tube frame performs the dual role of arch falsework and arch main reinforcement. After the steel tube truss frame is completed, concrete fill is pumped into the steel tubes to increase the capacity of the truss frame system. The stiffened truss frame is then encased by subsequent concrete placements to become the main reinforcement of the completed arch section.

Wanxian Parametric Study In first istance was calculated stress based on self-weight and overloads.

$$P_{pb} = 10 * 21,7\frac{kN}{m} = 217\frac{kN}{m}$$

$$P_f = 0,25m * 24m * 25\frac{kN}{m^3} = 150\frac{kN}{m}$$

$$P_{pv} = 24m * 2\frac{kN}{m^2} = 48\frac{kN}{m}$$

$$P_{tb} = \frac{1,70m * 1,30m * 24m * 25\frac{kN}{m^3}}{30,7m} = 43,20\frac{kN}{m}$$

$$P_l = 5\frac{kN}{m^2} * 24m = 120\frac{kN}{m}$$

$$P_p = 46,9\frac{kN}{m}$$

$$P_a = 25\frac{kN}{m^3} * 35,66m^2 + 25\frac{kN}{m^3} * 19,74m^2 = 692\frac{kN}{m}$$

Where:
P_{pb} is the precasted beam weight,
P_f is the flange weight,
P_{pv} is the pavement weight,
P_{tb} is the transversal beam weight,
P_l is the liveload,
P_p is the pile weight,
P_a is the arch self-weight.

$$P_{tot,l} = P_{pb} + P_f + P_{pv} + P_{tb} + P_l + P_p + P_a$$

The total stress is $P_{tot,l} = 1317,6kN/m$ and it will be used to calculate the axial force in the foundation.

$$N_l = \frac{P_{tot,l}l^2}{8fcos(\alpha)} = 468048kN$$

Remembering the value of the Area $A = 35,6m^2$ of the arch section, the stress σ_l is evalueted in:

$$\sigma_l = \frac{N_l}{A} = 13125\frac{kN}{m^2}$$

And the total stress without the liveload is $P_{tot} = 1197kN/m$ and the axial force in the foundation is:

$$N = \frac{P_{tot}l^2}{8fcos(\alpha)} = 425423kN$$

Finally is calculated a stress σ without the contribute of liveload evalueted in:

$$\sigma = \frac{N}{A} = 11930\frac{kN}{m^2}$$

Where:
l si the total span of the bridge,
f is the ratio of the bridge,
α is the slope of arch in foundation.

3.1.2 Krk Bridge

The idea of building a bridge which would link the Mainland with the biggest Croatian island Krk has been pursued for a very long time, though many years have passed from idea to realization. Finally in 1975, construction funds were raised and it was to be decided about the future bridge structure. In a very tough competition with different domestic and foreign proposals (suspended bridges, continuous beam structures, beam structures with inclined cables, steel arches), the solution with reinforced concrete arches was chosen as the best one in technical, economical and aesthetical respects.
The Krk I bridge arch between the Mainland and St. Marc Island with its 390 m span and its 60 m rise figure 3 with the rise to span ratio of $\frac{1}{6,5}$ was at that time the world record holder for classically built concrete arches.
The cross-section is a three-cell box type with constant outer dimensions along the entire length of the bridge figure 4.
The arch width was defined as 1/30 of the arch span and the depth as approximately 1/60 of the arch span.

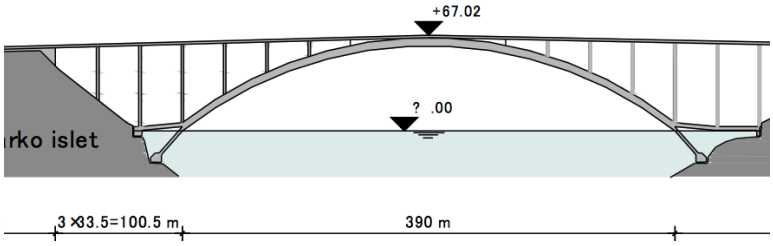

Figure 3: Krk Span

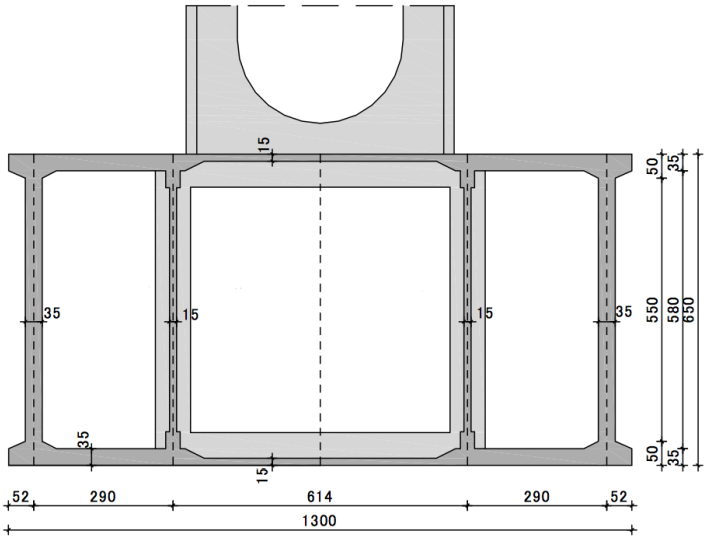

Figure 4: Krk Section

Krk Parametric Study The horizontal beams of 33,5 m span, extending to the shores, are of box type cross section of varying dimensions from 4,82*13,0 m at the arch connection to 3,0*20,0 m at the other hinged end of the beam, highlights in [9].

$$P_{pb} = 3 * 12,0 \frac{kN}{m} = 36 \frac{kN}{m}$$

$$P_f = 0,18m * 11,4m * 25 \frac{kN}{m^3} = 51,3 \frac{kN}{m}$$

$$P_{pv} = 11,4m * 2 \frac{kN}{m^2} = 22,8 \frac{kN}{m}$$

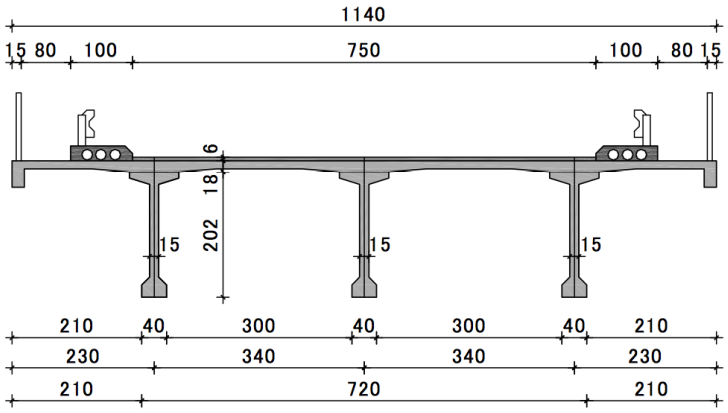

Figure 5: Krk Deck

$$P_{tb} = \frac{1,70m * 1,30m * 11,4m * 25\frac{kN}{m^3}}{33,5m} = 18,8\frac{kN}{m}$$

$$P_l = 5\frac{kN}{m^2} * 11,4m = 57\frac{kN}{m}$$

$$P_p = 16,5\frac{kN}{m}$$

$$P_a = 25\frac{kN}{m^3} * 43,7m^2 = 330\frac{kN}{m}$$

Where:
P_{pb} is the precasted beam weight,
P_f is the flange weight,
P_{pv} is the pavement weight,
P_{tb} is the transversal beam weight,
P_l is the liveload,
P_p is the pile weight,
P_a is the arch self-weight.

$$P_{tot,l} = P_{pb} + P_f + P_{pv} + P_{tb} + P_l + P_p + P_a$$

The total stress is $P_{tot,l} = 532,4kN/m$ and it will be used to calculate the axial force in the foundation.

$$N_l = \frac{P_{tot,l}l^2}{8fcos(\alpha)} = 180090kN$$

Remembering the value of the Area $A = 13,2m^2$ of the arch section, the stress σ_l is evalueted in:

$$\sigma_l = \frac{N_l}{A} = 15279\frac{kN}{m^2}$$

And the total stress without the liveload is $P_{tot} = 475,4kN/m$ and the axial force in the foundation is:

$$N = \frac{P_{tot} * l^2}{8 * fcos(\alpha)} = 217547kN$$

Finally is calculated a stress σ without the contribute of liveload evalueted in:

$$\sigma = \frac{N}{A} = 13643\frac{kN}{m^2}$$

Where:
l si the total span of the bridge,
f is the ratio of the bridge,
α is the slope of arch in foundation.

3.1.3 Hoover Dam Bridge

This 1060 foot (323 m) long arch span is the 4th longest concrete arch in the world, and the longest in the United States figure **??**. With a rise of 277 feet (84,43m) it has a rise-to-span ratio of $\frac{1}{4}$.
A 14,0m wide and 4,3m deep two-cell reinforced concrete box section was selected for the arch rib figure 6.
The scale of concrete construction for the bridge is impressive. Four form travelers advanced to the crown of the cast-in-place arch supported by 88 carefully tuned stay cables, while precast segmental construction was used for the tallest precast columns erected to date.

Hoover Parametric Study Here there are the self-weight and overloads stress.

$$P_{sb} = 4 * 0,1723m^2 * 78,5\frac{kN}{m^3} = 54,1\frac{kN}{m}$$

$$P_f = 0,25m * 26,8m * 25\frac{kN}{m^3} = 167,5\frac{kN}{m}$$

$$P_{pv} = 26,8m * 2\frac{kN}{m^2} = 53,6\frac{kN}{m}$$

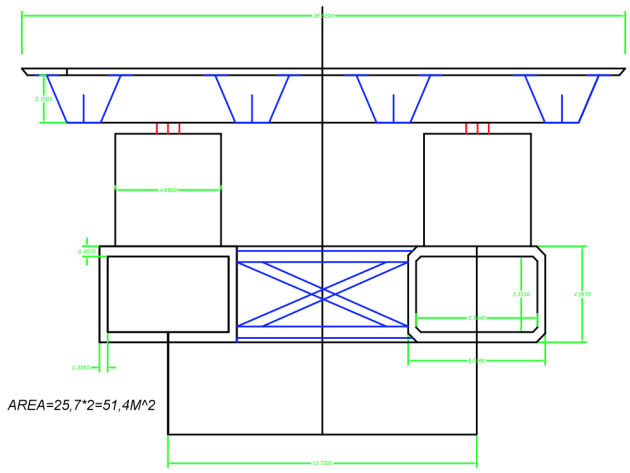

Figure 6: Hoover Section

$$P_{tb} = \frac{2,10m * 3,00m * 26,8m * 25\frac{kN}{m^3}}{36,5m} = 115,6\frac{kN}{m}$$

$$P_l = 5\frac{kN}{m^2} * 26,8m = 134\frac{kN}{m}$$

$$P_p = 71,2\frac{kN}{m}$$

$$P_a = 25\frac{kN}{m^3} * 15,5m^2 = 387,5\frac{kN}{m}$$

Where:
P_{sb} is the steel beam weight,
P_f is the flange weight,
P_{pv} is the pavement weight,
P_{tb} is the transversal beam weight,
P_l is the liveload,
P_p is the pile weight,
P_a is the arch self-weight.

$$P_{tot,l} = P_{sb} + P_f + P_{pv} + P_{tb} + P_l + P_p + P_a$$

The total stress is $P_{tot,l} = 983kN/m$ and it will be used to calculate the axial force in the foundation.

$$N_l = \frac{P_{tot} l^2}{8 f cos(\alpha)} = 252774kN$$

Remembering the value of the Area $A = 15,5m^2$ of the arch section, the stress σ_l is evalueted in:

$$\sigma_l = \frac{N_l}{A} = 16308 \frac{kN}{m^2}$$

And the total stress without the liveload is $P_{tot} = 849kN/m$ and the axial force in the foundation is:

$$N = \frac{P_{tot} l^2}{8 f cos(\alpha)} = 218335kN$$

Finally is calculated a stress σ without the contribute of liveload evalueted in:

$$\sigma = \frac{N}{A} = 14086 \frac{kN}{m^2}$$

Where:
l si the total span of the bridge,
f is the ratio of the bridge,
α is the slope of arch in foundation.

3.1.4 Infante Henrique

The new bridge, Infante Henrique [8] on Duero river in Oporto, needed to connect the old central part of Oporto city with Gaia city. The Infante Henrique bridge with its 280 m of span, was the winner in the International Challange of Projects and Constructions convened from Metro de Oporto.

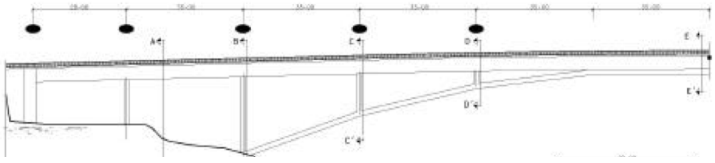

Figure 7: Infante Henrique Span

Infante Henrique Parametric Study In this bridge, designers were finding the minimum visual alteration, this is the reason why this bridge has an important span and a huge abasement, with a relation rise/span of 1/11,20. The deck is 20 m large.

$$P_b = 190,0\frac{kN}{m}$$

$$P_{pv} = 20,0m * 2\frac{kN}{m^2} = 40\frac{kN}{m}$$

$$P_l = 5\frac{kN}{m^2} * 20m = 100\frac{kN}{m}$$

$$P_p = 95,2\frac{kN}{m}$$

$$P_a = 25\frac{kN}{m^3} * 22,5m^2 = 562,5\frac{kN}{m}$$

Where:
P_b is the beam weight,
P_f is the flange weight,
P_{pv} is the pavement weight,
P_{tb} is the transversal beam weight,
P_l is the liveload,
P_p is the pile weight,
P_a is the arch self-weight.

$$P_{tot,l} = P_{sb} + P_f + P_{pv} + P_{tb} + P_l + P_p + P_a$$

The total stress is $P_{tot,l} = 987,7kN/m$ and it will be used to calculate the axial force in the foundation.

$$N_l = \frac{P_{tot}l^2}{8fcos(\alpha)} = 409473,8kN$$

Remembering the value of the Area $A = 30,0m^2$ of the arch section, the stress σ_l is evalueted in:

$$\sigma_l = \frac{N_l}{A} = 13649,1\frac{kN}{m^2}$$

And the total stress without the liveload is $P_{tot} = 887,7kN/m$ and the axial force in the foundation is:

$$N = \frac{P_{tot} l^2}{8 f cos(\alpha)} = 368017,4kN$$

Finally is calculated a stress σ without the contribute of liveload evalueted in:

$$\sigma = \frac{N}{A} = 12267,2 \frac{kN}{m^2}$$

Where:
l si the total span of the bridge,
f is the ratio of the bridge,
α is the slope of arch in foundation.

3.1.5 Bloukrans Bridge

As built, the chord was 272 metres and the rise was 62 m, the rise chord thus being 0,228.
The 19-metre spacing between the columns was set right from the first, the 19-m lenghts also meant an improved distribution of the liveloads over the arch, together with cutting down the bending moment peaks.

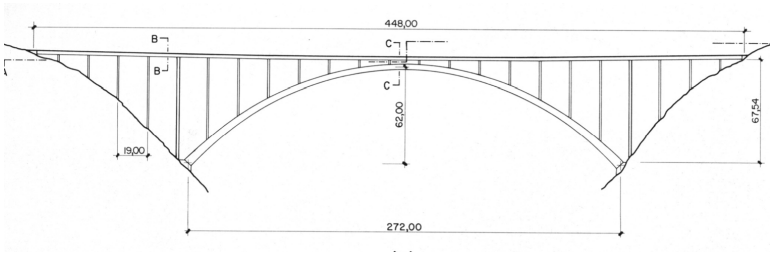

Figure 8: Bloukrans Span

Bloukrans Parametric Study The reinforced-concrete arch has a 12 m wide three-cell box cross section whose depth varies from 3,6 m at the crown lo 5,6 m at the sprI`ngers, where it has a slope of 46,2°. The box comprises: two slabs, upper and lower, of the same depth, running from 36 cm at the crown lo 43,5 cm near the abutments, al the abutments reaching 75 cm; two side webs 36 cm thick; and two inside webs 30 cm thick. The arch's parabolic curve is very close lo the dead load funicular, with a rise/chord of 0,228, since its chord is 272 m long and its rise is 62 m.

$$P_b = 200,7 \frac{kN}{m}$$

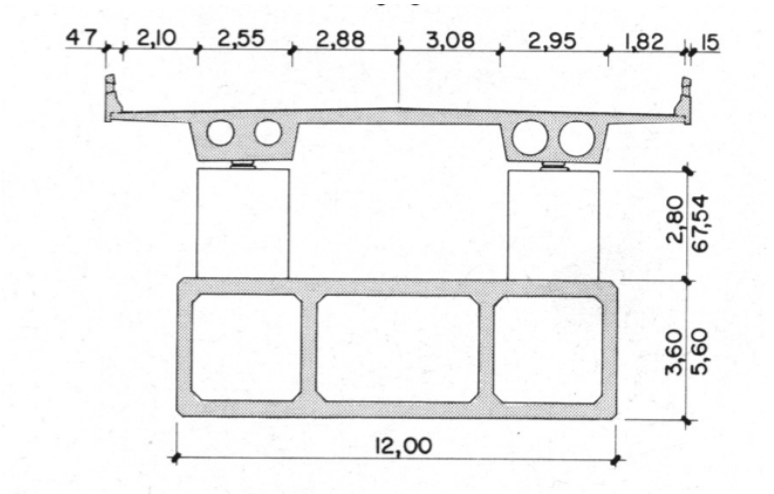

Figure 9: Bloukrans Section

$$P_{pv} = 14,2m * 2\frac{kN}{m^2} = 32\frac{kN}{m}$$

$$P_l = 5\frac{kN}{m^2} * 16m = 80\frac{kN}{m}$$

$$P_p = 28,9\frac{kN}{m}$$

$$P_a = 25\frac{kN}{m^3} * 20,4m^2 = 510\frac{kN}{m}$$

Where:
P_b is the beam weight,
P_f is the flange weight,
P_{pv} is the pavement weight,
P_{tb} is the transversal beam weight,
P_l is the liveload,
P_p is the pile weight,
P_a is the arch self-weight.

$$P_{tot,l} = P_{sb} + P_f + P_{pv} + P_{tb} + P_l + P_p + P_a$$

The total stress is $P_{tot,l} = 852kN/m$ and it will be used to calculate the axial force in the foundation.

$$N_l = \frac{P_{tot} l^2}{8 f cos(\alpha)} = 175344kN$$

Remembering the value of the Area $A = 23,41m^2$ of the arch section, the stress σ_l is evalueted in:

$$\sigma_l = \frac{N_l}{A} = 7490 \frac{kN}{m^2}$$

And the total stress without the liveload is $P_{tot} = 772kN/m$ and the axial force in the foundation is:

$$N = \frac{P_{tot} l^2}{8 f cos(\alpha)} = 158886kN$$

Finally is calculated a stress σ without the contribute of liveload evalueted in:

$$\sigma = \frac{N}{A} = 6787 \frac{kN}{m^2}$$

Where:
l si the total span of the bridge,
f is the ratio of the bridge,
α is the slope of arch in foundation.

3.1.6 Contreras Bridge

The reinforced concrete arch bridge of a 261 m span [7], with an upper prestressed concrete deck and a total length of 587.25 m, spans the Contreras Reservoir on the Madrid-Levante high-speed railway line. The mid-span sag is 36.944 m thus determining a span-to-rise ratio of over 6.77 to 1, which is a low rising arch although not excessively so. On the construction completion date, the span between the arch supports was holder of the world record for a concrete railway arch bridge 10.

The cross section is a box girder with a variable depth ranging from 2.8 m at mid-span to 3.4 m at the ends figure 11. The box girder width is also variable ranging from 6.0 m in the centre of the arch to 12.0 at the foundations embedding, which is the width required to resist the great bending moments of the vertical axis produced by the plan curvature of the arch and the crosswind. The box girder walls range from 0.6 to 1.35 m

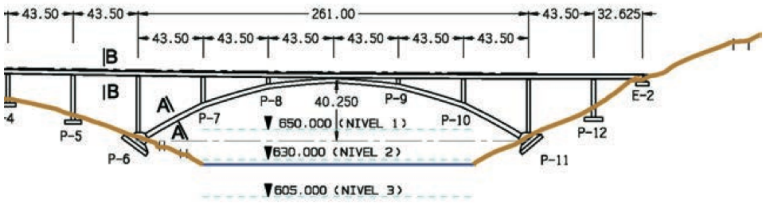

Figure 10: Contreras Span

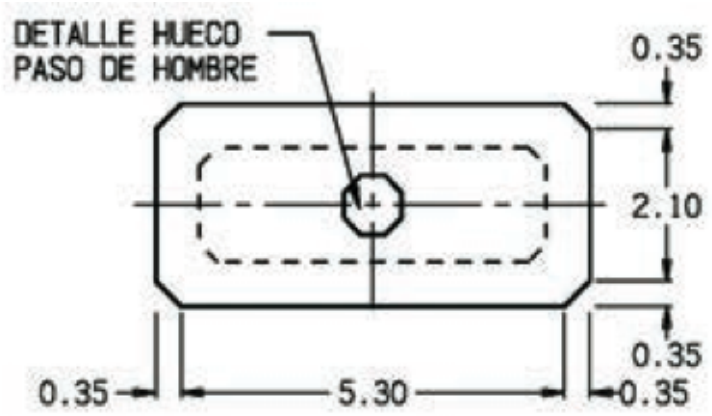

Figure 11: Contreras Section

Contreras Parametric Study

$$P_b = 262,1\frac{kN}{m}$$

$$P_f = 0,25m * 14,2m * 25\frac{kN}{m^3} = 88,75\frac{kN}{m}$$

$$P_{pv} = 14,2m * 2\frac{kN}{m^2} = 28,4\frac{kN}{m}$$

$$P_l = 78,48\frac{kN}{m} * 1,21 * 2 = 189\frac{kN}{m}$$

$$P_p = 16\frac{kN}{m}$$

$$P_a = 25\frac{kN}{m^3} * 25,7m^2 = 749\frac{kN}{m}$$

Where:
P_b is the beam weight,
P_f is the flange weight,
P_{pv} is the pavement weight,
P_{tb} is the transversal beam weight,
P_l is the liveload,
P_p is the pile weight,
P_a is the arch self-weight.

$$P_{tot,l} = P_{sb} + P_f + P_{pv} + P_{tb} + P_l + P_p + P_a$$

The total stress is $P_{tot,l} = 1058kN/m$ and it will be used to calculate the axial force in the foundation.

$$N_l = \frac{P_{tot}l^2}{8fcos(\alpha)} = 271588kN$$

Remembering the value of the Area $A = 43m^2$ of the arch section, the stress σ_l is evalueted in:

$$\sigma_l = \frac{N_l}{A} = 7559\frac{kN}{m^2}$$

And the total stress without the liveload is $P_{tot} = 868kN/m$ and the axial force in the foundation is:

$$N = \frac{P_{tot}l^2}{8fcos(\alpha)} = 222842kN$$

Finally is calculated a stress σ without the contribute of liveload evalueted in:

$$\sigma = \frac{N}{A} = 6202\frac{kN}{m^2}$$

Where:
l si the total span of the bridge,
f is the ratio of the bridge,
α is the slope of arch in foundation.

3.1.7 Los Tilos Bridge

The following is a description of the main characteristics of the Los Tilos arch (figure 2). The complete structure includes the arch itself and two access viaducts on either side. The complete bridge length is 319 m. The

access viaducts are 32 m long at both sides of the main span, with two spans each of 15 and 17 m. Over the arch, the deck is connected with the arch in another 15 spans of 17 m in length. The arch has a span of 255 m and its rise is of 46.20 m; therefore the span rise ratio is 5.52.

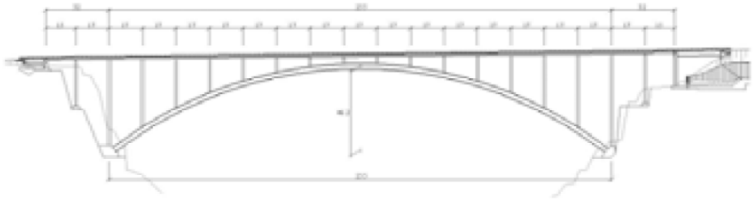

Figure 12: Los Tilos Span

Los Tilos Parametric Study

$$P_f = 0,28m * 12,00m * 25\frac{kN}{m^3} = 84,00\frac{kN}{m}$$

$$P_{sb} = 61,6\frac{kN}{m}$$

$$P_{pv} = 12,0m * 2\frac{kN}{m^2} = 24,0\frac{kN}{m}$$

$$P_l = 5\frac{kN}{m^2} * 12,0m = 60\frac{kN}{m}$$

$$P_p = 39\frac{kN}{m}$$

$$P_a = 25\frac{kN}{m^3} * 17,5m^2 = 438\frac{kN}{m}$$

Where:
P_{sb} is the steel beam weight,
P_f is the flange weight,
P_{pv} is the pavement weight,
P_l is the liveload,
P_p is the pile weight,
P_a is the arch self-weight.

$$P_{tot,l} = P_{sb} + P_f + P_{pv} + P_l + P_p + P_a$$

The total stress is $P_{tot,l}707 = kN/m$ and it will be used to calculate the axial force in the foundation.

$$N_l = \frac{P_{tot}l^2}{8fcos(\alpha)} = 157853kN$$

Remembering the value of the Area $A = 17,52m^2$ of the arch section, the stress σ_l is evalueted in:

$$\sigma_l = \frac{N_l}{A} = 9009\frac{kN}{m^2}$$

And the total stress without the liveload is $P_{tot} = 647kN/m$ and the axial force in the foundation is:

$$N = \frac{P_{tot}l^2}{8fcos(\alpha)} = 144457kN$$

Finally is calculated a stress σ without the contribute of liveload evalueted in:

$$\sigma = \frac{N}{A} = 8245\frac{kN}{m^2}$$

Where:
l si the total span of the bridge,
f is the ratio of the bridge,
α is the slope of arch in foundation.

3.1.8 Almonte Bridge

The arches for both carriageways are identical, with 184 metres span and 42 metres deflection, and, therefore, the sag/span ratio is 1/4.

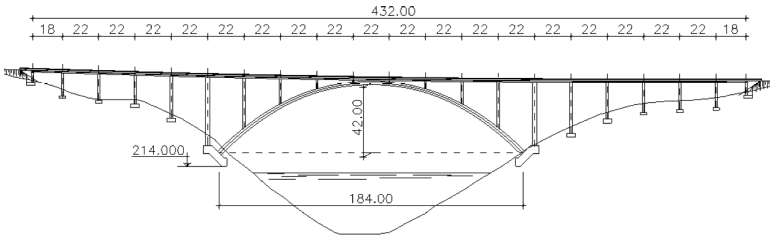

Figure 13: Almonte Span

Almonte Parametric Study The section is a single cell box with a thickness varying linearly between 3.00 metres at springings and 1.80 metres at the crown, with slenderness ratios of 1/61.33 and 1/102.22.
The width is kept constant at 6.00 metres, with 0.35 metre web and top and bottom slab thicknesses, and tapered beams in the slabs 0.50 metres long and 0.30 metres thick inside and, 0.30x0.30 outside, with which the overall width of the slabs is 6.60 metres

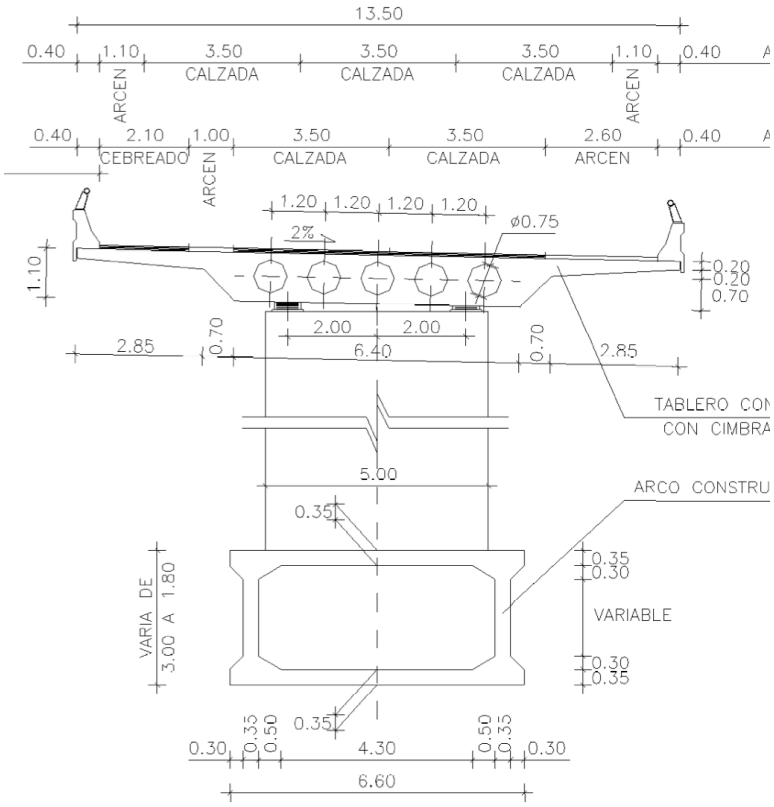

Figure 14: Almonte Section

$$P_b = 190\frac{kN}{m}$$

$$P_{pv} = 14,2m * 2\frac{kN}{m^2} = 27\frac{kN}{m}$$

$$P_l = 78,48\frac{kN}{m} * 1,21 * 2 = 67\frac{kN}{m}$$

$$P_p = 53\frac{kN}{m}$$

$$P_a = 25\frac{kN}{m^3} * 25,7m^2 = 157,5\frac{kN}{m}$$

Where:
P_b is the beam weight,
P_f is the flange weight,
P_{pv} is the pavement weight,
P_{tb} is the transversal beam weight,
P_l is the liveload,
P_p is the pile weight,
P_a is the arch self-weight.

$$P_{tot,l} = P_{sb} + P_{pv} + P_{tb} + P_l + P_p + P_a$$

The total stress is $P_{tot,l} = 495kN/m$ and it will be used to calculate the axial force in the foundation.

$$N_l = \frac{P_{tot}l^2}{8fcos(\alpha)} = 71901kN$$

Remembering the value of the Area $A = 6,7m^2$ of the arch section, the stress σ_l is evalueted in:

$$\sigma_l = \frac{N_l}{A} = 10731\frac{kN}{m^2}$$

And the total stress without the liveload is $P_{tot} = 428kN/m$ and the axial force in the foundation is:

$$N = \frac{P_{tot}l^2}{8fcos(\alpha)} = 62101kN$$

Finally is calculated a stress σ without the contribute of liveload evalueted in:

$$\sigma = \frac{N}{A} = 9268\frac{kN}{m^2}$$

Where:
l si the total span of the bridge,
f is the ratio of the bridge,
α is the slope of arch in foundation.

3.1.9 Traneberg Bridge

The arch bridge over Tranebergssund [4] in Stockholm built during 1932 to 1934 combining railway and road bridge is at present the widest arch bridge in the world having a span of 181 m figure 15. It has a relation rise/span of 1/7.

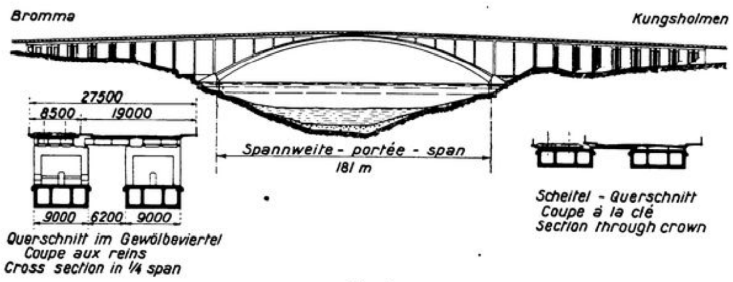

Figure 15: Traneberg Span

Traneberg Parametric Study

$$P_b = 190,0\frac{kN}{m}$$

$$P_{pv} = 27,5m * 2\frac{kN}{m^2} = 55,0\frac{kN}{m}$$

$$P_l = 11,7m * 5\frac{kN}{m^2} = 250,0\frac{kN}{m}$$

$$P_p = 54,1\frac{kN}{m}$$

$$P_a = 25\frac{kN}{m^3} * 16,0m^2 = 400\frac{kN}{m}$$

Where:
P_b is the beam weight,
P_{pv} is the pavement weight,
P_{tb} is the transversal beam weight,
P_l is the liveload,
P_p is the pile weight,
P_a is the arch self-weight.

$$P_{tot,l} = P_{sb} + P_{pv} + P_{tb} + P_l + P_p + P_a$$

The total stress is $P_{tot,l} = 949,7kN/m$ and it will be used to calculate the axial force in the foundation.

$$N_l = \frac{P_{tot}l^2}{8fcos(\alpha)} = 171376,4kN$$

Remembering the value of the Area $A = 16,0m^2$ of the arch section, the stress σ_l is evalueted in:

$$\sigma_l = \frac{N_l}{A} = 7772,2\frac{kN}{m^2}$$

And the total stress without the liveload is $P_{tot} = 700kN/m$ and the axial force in the foundation is:

$$N = \frac{P_{tot}l^2}{8fcos(\alpha)} = 126277,0kN$$

Finally is calculated a stress σ without the contribute of liveload evalueted in:

$$\sigma = \frac{N}{A} = 5726,8\frac{kN}{m^2}$$

Where:
l si the total span of the bridge,
f is the ratio of the bridge,
α is the slope of arch in foundation.

3.1.10 Ulla Bridge

The Ulla Viaduct [3] is the crossing of the N-NW Spanish High Speed Railway over the "Ulla-Deza Fluvial System", Place of Community Interest (LIC), with height above that level of 115m. Strong winds are usual in this valley. The viaduct is 630 m long. A lightly pointed arch, 168 m of span and 105 m of rise, crosses over the river.
The access viaducts are made of spans that are 52m lengtheach. The deck is a prestressed concrete box, 3,89 m height constant. It is made using a self-cast formwork. The architself is a boxsection, dimensions 7,7x3,50 m;the archaxis is a polygonal line.

Ulla Parametric Study Is now evalueted the tension that is working on the basement of the bridge.

$$P_f = 0,28m * 12,00m * 25\frac{kN}{m^3} = 84,00\frac{kN}{m}$$

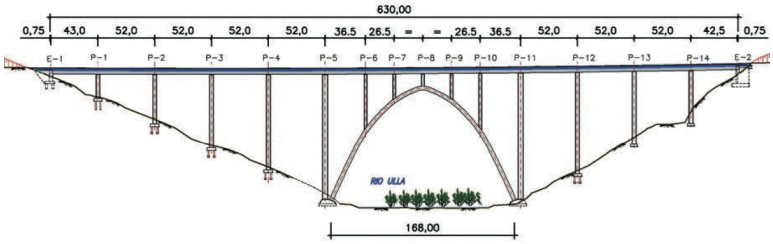

Figure 16: Ulla Span

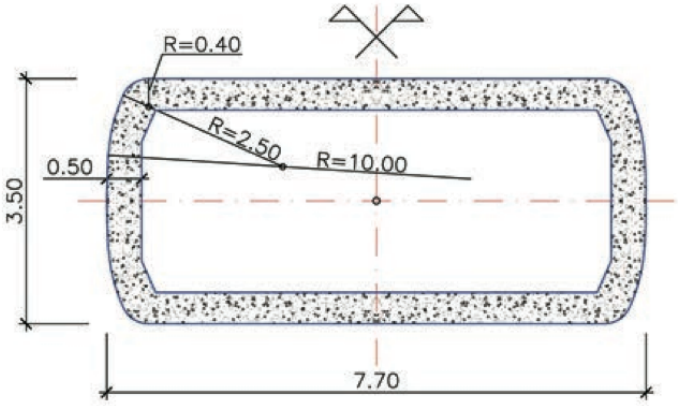

Figure 17: Ulla Section

$$P_{sb} = 61,6\frac{kN}{m}$$

$$P_{pv} = 12,0m * 2\frac{kN}{m^2} = 24,0\frac{kN}{m}$$

$$P_l = 5\frac{kN}{m^2} * 12,0m = 60\frac{kN}{m}$$

$$P_p = 149\frac{kN}{m}$$

$$P_a = 25\frac{kN}{m^3} * 17,5m^2 = 438\frac{kN}{m}$$

Where:
P_{sb} is the steel beam weight,
P_f is the flange weight,
P_{pv} is the pavement weight,

P_l is the liveload,
P_p is the pile weight,
P_a is the arch self-weight.

$$P_{tot,l} = P_{sb} + P_f + P_{pv} + P_l + P_p + P_a$$

The total stress is $P_{tot,l}889 = kN/m$ and it will be used to calculate the axial force in the foundation.

$$N_l = \frac{P_{tot}l^2}{8fcos(\alpha)} = 46013kN$$

Remembering the value of the Area $A = 17,52m^2$ of the arch section, the stress σ_l is evalueted in:

$$\sigma_l = \frac{N_l}{A} = 3098\frac{kN}{m^2}$$

And the total stress without the liveload is $P_{tot} = 793,8kN/m$ and the axial force in the foundation is:

$$N = \frac{P_{tot}l^2}{8fcos(\alpha)} = 41096,7kN$$

Finally is calculated a stress σ without the contribute of liveload evalueted in:

$$\sigma = \frac{N}{A} = 2686\frac{kN}{m^2}$$

Where:
l si the total span of the bridge,
f is the ratio of the bridge,
α is the slope of arch in foundation.

3.1.11 Burguillo Bridge

The Burguillo Bridge has a 161m span and a 25m rise with the rise to span ratio of $\frac{1}{6,4}$.

Burguillo Parametric Study

$$P_b = 171\frac{kN}{m}$$

$$P_{pv} = 12,0m * 2\frac{kN}{m^2} = 24,0\frac{kN}{m}$$

$$P_l = 12,0m * 5\frac{kN}{m^2} = 60\frac{kN}{m}$$

$$P_p = 20,9\frac{kN}{m}$$

$$P_a = 258\frac{kN}{m}$$

Where:
P_b is the beam weight,
P_{pv} is the pavement weight,
P_l is the liveload,
P_p is the pile weight,
P_a is the arch self-weight.

$$P_{tot,l} = P_{sb} + P_{pv} + P_{tb} + P_l + P_p + P_a$$

The total stress is $P_{tot,l} = 534,4kN/m$ and it will be used to calculate the axial force in the foundation.

$$N_l = \frac{P_{tot}l^2}{8fcos(\alpha)} = 85043kN$$

Remembering the value of the Area $A = 12,4m^2$ of the arch section, the stress σ_l is evalueted in:

$$\sigma_l = \frac{N_l}{A} = 6858,3\frac{kN}{m^2}$$

And the total stress without the liveload is $P_{tot} = 474,4kN/m$ and the axial force in the foundation is:

$$N = \frac{P_{tot}l^2}{8fcos(\alpha)} = 75495kN$$

Finally is calculated a stress σ without the contribute of liveload evalueted in:

$$\sigma = \frac{N}{A} = 6088\frac{kN}{m^2}$$

Where:
l si the total span of the bridge,
f is the ratio of the bridge,
α is the slope of arch in foundation.

3.1.12 Cieza Bridge

The arch has a 141m span between both roots and is 32m in height.
It fallows a 2° parabola and the edge varies between 2,6m at the root and 1,8m at the crown section.

Cieza Parametric Study

$$P_b = 144,2\frac{kN}{m}$$

$$P_{pv} = 11,7m * 2\frac{kN}{m^2} = 23,4\frac{kN}{m}$$

$$P_l = 11,7m * 5\frac{kN}{m^2} = 58,5\frac{kN}{m}$$

$$P_p = 41,8\frac{kN}{m}$$

$$P_a = 25\frac{kN}{m^3} * 5,2m^2 = 130\frac{kN}{m}$$

Where:
P_b is the beam weight,
P_{pv} is the pavement weight,
P_{tb} is the transversal beam weight,
P_l is the liveload,
P_p is the pile weight,
P_a is the arch self-weight.

$$P_{tot,l} = P_{sb} + P_{pv} + P_{tb} + P_l + P_p + P_a$$

The total stress is $P_{tot,l} = 397,9kN/m$ and it will be used to calculate the axial force in the foundation.

$$N_l = \frac{P_{tot}l^2}{8fcos(\alpha)} = 43405kN$$

Remembering the value of the Area $A = 5,2m^2$ of the arch section, the stress σ_l is evalueted in:

$$\sigma_l = \frac{N_l}{A} = 8347\frac{kN}{m^2}$$

And the total stress without the liveload is $P_{tot} = 339kN/m$ and the axial force in the foundation is:

$$N = \frac{P_{tot} l^2}{8 f cos(\alpha)} = 37024 kN$$

Finally is calculated a stress σ without the contribute of liveload evalueted in:

$$\sigma = \frac{N}{A} = 7120 \frac{kN}{m^2}$$

Where:
l si the total span of the bridge,
f is the ratio of the bridge,
α is the slope of arch in foundation.

3.2 Statistical Analysis

It is necessary create a cloud of informations about areas and tensions (Axil in correspondence of the support) of bridges analysied in the previous section and a cloud of informations about medium and small area. Finally using excell functions it will be possible to find the equation that governs the scattergram distribution of the cloud of points.

In first instance it is necessary to build a summary table with all area velues calculate in chapter 2.

Bridge	Max Area $[m^2]$	Med Area $[m^2]$	Min Area $[m^2]$
Wanxian	35,7	27,9	20,2
Krk	13,2	13,2	13,2
Hoover	15,5	15,5	15,5
Infante Henrique	30,0	22,5	15,0
Bloukrans	23,4	20,4	17,4
Contreras	35,9	22,5	9,0
Los tilos	17,5	17,5	17,5
La Regenta	10,6	9,0	7,3
Almonte	6,7	6,3	5,9
Traneberg	22,0	13,2	12,8
Ulla	21,4	14,3	10,2
Burguillo	10,3	10,3	10,3
Cieza	5,4	5,2	5,0

Table 1: Areas Bridge's Summary

Maximum Arch Area This is a scattergram of the Maximum Area of the analyzed bridges. Specifically is the Area of the Section in correspondence of the supports. On the x-axis we find the span and in the y-axis the value of the Maximum Area.

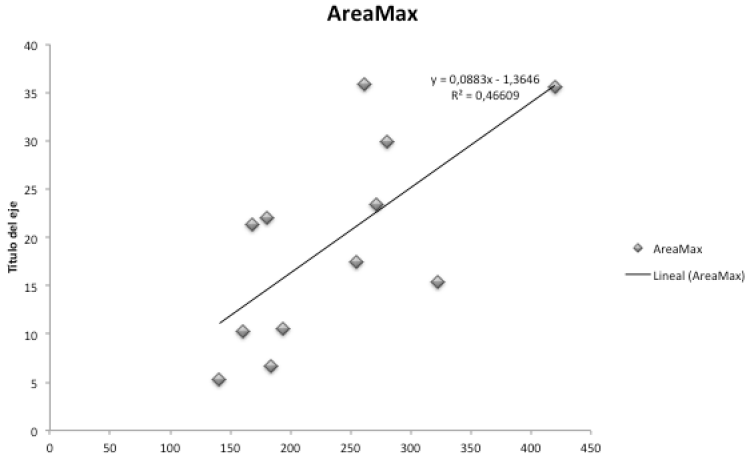

Figure 18: Maximum Area

And the equation that governs the scattergram distribution in [figure 18] is:

$$y = 0,0883x - 1,3646 \tag{8}$$

Median Arch Area This graphic represents a cloud of points, in which every point is the Median Arch Area per each bridge analyzed.

On the x-axis we find the span and in the y-axis the value of the Median Area.

And the equation that governs the scattergram distribution in [figure 19] is:

$$y = 0,0734x - 1,9981 \tag{9}$$

Minimum Arch Area This graphic represents a cloud of points, in which every point is the Minimum Arch Area per each bridge analyzed. This is going to happens in the midspan of the bridge and in the very next parts to it. On the x-axis we find the span and in the y-axis the value of the Minimum Area.

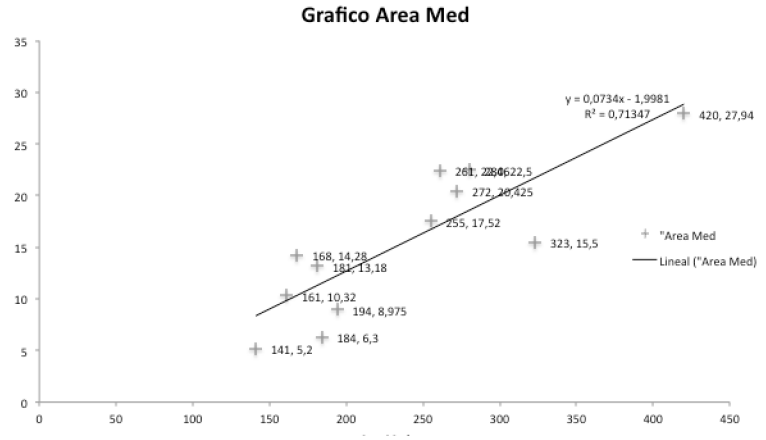

Figure 19: Median Area

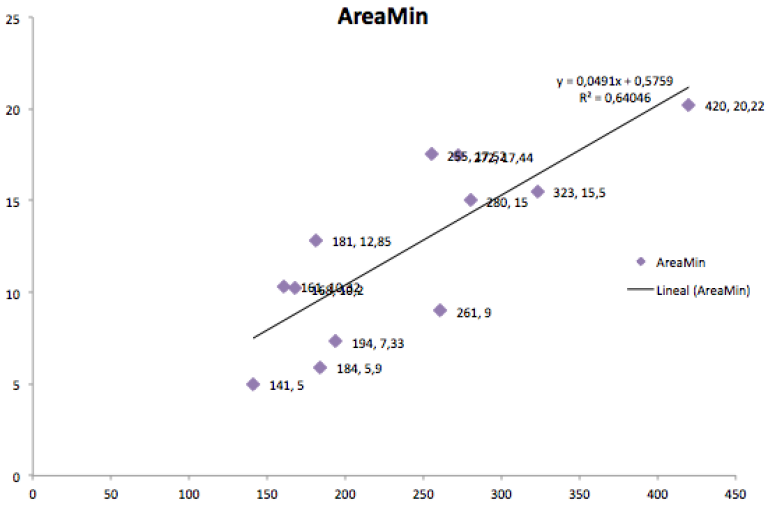

Figure 20: Minimum Area

And the equation (regression line) that governs the scattergram distribution in [figure 20] is:

$$y = 0,0491x + 0,5759 \tag{10}$$

3.2.1 Upper and Lower Bounds of Arch Cross Section

It is necessary now to avaluete a range between the estimated regression line and massive bridges (upper limit) and between the estimated regression line and light bridges (lower limit).

3.2.2 Standard Deviation

It is necessary to estimate $\sqrt{\sigma^2}$, the assumed constant standard deviation (following called SD) of Y given x.
The obvious estimator of σ^2, is the average of the squared residuals.
This method has been taken from [2].

That is:

$$s^2 = \sigma^2 = \frac{1}{n-2}\sum_{n=1}^{n}[yi - (\alpha + \beta * xi)]^2 \tag{11}$$

The average value of the area is:

$$ymed = \sum_{i=1}^{12}\frac{yi}{n} \tag{12}$$

The average value of the span is:

$$xmed = \sum_{i=1}^{12}\frac{xi}{n} \tag{13}$$

Is now possible to estimate the two parameters α and β:

$$\beta = \sum_{i=1}^{12}\frac{xiyi - nymedxmed}{xi^2 - nxmed^2} \tag{14}$$

$$\alpha = (ymed - \beta)xmed \tag{15}$$

Where:
n is the number of bridges analyzed.
yi is the ordinate of the graphic representing the area of the bridge.
xi is the abscissa of the graphic representing the span of the bridge.

It is required now to apply this equations to the regression lines functions. In this way, we will obtain the standard constant deviation for each graphic showed in subsection 3.2

Maximum Arch Area SD Remembering the equation (8), we are going to evaluate its SD.
Using the equation (12) we estimate:

$$ymed = 19,54$$

Using the equation (13):

$$xmed = 236,66$$

Using the equation (21):

$$\beta = 0,0883$$

Using the equation (15):

$$\alpha = -1,364$$

Using the equation (11):

$$s^2 = 64,79$$

Finally the value of the SD for the Maximum Arch Area graphic regression line is:

$$s = \sqrt{s^2} = 8,049$$

So now the value of s will be used to "move" the regression line up with a value of $y = f(x) + 8,049$ and down with a value of $y = f(x) - 8,049$. Where y=f(x) is the equation (8).

Median Arch Area SD Remembering the equation (9), we are going to evaluate its SD.
Using the equation (12) we estimate:

$$ymed = 15,38$$

Using the equation (13):

$$xmed = 236,66$$

Using the equation (21):

$$\beta = 0,073$$

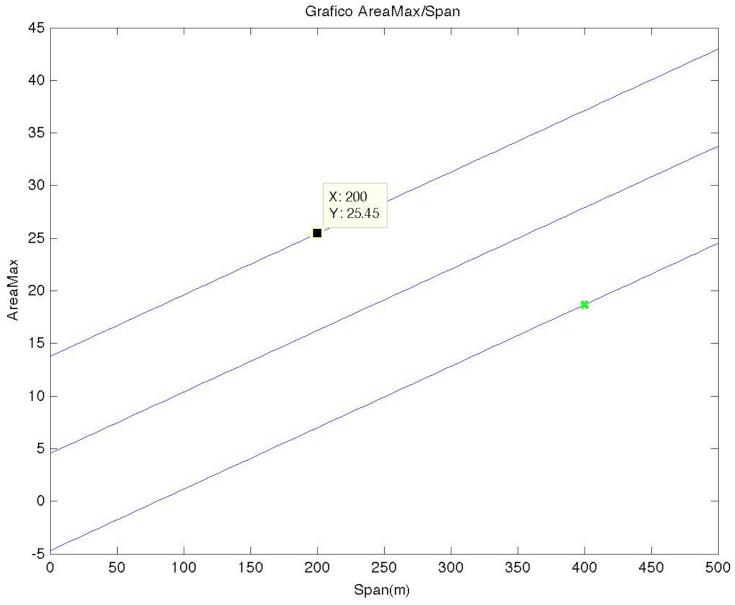

Figure 21: SD Area on Supports

Using the equation (15):

$$\alpha = -1,998$$

Using the equation (11):

$$s^2 = 15,68$$

Finally the value of the SD for the Median Arch Area graphic regression line is:

$$s = \sqrt{s^2} = 3,96$$

So now the value of s will be used to "move" the regression line up with a value of $y = f(x) + 3,96$ and down with a value of $y = f(x) - 3,96$. Where y=f(x) is the equation (9).

Minimum Arch Area SD Remembering the equation (10), we are going to evaluate its SD.

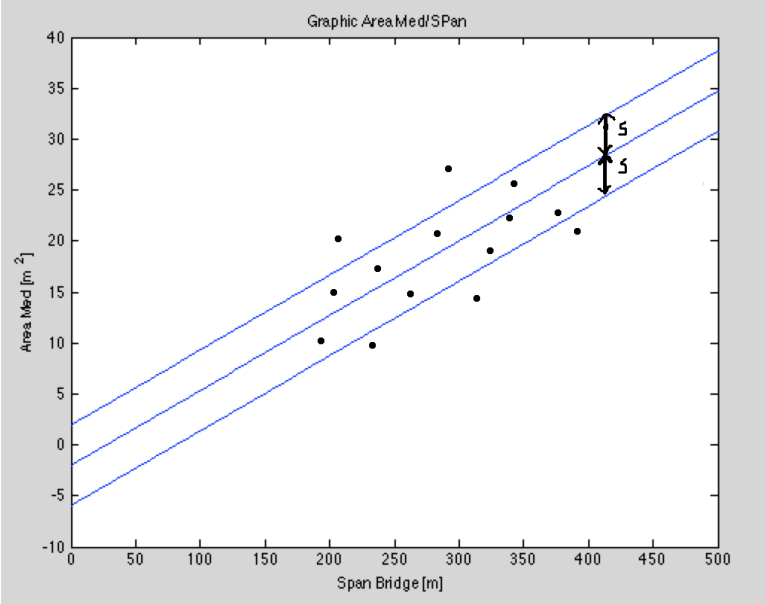

Figure 22: SD Area in The Center of The Rib

Using the equation (12) we estimate:

$$ymed = 12,19$$

Using the equation (13):

$$xmed = 236,66$$

Using the equation (21):

$$\beta = 0,049$$

Using the equation (15):

$$\alpha = 0,576$$

Using the equation (11):

$$s^2 = 9,79$$

Finally the value of the SD for the Median Arch Area graphic regression line

is:

$$s = \sqrt{s^2} = 3,13$$

So now the value of s will be used to "move" the regression line up with a value of $y = f(x) + 3,13$ and down with a value of $y = f(x) - 3,13$. Where y=f(x) is the equation (10).

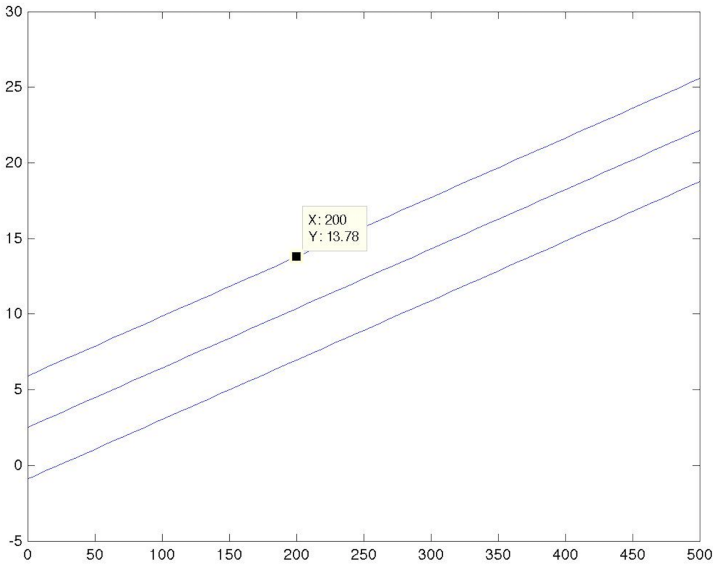

Figure 23: SD Area in Midspan

4 Contreras Arch Bridge Like a Sample

The reinforced concrete arch bridge of a 261 m span, with an upper prestressed concrete deck and a total length of 587.25 m, spans the Contreras Reservoir on the Madrid-Levante high-speed railway line. The mid-span sag is 36.944 m thus determining a span-to-rise ratio of over 6.77 to 1, which is a low rising arch although not excessively so. On the construction completion date, the span between the arch supports was holder of the world record for a concrete railway arch bridge. It was built by free cantilever system using a temporary pier that was dismantled once the two semi-arches had been joined. The deck was built span by span with a scaffolding truss on either side of the arch. Jacks at the crown of the bridge were not used since they would not have improved significantly the global forces in the bridge.

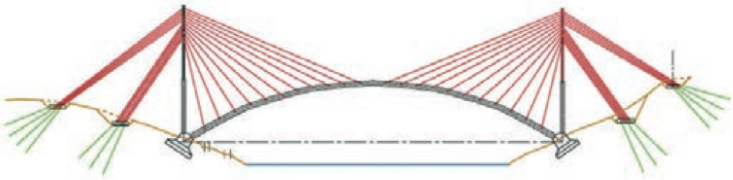

Figure 24: Contreras' Temporary Supporting System

4.1 Construction Process

Various preliminary calculations were carried out to check the construction process, among which was arranging a lattice in the trapeziums resulting from the piers, arch and deck (Fig. 26).

This classic and intuitively logical solution consists of forming a lattice in the course of the process. Within this lattice, the arch acts as the lower compression chord, the deck is the upper tension chord and the piers supported on the arch serve as vertical bars. Temporary elements act as diagonals, resisting tensile stresses.
The first conceptual problem in this construction process is encountered when a concrete element such as the deck is used as a stay cable for the lattice. Nevertheless, as this is a prestressed element, this solution may be convenient in case the tension during the process is resisted through a moderate increase of prestressing required for the service situation.

Figure 25: Free Cantilever Construction of The Arch With Temporary cable-staying from the pier at the springs

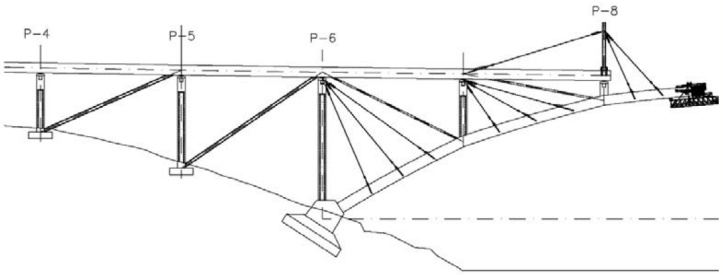

Figure 26: Cantilever construction between de Arch and the Deck

After carrying out the corresponding analysis, this solution turned out clearly unfavourable from the economic point of view. The magnitude of the length spanned by each semi-arch implied having to solve great tension in the deck, which in its turn required a large amount of reinforcement. The extra cost of the said prestressing, as well as the difficulty of its installation, makes this method more expensive and than others, even those that require additional auxiliary means. This is, therefore, the least economical construction system for large-span arches such as this one. It is, however, quite competitive for smaler arches.
The construction method eventually chosen for this bridge and given its situation with respect to the water of the reservoir and the land was the cable-stayed free cantilever launching of the two semi-arches embedded in their foundations Fig. 26.

However, this process was modified at the request of the Construction Company and of EIPSA, acting as technical advisor of the construction company throughout the proj- ect execution. The proposal was to build

the arch by cable- stayed incremental launching as well, only it was to be launched from the first pier of the arch, which was to be extended until reaching the ground where it was then appropriately founded. At the beginning of the construction, after a particularly favourable hydrological year for our purposes, the reservoir water level was such that the foundations of the temporary pier were above water level for months on end.

Moving the cable-staying pier forward considerably lowers the costs of the construction process, since it reduces the weight of the arch to be supported, with the subsequent reduction of the number and length of temporary stay cables. Nevertheless, this is not a universal solution (bathymetry, geotechnical engineering, etc.).

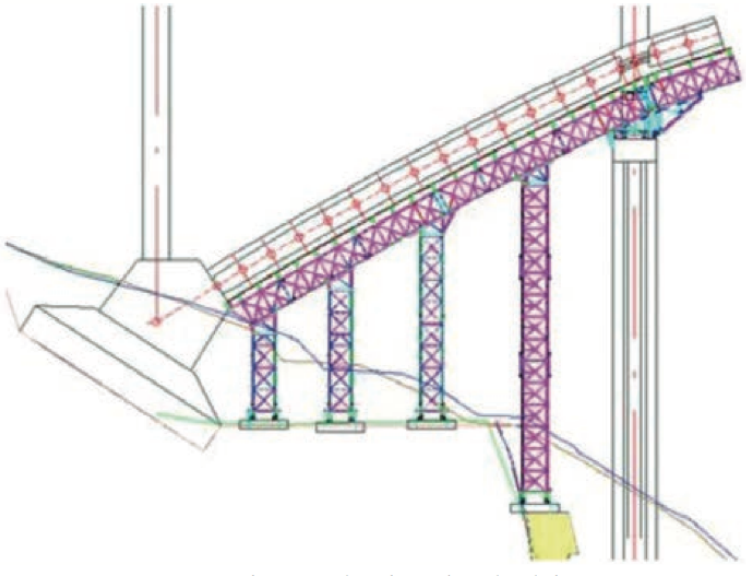

Figure 27: Centering Supported on the Ground

At this point the execution of the arch begins. The first section of each semi-arch, between the foundation and temporary piers, is built upon a centering supported on the ground (Fig. 27). For that purpose, a series of temporary steel supports are arranged to support the arch formwork. We must emphasise the need for a perfect conception and revision of all the details of the auxiliary structures, which are essential in this stage of

construction.
The centering is then dismantled and the advance of the semi-arches is initiated using cable stayed free cantilevers. To this end we placed metal pylons on the deck, following the vertical line of the temporary piers. From this moment on, the semi-arches advanced in free cantilevers while concreted in situ using form traveller. To enable such proce- dure, we placed nine successive bundles of stay cables on each semi-arch. Each bundle consisted of a couple of front cables anchored in the executed arch segments and a couple of rear ones anchored in the arch plinths.

5 Previously Approximate Evaluations To The Calibration Of The TOA Method

For a pre planning, the estimation of the tensions the values of the static tensions in the tiebacks have been done considering pins among the cantilevered sections as is possible to view in the picture **??**.

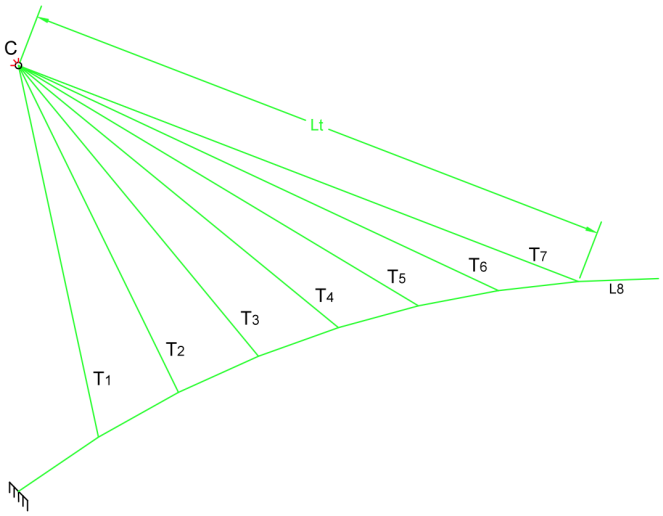

Figure 28: Emiarch And Tieback Lenght L_t

5.1 Beam on Elastic Supports - Winkler foundation

It is obvious that is possible to compare the static model of the emiarch (Picture 29) with a Winkler foundation, a simplified elastic-support model showed in the picture 30.

The elastic constant k of a single tieback is equal to:

$$k = \frac{E_s A}{L_t} \tag{16}$$

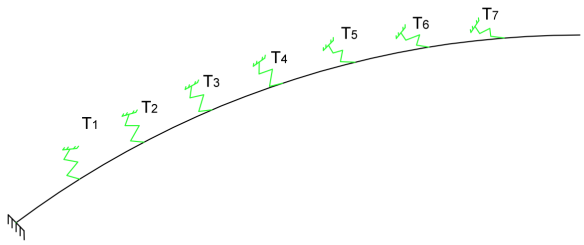

Figure 29: Emiarch Compared to a Winkler Beam

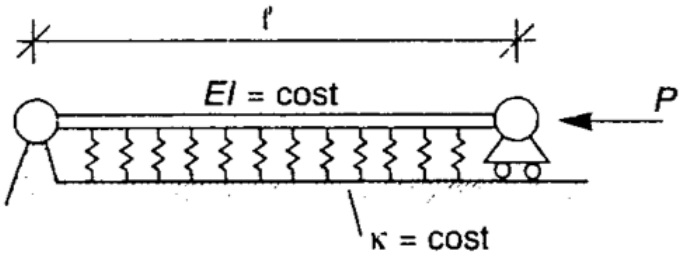

Figure 30: Winkler foundation

with E_s Young Modulus of the steel.

And L_t is the avarage lenght of the tieback:

$$L_t \sim \alpha * H \tag{17}$$

Where:
H is the height of the tower,
EA is the stiffness of the tieback.

Indeed the total stiffness K of the system "tiebacks" is:

$$K = \frac{k}{\delta} \tag{18}$$

Where δ is:

$$\delta = \frac{L_t}{2n} \tag{19}$$

with n number of tiebacks.

And the stiffness of the emiarch is:

$$w = \frac{E_c I}{L^4} \tag{20}$$

with L lenght of the emiarch.

Finally the relation between the stiffnesses of the two components, for better say, K for the tieback's system and w for the emiarch will be:

$$\beta = \frac{K}{w} = \frac{E_s A L^4}{E_c I L_t \delta} \tag{21}$$

Remembering the equations 19 and 17 and replacing them in the equation 21 is obtained:

$$\beta = \frac{E_s A L^4 2n}{E_c I H^2} \tag{22}$$

Here it is showed a table summerizing a step of values of diameters for different types of tiebacks:

$D[m]$	A $[m^2]$	β	$\frac{R_x}{R_y}$	$\frac{T_1}{V_1}$	$\frac{T_2}{V_2}$	$\frac{T_3}{V_3}$	$\frac{T_4}{V_4}$	$\frac{T_5}{V_5}$	$\frac{T_6}{V_6}$	$\frac{T_7}{V_7}$	$\frac{T_8}{V_8}$	$\sum \frac{T_i}{V_i}$
0.01	$7.85.10^{-5}$	0.15	$\frac{10527}{6397}$	$\frac{554}{541}$	$\frac{1264}{1136}$	$\frac{1875}{1436}$	$\frac{2173}{1368}$	$\frac{2185}{1126}$	$\frac{2047}{866}$	$\frac{1861}{668}$	$\frac{1676}{519}$	$\frac{13635}{7660}$
0.10	$7.80.10^{-3}$	15	$\frac{10527}{7837}$	$\frac{275}{271}$	$\frac{660}{606}$	$\frac{1158}{928}$	$\frac{1687}{1118}$	$\frac{2109}{1128}$	$\frac{2336}{1017}$	$\frac{2373}{863}$	$\frac{2278}{720}$	$\frac{12876}{6651}$
0.20	$3.14.10^{-2}$	62	$\frac{10179}{8462}$	$\frac{324}{318}$	$\frac{592}{543}$	$\frac{903}{724}$	$\frac{1409}{933}$	$\frac{2027}{1085}$	$\frac{2524}{1099}$	$\frac{2747}{999}$	$\frac{2721}{860}$	$\frac{13247}{6561}$
0.30	$7.07.10^{-2}$	140	$\frac{11828}{9000}$	$\frac{433}{425}$	$\frac{651}{597}$	$\frac{827}{663}$	$\frac{1269}{841}$	$\frac{1999}{1070}$	$\frac{2719}{1183}$	$\frac{3122}{1136}$	$\frac{3161}{998}$	$\frac{14181}{6913}$
0.40	$1.256.10^{-1}$	247	$\frac{12966}{9732}$	$\frac{522}{513}$	$\frac{700}{642}$	$\frac{803}{643}$	$\frac{1199}{794}$	$\frac{2010}{1076}$	$\frac{2955}{1287}$	$\frac{3578}{1302}$	$\frac{3711}{1172}$	$\frac{15478}{7429}$
				P_1	P_2	P_3	P_4	P_5	P_6	P_7	P_8	P_{Tot}
				1823	1823	1823	1823	1823	1823	1823	1823	14584

Table 2: Characteristics of λ and the tiebacks in A_t Variation

In particular the diameter elected for the next samples will be $D = 10cm$ because of the homogeneous distribution among the tensions in the tiebacks.

For better explain, if the system of tiebacks is very stiff ($D = 0.30/0.40$m) the tensions are concentreted in the zone next to the mid-span, otherwise if the tiebacks' system is not so stiff ($D = 0.01$m), then the tensions are concentreted in the central zone of the rib.

6 Optimization Of The Construction Process

6.1 Tiebacks' Optimization Algorithms TOA

Take in account what has been study in the article write by Au, Wang and Liu [10], and in particular if we consider a typical stage i during the cantilever erection of the arch rib of a bridge we need to ensure not only the stability of the assembly but also that the stresses are within the allowable limits. In this case limits will be represented from Admissible Bending Moments.

What they proposed in [10] is to determinate the minimum tieback forces and the maximum tieback forces from the following equation:

$$\{f^t\} = \{g^t\} + [A]\{T\} \tag{23}$$

$$\{f^b\} = \{g^b\} + [B]\{T\} \tag{24}$$

Where the vectors f^t and f^b contain the stresses at the top and bottom fibers, respectively, and the vectors g^t and g^b contain the stresses due to dead load at the top and bottom fibers, respectively, of the control sections if the incomplete arch rib is assumed to be cantilevered from the abutment; [A] and [B]= influence matrices for the top and bottom fibers, respectively, of the control sections due to tieback forces; and T contains the tieback forces T_j.

Similar to what has been done in [10] we can consider a clamped semi-arch and a number j of ties applied at S-sections along the acting as suspenders before crown closing as shown in Figure 31.

If M_G is the vector of the bending moments in the M-sections due to the arch self weight, A is the influence matrix, T is the vector of the tieback forces and M is the vector contains the Bending Moment along the arch rib one can write:

$$\{M\} = \{M_G\} + [A]\{T\} \tag{25}$$

The equation 25 will be study in detail in the following section.

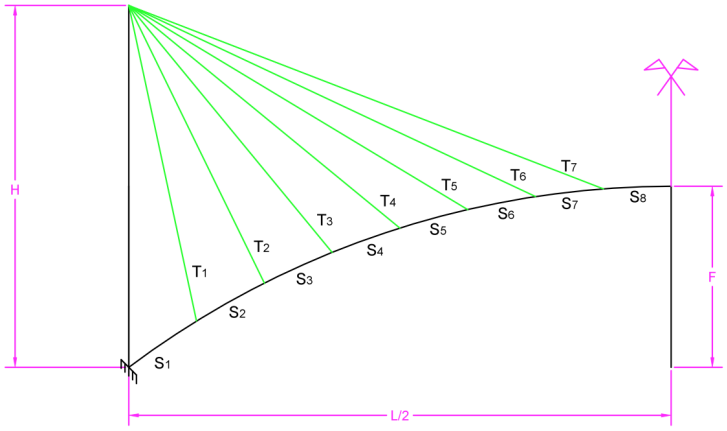

Figure 31: Before Crown Closing

6.1.1 Value of T Optimizing The Static Response

Being A_{ij} the influence coefficients defining the target internal actions (i.e. M) in a number i of M-sections and being T_j the value of the optimized tensions, a simple formulation is derived:

$$M_{T,i} = \sum A_{ij} T_j \tag{26}$$

$$A \rightarrow A_{ij} \tag{27}$$

Denoting with $M_{G,i}$ the moments in M-sections due to the arch self weight, it is possible to write and calling now, A the total matrix of the influence coefficients:

$$M_i = M_{G,i} + \sum A_{ij} T_j \tag{28}$$

Finally it is possble to establish in matrix terms:

$$M = M_G + AT \tag{29}$$

The optimal design problem requires to determine the values T optimizing the static response, in fact:

$$min \sum M_i^2 = min(M^t M) \tag{30}$$

that is:

$$\frac{\partial}{\partial T}(M^t M) = 2\frac{\partial M^t}{\partial T} M = 0 \tag{31}$$

replacing the equation 29 in the equation 31 it is obtained:

$$A^t(M_G + AT) = 0 \tag{32}$$

finally:

$$(A^t A)T = -A^t M_G \tag{33}$$

with solution:

$$T = -(A^t A)^{-1} A^t M_G \tag{34}$$

The equation 34 is suitable to every arch bridge erected with the Cantilever Launching Method.
The values of the optimized tensions in the vector T will produce the best diagram of Bending Moment along the emiarch.

6.1.2 Pretensions Applied to Tiebacks

An other algorithm has been realized to obtain the tiebacks' forces distribution already deduced from the equation (34).
In other words, if it is applied to the tiebacks the pretensions gains from the equation (34) directly to the tiebacks, the output of the Solver in Straus7 will give back a wrong moment distribution, this is because of the static contribution in the tiebacks.
Indeed, to ensure that tiebacks work at the rate T_i determinated by the equation (34) like the optimal one it is possible to follow a similar strategy of calculus used to define the T_i selves.
First of all has been calculated the vector N_G, the vector of the axial forces into the tiebacks due to selfweight of the semiarch.
In a second step the matrix D_{ij} has been calculated, which supply in columns the axial forces per each tieback under the effect of a pre-tension N^o unitary.
So the forces per each tieback is given by the equation:

$$N_i = N_{Gi} + D_{ij} N_j^o \tag{35}$$

Imposing the relation:

$$Ni = Ti \tag{36}$$

$$D = D_{ij} \tag{37}$$

it is obtained:

$$D_{ij} N_j^o = T_i - N_{Gi} \tag{38}$$

in matrix terms:

$$DN^o = T - N_G \tag{39}$$

To finally obtain the equation:

$$N^o = D^{-1}(T - N_G) \tag{40}$$

The values N^o (i.e. pretensions) obtained from the equation (40) have to be applied to the tiebacks as pretensions to ensure that the tiebacks are working at the forces extracted from the equation (34).

6.2 Sample TOA Bridge Application

In this section will be applied the previous algorithms to a pratical case, showed in the picture 32

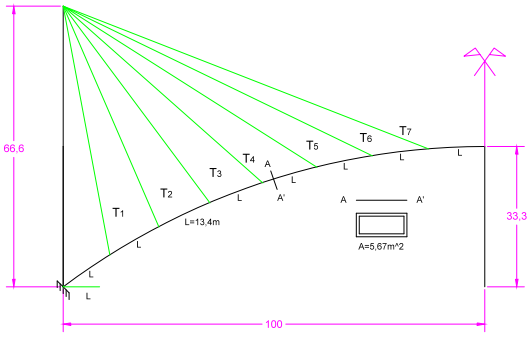

Figure 32: Sample Bridge

The bridge has a span of 200m and the relation $\frac{rise}{span}$ is $\frac{r}{s} = \frac{1}{6}$, in fact the rise is 33,3 m. This $\frac{r}{s}$ value has been choose because of the avarage of bridges already constructed.
Here it is a table summarizing all the characteristics of this bridge:

Span $[m]$	Rise $[m]$	A $[m^2]$	f_{yk} [MPa]	f_{ck} [MPa]	E_c [MPa]	E_s [MPa]
200	$33,3$	$5,67m^2$	450	40	34290	200000

Table 3: Sample Bridge' Characteristics

Where:
A is the area of the arch section,
f_{yk} is the specified characteristics yield stress of bars,
f_{ck} is the specified characteristics yield stress of the concrete,
E_c is the Young Modulus of the concrete,
E_s is the Young Modulus of steel (i.e. bars and steel),

6.2.1 Application Of The Optimizing Alghorithms to The Sample Case

The configuration of tiebacks is the one showed in the picture 32.
First of all is important to construct a model in which is applied a force equal to the unit per each tieback, so it is possible to compose the matrix A, the one containing the influence coefficients defining the target internal actions (i.e. M) settle in the section 6.1.1.

Unitary Force in tieback 1 position:

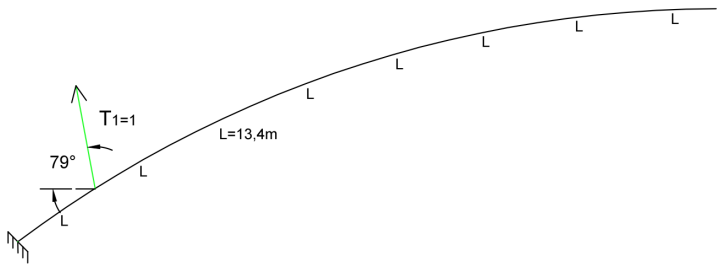

Figure 33: Unit Force T1

Decompose of the unitary force in tieback 1 position:

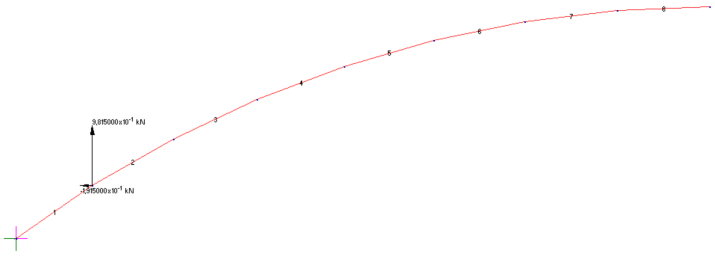

Figure 34: Decompose Force T1

Coefficients:

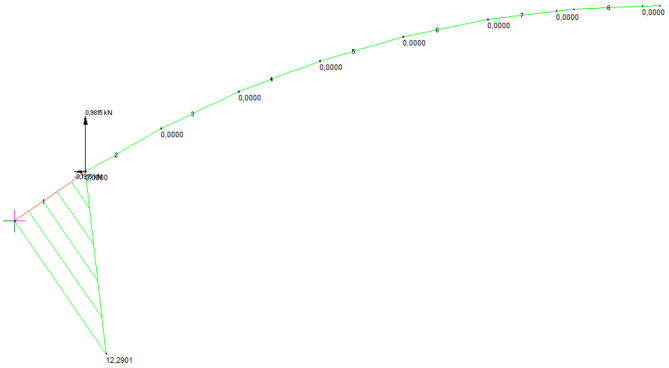

Figure 35: Coefficients Product From Force T1

Unitary Force in tieback 2 position:

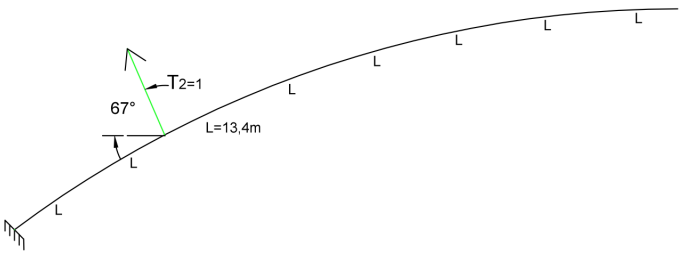

Figure 36: Unit Force T2

Decompose of the unitary force in tieback 2 position:

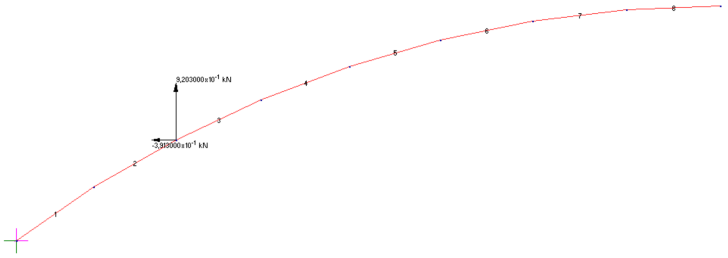

Figure 37: Decompose Force T2

Coefficients:

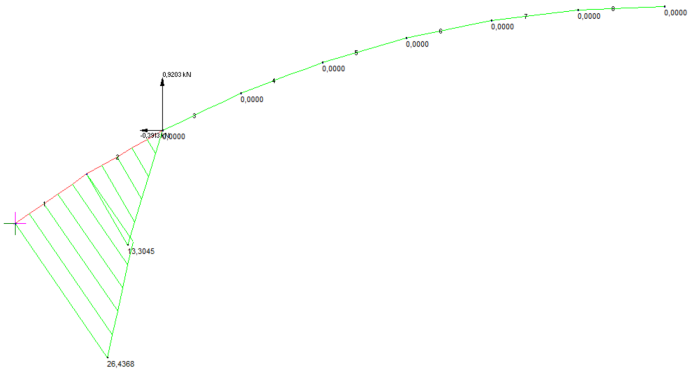

Figure 38: Coefficients Product From Force T2

Unitary Force in tieback 3 position:

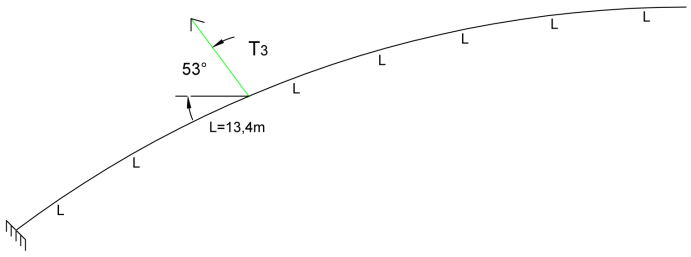

Figure 39: Unit Force T3

Decompose of the unitary force in tieback 3 position:

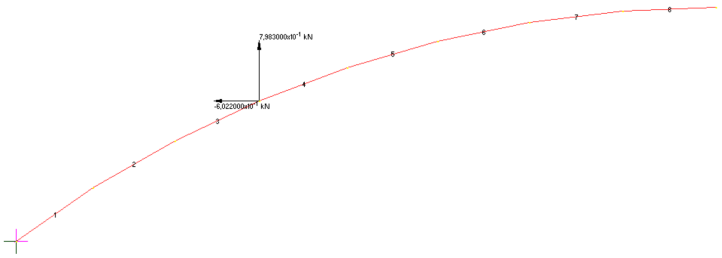

Figure 40: Decompose Force T3

Coefficients:

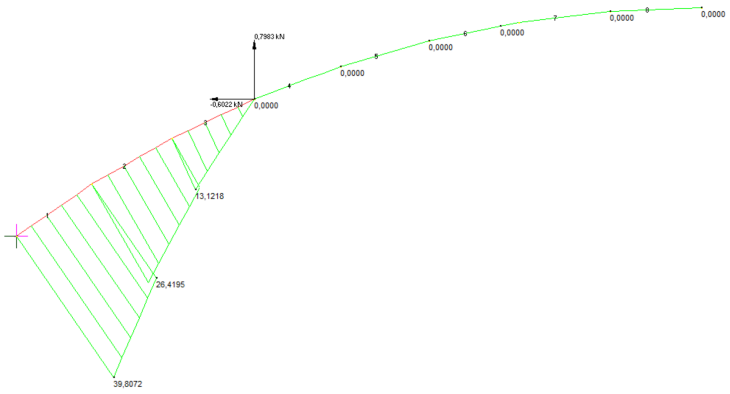

Figure 41: Coefficients Product From Force T3

Unitary Force in tieback 4 position:

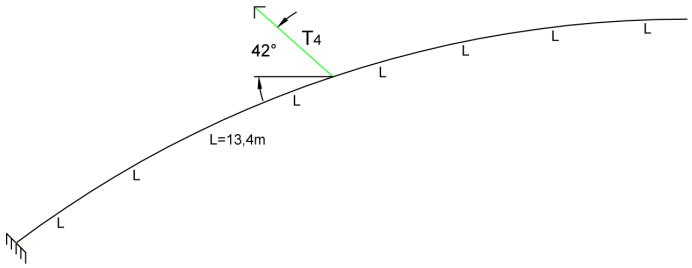

Figure 42: Unit Force T4

Decompose of the unitary force in tieback 4 position:

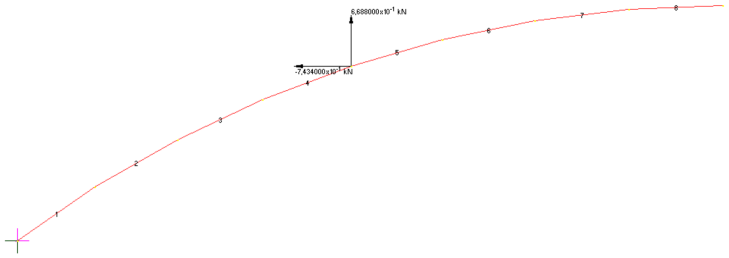

Figure 43: Decompose Force T4

Coefficients:

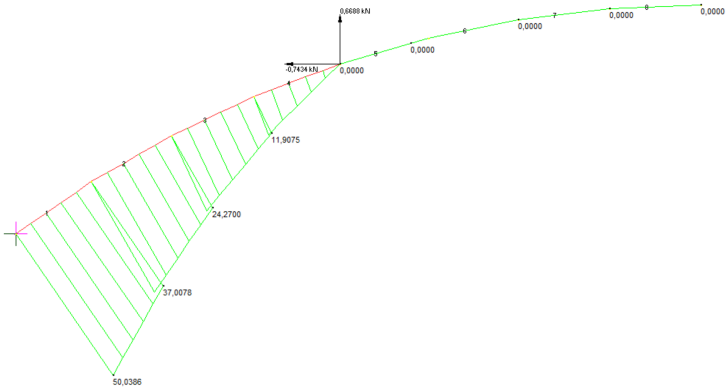

Figure 44: Coefficients Product From Force T4

Unitary Force in tieback 5 position:

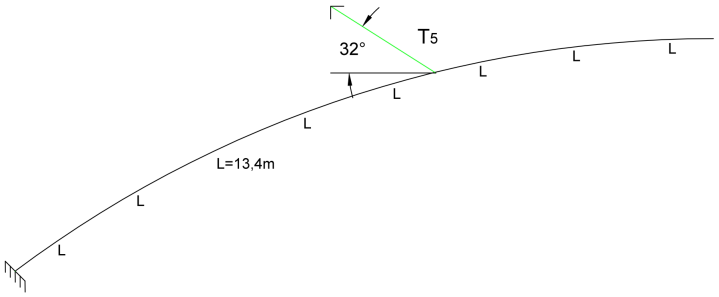

Figure 45: Unit Force T5

Decompose of the unitary force in tieback 5 position:

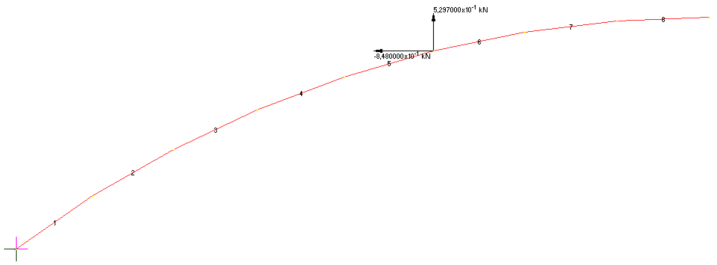

Figure 46: Decompose Force T5

Coefficients:

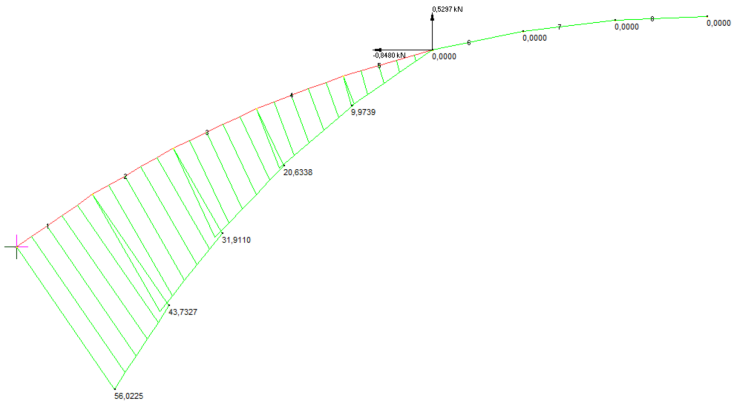

Figure 47: Coefficients Product From Force T5

Unitary Force in tieback 6 position:

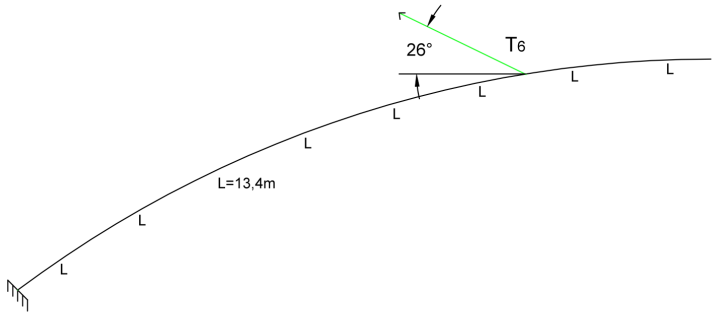

Figure 48: Unit Force T6

Decompose of the unitary force in tieback 6 position:

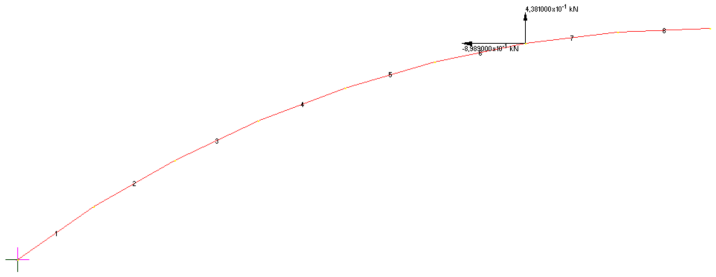

Figure 49: Decompose Force T6

Coefficients:

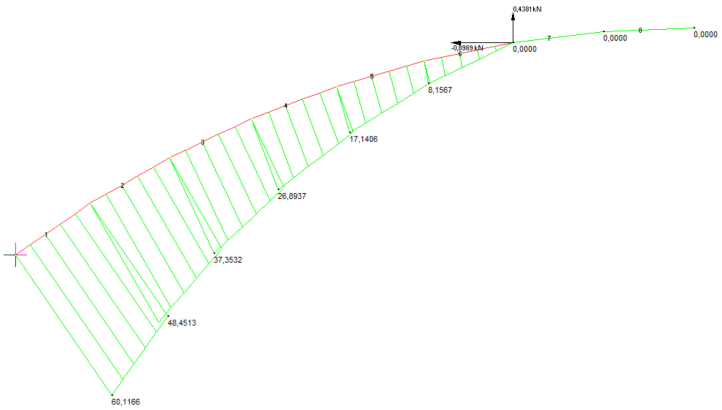

Figure 50: Coefficients Product From Force T6

Unitary Force in tieback 7 position:

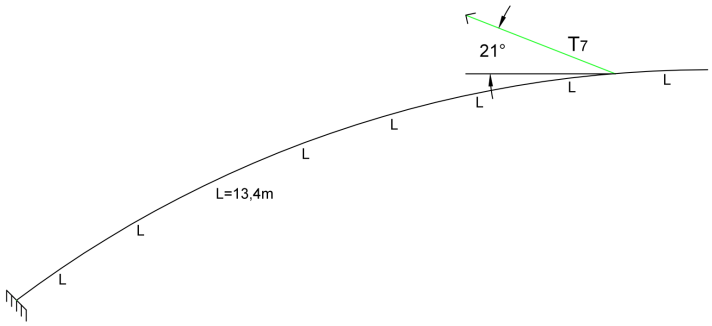

Figure 51: Unit Force T7

Decompose of the unitary force in tieback 7 position:

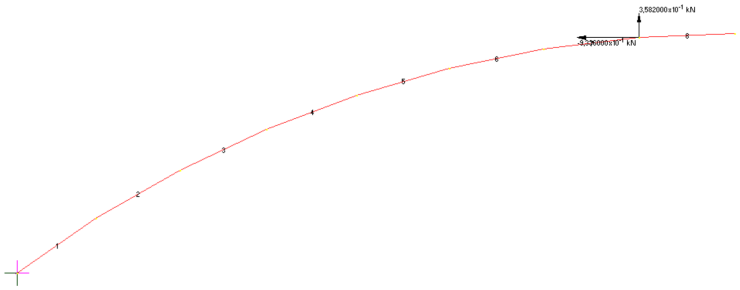

Figure 52: Decompose Force T7

Coefficients:

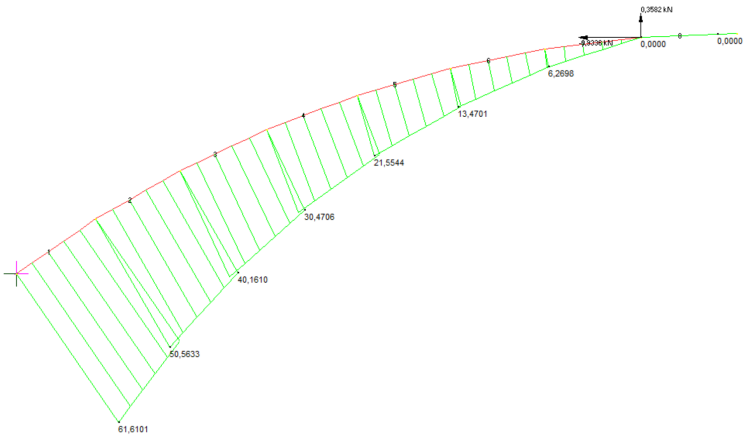

Figure 53: Coefficients Product From Force T7

And finally, this is the contribution of the Bending Moment products by the self weight:

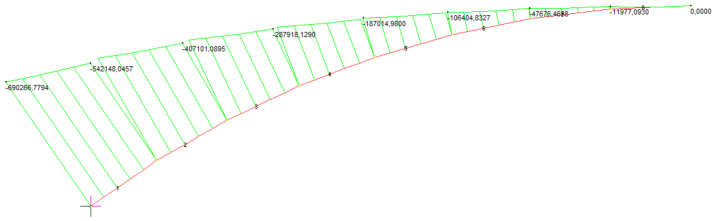

Figure 54: Self Weight Bending Moment' s Contribution

Considering the equation 27 this is the matrix containing influence coefficents:

```
A =

   12.2901   26.4368   39.8072   50.0386   56.0225   60.1166   61.6101
    6.1451   19.8706   33.1133   43.5232   49.8776   54.2840   56.0867
         0   13.3045   26.4195   37.0078   43.7327   48.4513   50.5633
         0    6.6522   19.7706   30.6389   37.8218   42.9022   45.3622
         0         0   13.3045   24.2700   28.6737   37.3532   40.1610
         0         0    6.6522   18.0888   26.2724   32.1234   35.3158
         0         0         0   11.9075   20.6338   26.8937   30.4706
         0         0         0    5.9537   15.3038   22.0172   26.0125
         0         0         0         0    9.9739   17.1406   21.5544
         0         0         0         0    4.9869   12.6486   17.5122
         0         0         0         0         0    8.1567   13.4701
         0         0         0         0         0    4.0783    9.8688
         0         0         0         0         0         0    6.2698
         0         0         0         0         0         0    3.1349
```

Figure 55: Influence Coefficients' Matrix A

And this is the contribution of the Self Weight's Bending Moment:

```
B =

   1.0e+05 *

   -6.9027
   -6.1384
   -5.4215
   -4.7213
   -4.0710
   -3.4491
   -2.8792
   -2.3478
   -1.8701
   -1.4395
   -1.0640
   -0.7422
   -0.4768
   -0.2697
```

Figure 56: Bending Moment' s Contribution

The vectonr $B = M_G$ in matlab.

Applying now the algorithm 34 is possible to calculate the values of optimized T expressed in the section 6.1.1:

```
T =

   1.0e+03 *

    0.9268
    0.1615
    1.0468
    1.2276
    1.3043
    0.5560
    7.5381
```

Figure 57: Optimized T

Conforming with all was established in the section 6.1.2 pretensions N^o are now evaluated.
First of all, an other influence coefficients' matrix must be calculated, the one explained in the equation 37.

In the following pictures is showed how these coefficients have been calculated:

A force $F = 1$ has been applied to the tieback 1:

And this is the corresponding influence coefficients:

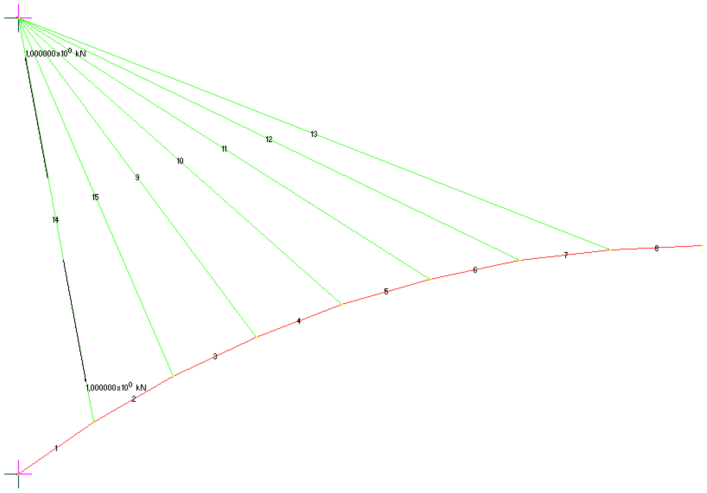

Figure 58: Unitary Pretension Applied into the Tieback 1

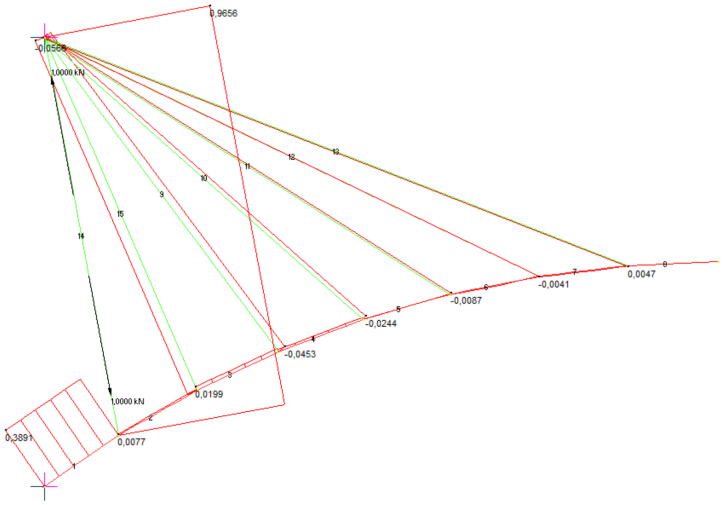

Figure 59: Coefficients Given by Tieback 1

A force $F = 1$ has been applied to the tieback 2:

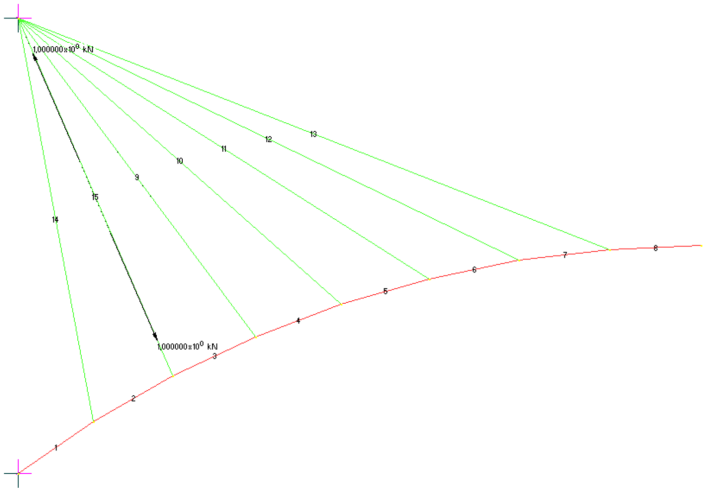

Figure 60: Unitary Pretension Applied into the Tieback 2

A force $F = 1$ has been applied to the tieback 3:

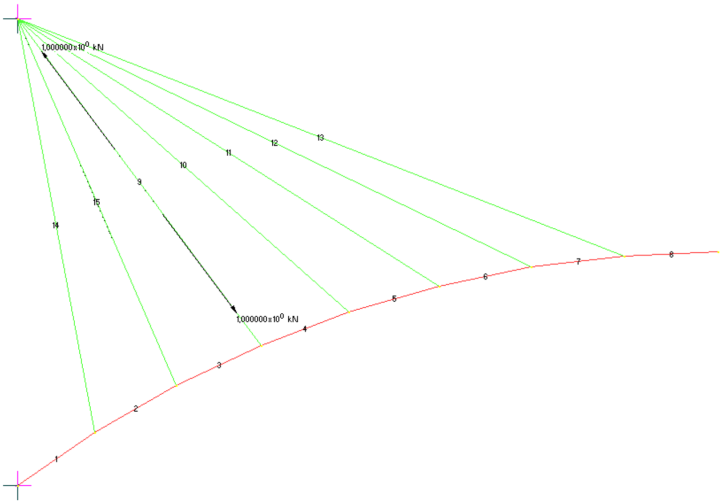

Figure 61: Unitary Pretension Applied into the Tieback 3

A force $F = 1$ has been applied to the tieback 4:

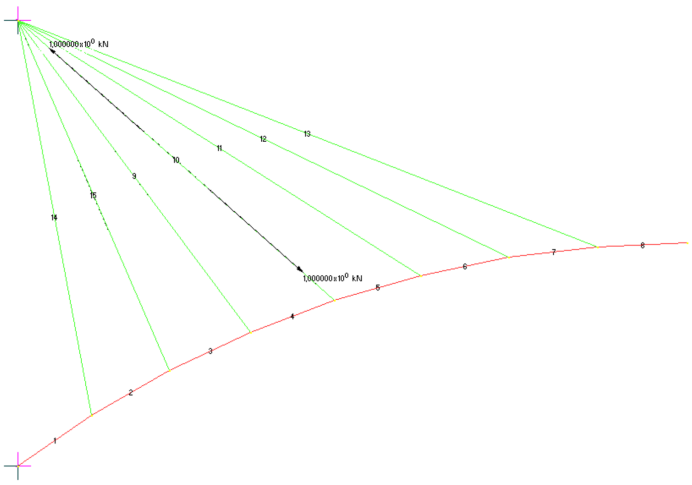

Figure 62: Unitary Pretension Applied into the Tieback 4

A force $F = 1$ has been applied to the tieback 5:

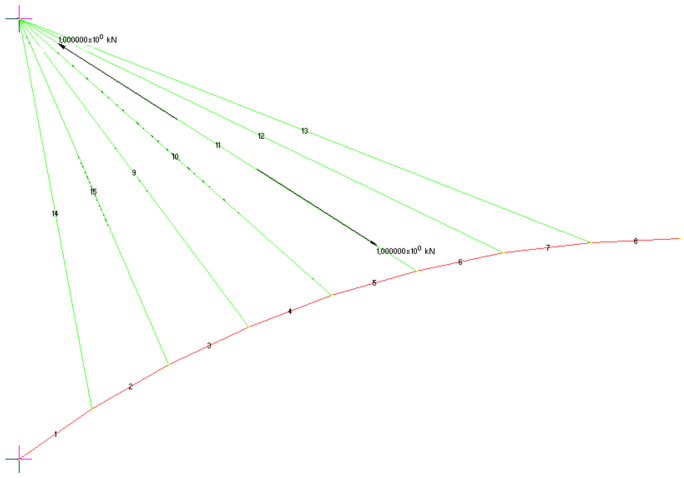

Figure 63: Unitary Pretension Applied into the Tieback 5

A force $F = 1$ has been applied to the tieback 6:

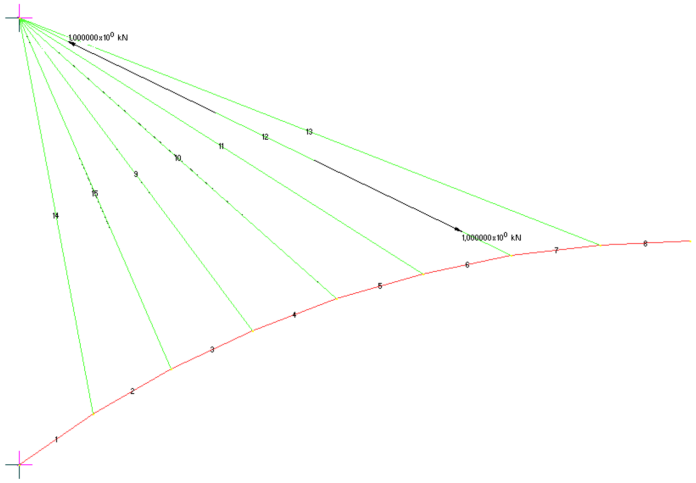

Figure 64: Unitary Pretension Applied into the Tieback 6

A force $F = 1$ has been applied to the tieback 7:

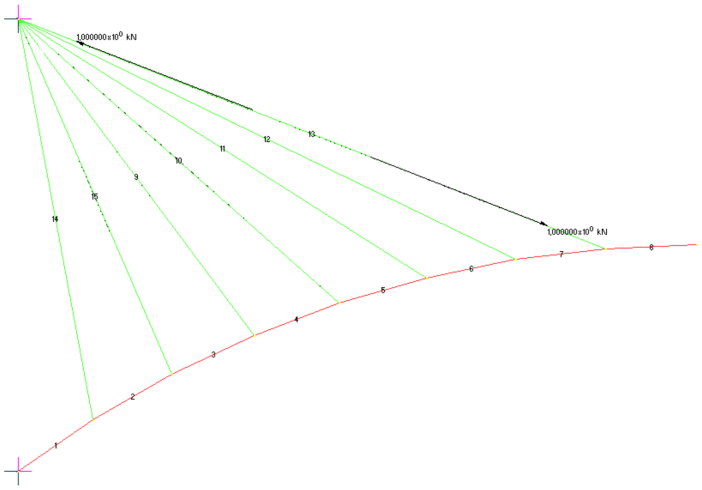

Figure 65: Unitary Pretension Applied into the Tieback 7

In the following picture is showed the value of matrix D:

```
D =

    0.9656   -0.0538   -0.0439   -0.0257   -0.0103    0.0003    0.0072
   -0.0566    0.8494   -0.1563   -0.1075   -0.0554   -0.0162    0.0105
   -0.0453   -0.1533    0.7655   -0.2071   -0.1367   -0.0734   -0.0278
   -0.0244   -0.0970   -0.1906    0.7567   -0.2148   -0.1626   -0.1195
   -0.0087   -0.0444   -0.1115   -0.1904    0.7578   -0.2450   -0.2335
    0.0002   -0.0113   -0.0524   -0.1261   -0.2143    0.7120   -0.3293
    0.0047    0.0064   -0.0174   -0.0811   -0.1789   -0.2884    0.6170
```

Figure 66: Matrix D

And this is the value of the static axial response in the cables:

N_G
$92,95$
$413,52$
$1025,22$
$1828,39$
$2591,52$
$3128,54$
$3379,11$

Table 4: Static Axial Forces in Tiebacks

And this is the vector $T - N_g$ in Matlab called E:

Appling the equation 6.1.2 is possible to deduce the values of pretensions N^o called F in Matlab:

Those values N^o must be applied to cables in the Straus7's Model, in this way is possible to let tiebacks' Axial Forces be the value desumed from the equation 34.

This is a table summarizing the values evaluated in this section.

```
E =

   1.0e+03 *

    0.8338
   -0.2520
    0.0216
   -0.6008
   -1.2872
   -2.5725
    4.1590
```

Figure 67: Vector T-Ng

```
F =

   1.0e+03 *

    0.8871
    0.0317
    0.8519
    1.0000
    1.0769
    0.3593
    7.3692
```

Figure 68: Pretensions N^o

Tieback Number	T $[kN]$	N_g $[kN]$	E $[kN]$	N_o $[kN]$
T1	$926,80$	$92,95$	$833,85$	$887,1$
T2	$161,50$	$413,52$	$-252,02$	$31,7$
T3	$1046,80$	$1025,22$	$21,58$	$851,9$
T4	$1227,60$	$1828,39$	$-600,79$	$1000,0$
T5	$1304,30$	$2591,52$	$-1287,22$	$1076,9$
T6	$556,00$	$3128,54$	$-2572,54$	$359,3$
T7	$7538,10$	$3379,11$	$4158,99$	$7369,2$

Table 5: Optimization Results' Summary

Finally is possible to apply the values of the pretensions N_o to the model; the Bending Moment diagram produced is the optimized one (Picture 69).

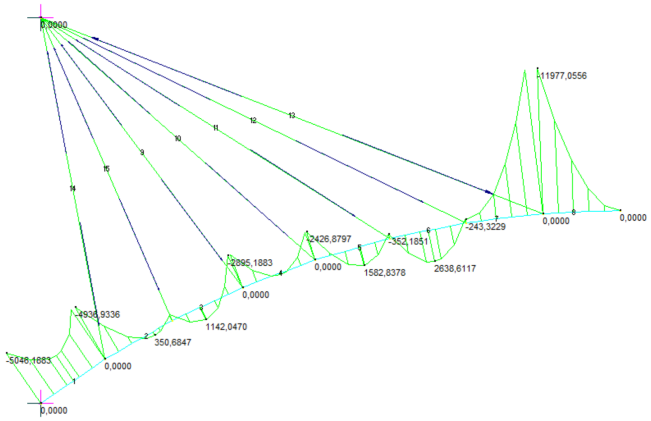

Figure 69: Closing Arch Configuration

Back Destruction It is important now evaluate how is the Bending Moment distribution variating when step by step we proceed in back destruction.
The starter configuration is the one showed in the picture 69.

The section number S8 [Fig. 31] has been deleted in the Step 1:

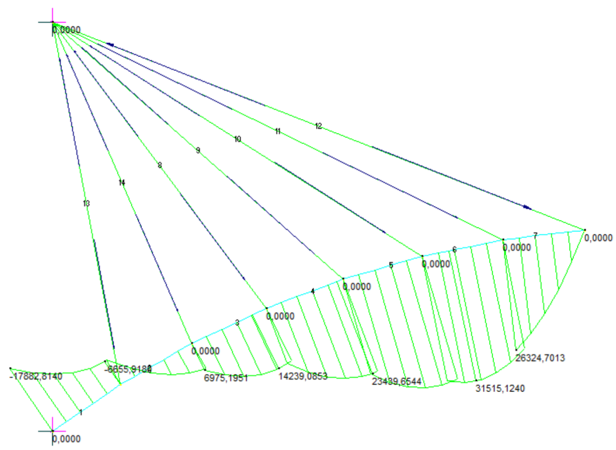

Figure 70: Section 8 Deleted

The tieback number T7 [Fig. 31] has been deleted in the Step 2:

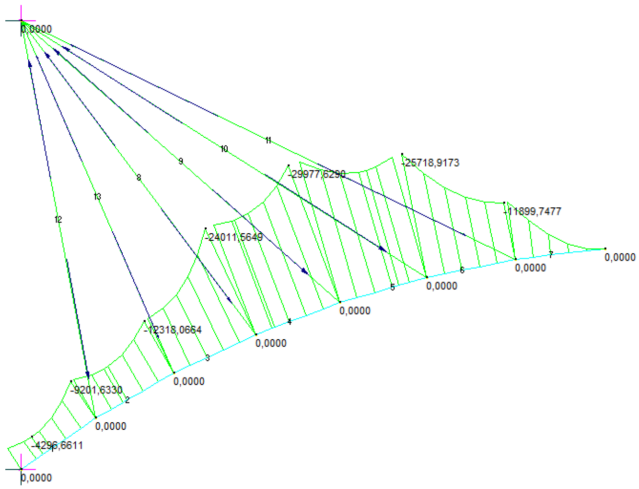

Figure 71: Tieback 7 Deleted

The section number S7 [Fig. 31] has been deleted in the Step 3:

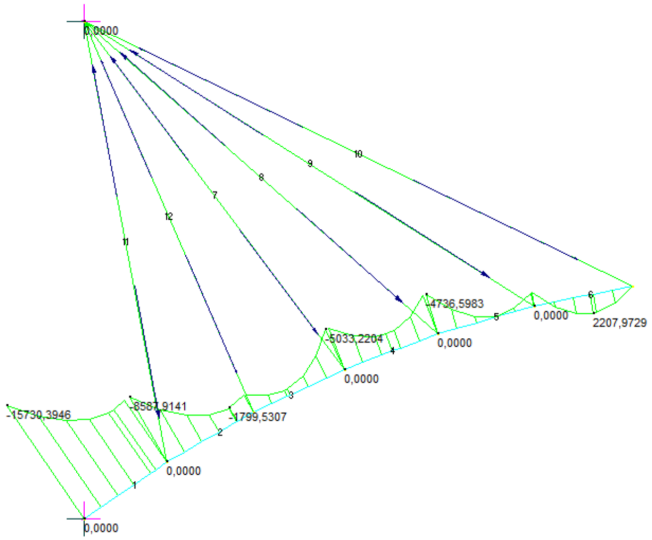

Figure 72: Section 7 Deleted

The tieback number T6 [Fig. 31] has been deleted in the Step 4:

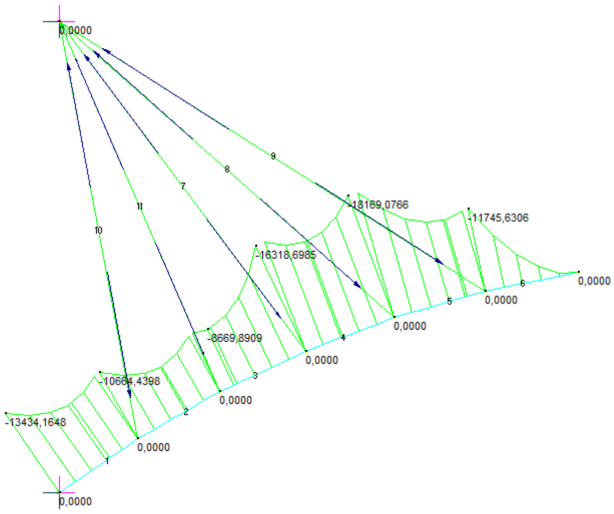

Figure 73: Tieback 6 Deleted

The section number S6 [Fig. 31] has been deleted in the Step 5:

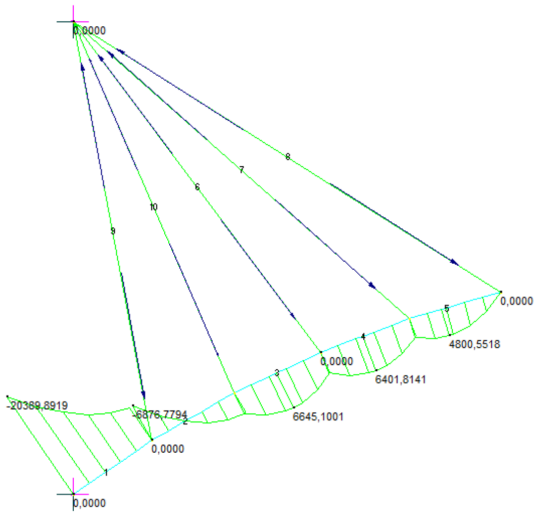

Figure 74: Section 6 Deleted

The tieback number T5 [Fig. 31] has been deleted in the Step 6:

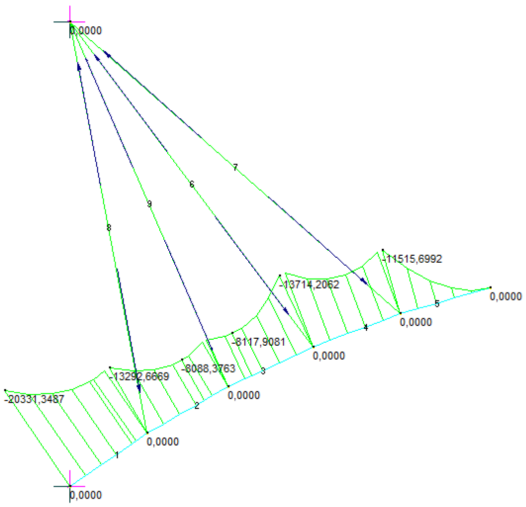

Figure 75: Tieback 5 Deleted

The section number S5 [Fig. 31] has been deleted in the Step 7:

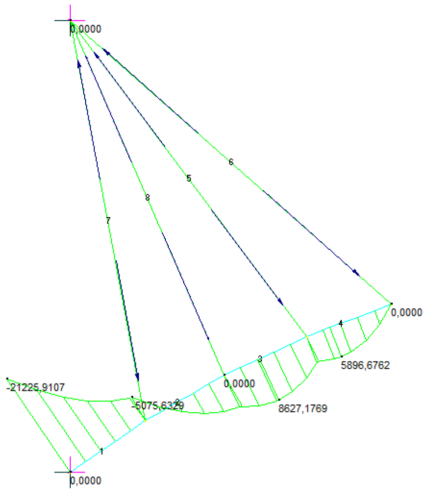

Figure 76: Section 5 Deleted

The tieback number T4 [Fig. 31] has been deleted in the Step 8:

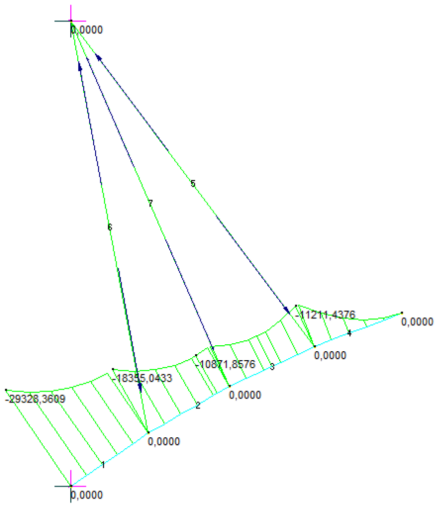

Figure 77: Tieback 4 Deleted

The section number S4 [Fig. 31] has been deleted in the Step 9:

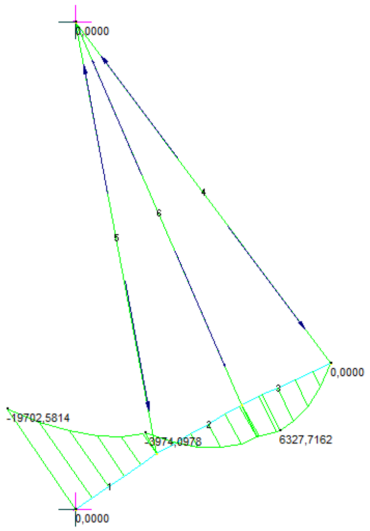

Figure 78: Section 4 Deleted

The tieback number T3 [Fig. 31] has been deleted in the Step 10:

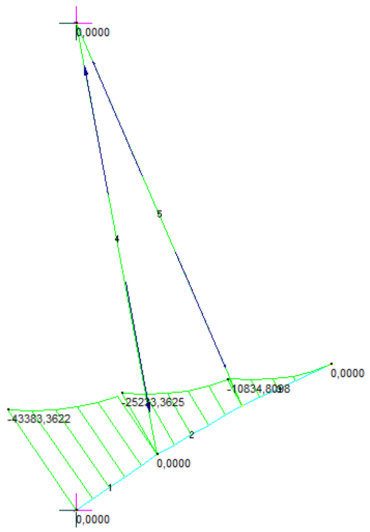

Figure 79: Tieback 3 Deleted

The section number S3 [Fig. 31] has been deleted in the Step 11:

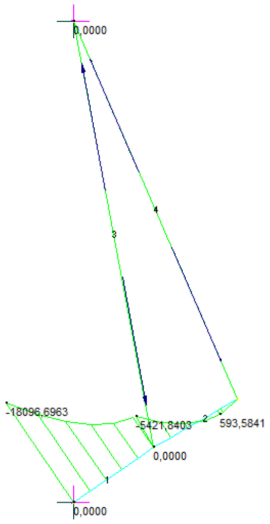

Figure 80: Section 3 Deleted

The tieback number T2 [Fig. 31] has been deleted in the Step 12:

Figure 81: Tieback 2 Deleted

The section number S2 [Fig. 31] has been deleted in the Step 13:

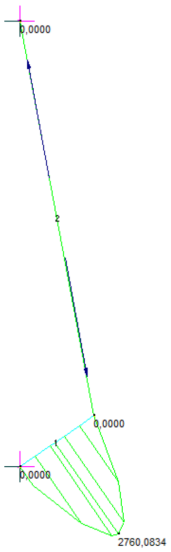

Figure 82: Section 2 Deleted

In all the process of back destruction the Maximum values of the Bending Moment are:

Step Number	M^+ $[kNm]$	M^- $[kNm]$
1	31515,124	-
10	-	-43383,3622

Table 6: Maximum Moments

6.2.2 Variable Distribution - VD

An other concept can be developed focus the attention on the fact that the angle along the emiarch is varying, for better say, the angle is decreasing from 33°(i.e. abutment) to 0°(i.e. midspan), like is shown in the picture [83]

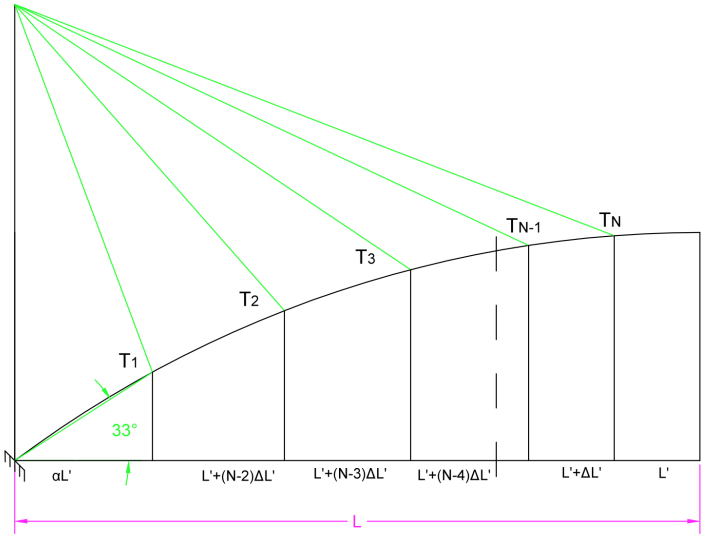

Figure 83: Angle Decreasing

Let's introduce a coefficent α like the increment of L', where L' in this case is the lenght of the last segment in projection, as it's easy to understand from the picture number 83.

Considering the first segment αL$'$ showed in the picture [83] and the last segment is L' it is possible develope a function for interpolation:

If we consider L the value of the lenght of the midspan known and invariable, N is the number of segments and α can be any.

It ensures that the lenght of the last segment L' is equal to:

$$L' = \frac{2L}{N(1+\alpha)} \tag{41}$$

And so the increment will be:

$$\Delta \text{Ł}' = \frac{L'(\alpha - 1)}{N - 1} \tag{42}$$

For differents values of α is possible to have a different distribution of tiebacks from the configuration analyzied in the section 6.2.1. In particular way, is possible to increase the lenght of the span $\alpha l'$ close to the abutment reducing the concentration of tiebacks in that zone and thicken the one next to the middspan. In this new configuration the Maximum Bending Moment will be less heavy.

And now, in the same way was made in the paragraph 6.2.1 pretensions N^o must be calculated.

Case in which $\alpha = 1,2$ and N=8 Let's evaluate differents situations, this one in particular has an $\alpha = 1,2$ and a number of segments N=8.

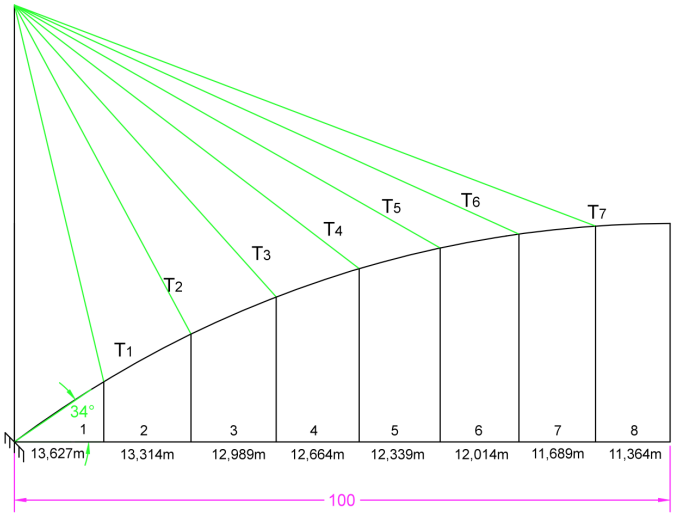

Figure 84: N=8 $\alpha = 1,2$

The last segment is:

$L' = \frac{2*100}{8(1+1,2)} = 11,364m$

The increment is:

$\Delta L' = \frac{11,364(1,2-1)}{8-1} = 0,325m$

In the picture 84 is showed the following configuration.

It is now useful apply the TOA and analyze the Bending Moment Diagram.

Now, appling the same procedure explained in the paragraph 6.2.1 is possible to evaluate the Bending Moment's Diagram:

Considering the equation 27 this is the matrix containing influence coefficents:

15.3416	31.4930	44.4582	52.7202	58.0759	60.2134	62.4386
7.6708	23.3227	36.3201	44.9519	50.6877	53.2450	55.7099
0	15.1523	28.1819	37.1835	43.2995	46.2766	48.9812
0	7.5762	20.8093	30.2847	36.8300	40.2588	43.2140
0	0	11.0579	23.3859	30.3605	34.2409	37.4468
0	0	5.5290	17.2219	24.6629	29.0180	32.4818
0	0	0	11.0579	18.9653	23.7951	27.5169
0	0	0	5.5290	13.9314	19.2528	23.2375
0	0	0	0	8.8974	14.7100	18.9582
0	0	0	0	4.4487	10.7661	15.2800
0	0	0	0	0	6.8218	11.6019
0	0	0	0	0	3.4109	8.4591
0	0	0	0	0	0	5.3164
0	0	0	0	0	0	2.6582

Figure 85: Influence Coefficients' Matrix in VD case $\alpha = 1, 2$

And finally, this is the contribution of the Self Weight Bending Moment products by the self weight:

```
1.0e+05 *

-6.9036
-5.9674
-5.1029
-4.3313
-3.6244
-3.0009
-2.4363
-1.9464
-1.5108
-1.1422
-0.8240
-0.5662
-0.3554
-0.1988
```

Figure 86: Self Weight Bending Moment' s Contribution in VD case $\alpha = 1, 2$

Applying now the algorithm 34 is possible to calculate the values of optimized T expressed in the section 6.1.1:

```
T =

   1.0e+03 *

    0.9386
    0.5411
    0.9726
    1.2623
    1.7450
    0.4589
    6.7130
```

Figure 87: Optimized T in VD case $\alpha = 1, 2$

And now, in the same way was made in the paragraph 6.2.1 pretensions N^o must be calculated.

In the following picture is showed the value of the matrix D:

```
D =

    0.9427   -0.0786   -0.0570   -0.0307   -0.0112    0.0017    0.0101
   -0.0814    0.8054   -0.1836   -0.1199   -0.0617   -0.0198    0.0086
   -0.0563   -0.1748    0.7537   -0.2097   -0.1422   -0.0852   -0.0446
   -0.0274   -0.1031   -0.1895    0.7683   -0.2089   -0.1705   -0.1392
   -0.0089   -0.0470   -0.1138   -0.1850    0.7693   -0.2397   -0.2375
    0.0012   -0.0133   -0.0603   -0.1335   -0.2121    0.7253   -0.3120
    0.0063    0.0052   -0.0281   -0.0972   -0.1872   -0.2780    0.6472
```

Figure 88: Matrix D in VD case $\alpha = 1, 2$

And this is the value of the static axial response in the cables:

And this is the vector $T - N_g$:

It is important to emphasize in this case that the value of the pretension N_7^o is negative, it means that i need to apply a "pre-detension".
Appling the equation 6.1.2 is possible to deduce the values of pretensions N^o:

N_i
$153,307$
$598,8755$
$1265,751$
$1960,67$
$2512,176$
$1851,458$
$2989,544$

Table 7: Static Axial Forces in Tiebacks in AF case $\alpha = 1, 2$

```
E =

   1.0e+03 *

    0.7853
   -0.0578
   -0.2931
   -0.6984
   -0.7672
   -2.3926
    3.7235
```

Figure 89: Vector T-Ng in VD case $\alpha = 1, 2$

```
F =

   1.0e+03 *

    0.8186
    0.1161
    0.2571
    0.3847
    0.8197
   -0.4458
    5.8588
```

Figure 90: Pretensions N^o in VD case $\alpha = 1, 2$

Those values N^o must be applied to cables in the Straus7's Model, in this way is possible to let tiebacks' Axial Forces be the value desumed from the equation 34.

This is a table summarizing the values evaluated in this section.

Tieback Number	$T\ [kN]$	$N_g\ [kN]$	$T - N_g\ [kN]$	$N^o\ [kN]$
T1	$938,60$	$153,307$	$785,29$	$818,6$
T2	$541,10$	$598,87$	$-57,78,$	$116,1$
T3	$972,60$	$1265,75$	$-293,15$	$257,1$
T4	$1262,30$	$1960,67$	$-698,37$	$384,7$
T5	$1745,00$	$2512,176$	$-767,18$	$819,7$
T6	$458,90$	$2851,458$	$-2392,56$	$-445,8$
T7	$6713,00$	$2989,54$	$3723,46$	$5858,8$

Table 8: Optimization Results' Summary in VD case $\alpha = 1,2$

Finally is possible to apply the values of the pretensions N_o to the model; the Bending Moment diagram produced is the optimized one (Picture **??**).

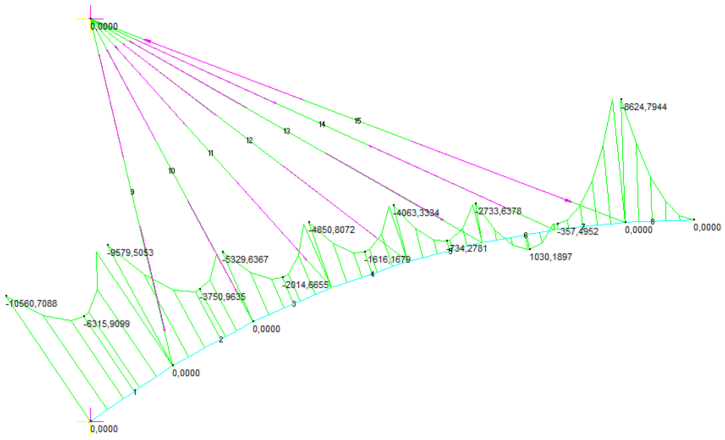

Figure 91: Closing Arch Configuration in VD case $\alpha = 1,2$

Comparing this Bending Moment diagram with the one in the picture 69 it's underline that the Maximum Moment in the Closing Arch Configuration has been reduced comparing with the one in the picture 69.

Precisely in this table are summarized the values of the Maximum Positive and Negative Bending Moment:

Configuration	M^+ $[kNm]$	M^- $[kNm]$
Standard Configuration	2638	-11977
AF $\alpha = 1,2$	981,68	-10828,03

Table 9: Maximum Moments in VD case $\alpha = 1,2$ Closing Arch Configuration

Back Destruction It is important now evaluate how is the Bending Moment distribution variating when step by step we proceed in back destruction in the same way has been done in the section 6.2.1.
The starter configuration is the one showed in the picture 112.

The section number S8 [Fig. 31] has been deleted in the Step 1:

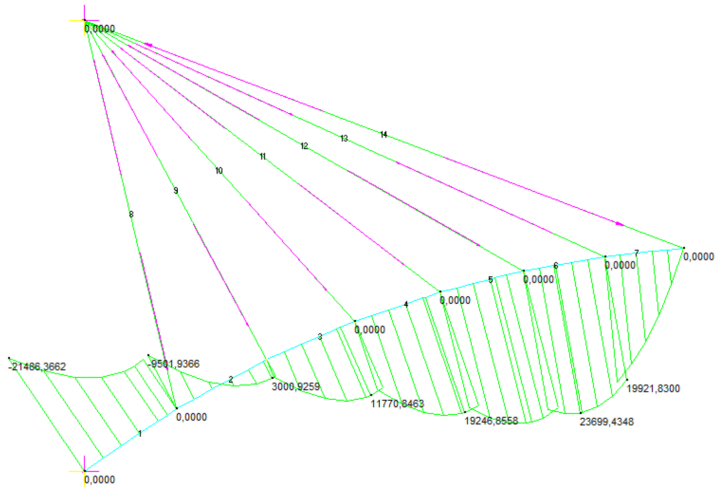

Figure 92: Section 8 Deleted in VD case $\alpha = 1,2$

The tieback number T7 [Fig. 31] has been deleted in the Step 2:

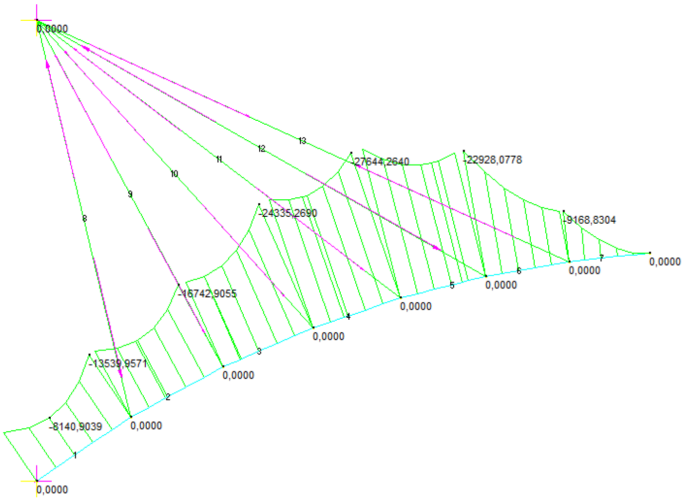

Figure 93: Tieback 7 Deleted in VD case $\alpha = 1, 2$

The section number S7 [Fig. 31] has been deleted in the Step 3:

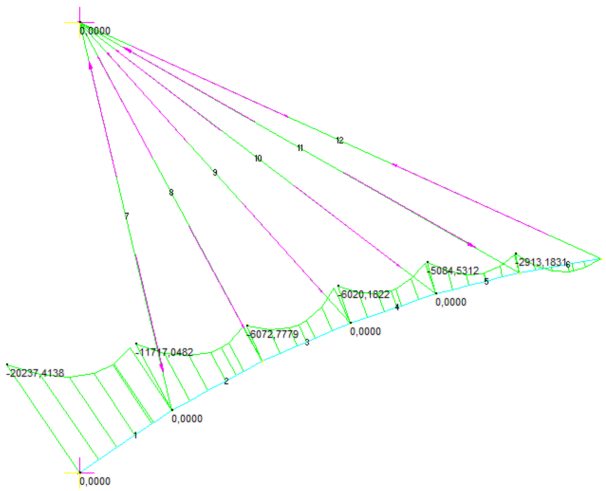

Figure 94: Section 7 Deleted in VD case $\alpha = 1, 2$

The tieback number T6 [Fig. 31] has been deleted in the Step 4:

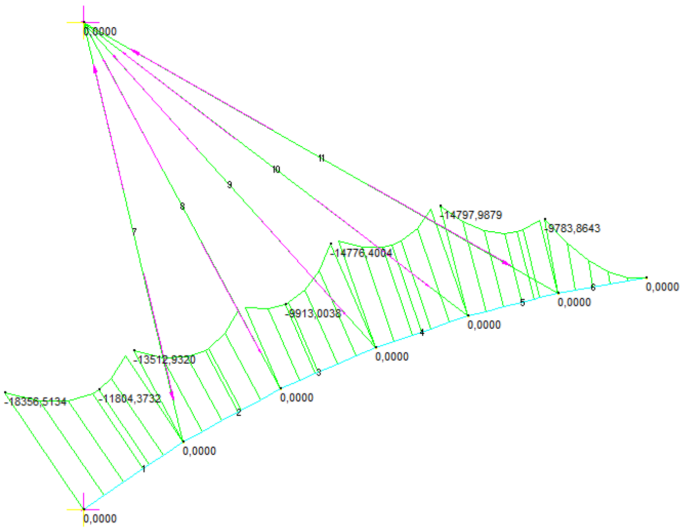

Figure 95: Tieback 6 Deleted in VD case $\alpha = 1, 2$

The section number S6 [Fig. 31] has been deleted in the Step 5:

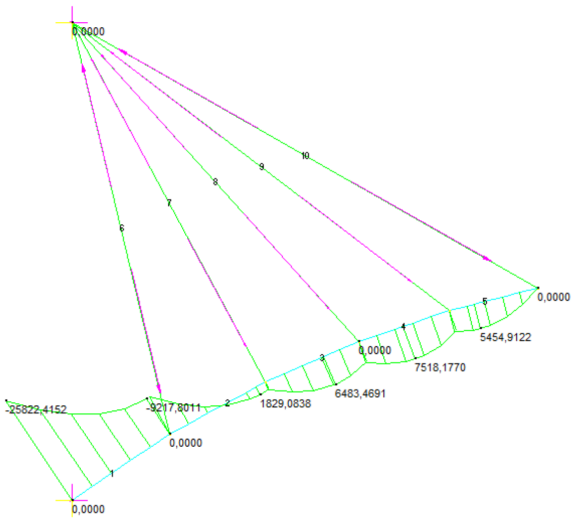

Figure 96: Section 6 Deleted in VD case $\alpha = 1, 2$

The tieback number T5 [Fig. 31] has been deleted in the Step 6:

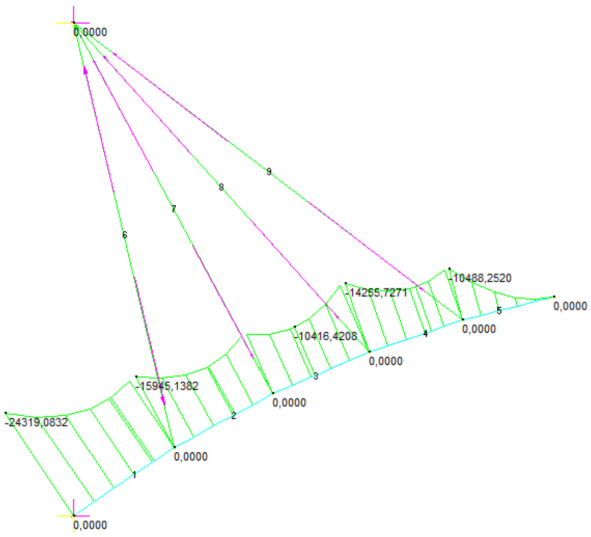

Figure 97: Tieback 5 Deleted in VD case $\alpha = 1,2$

The section number S5 [Fig. 31] has been deleted in the Step 7:

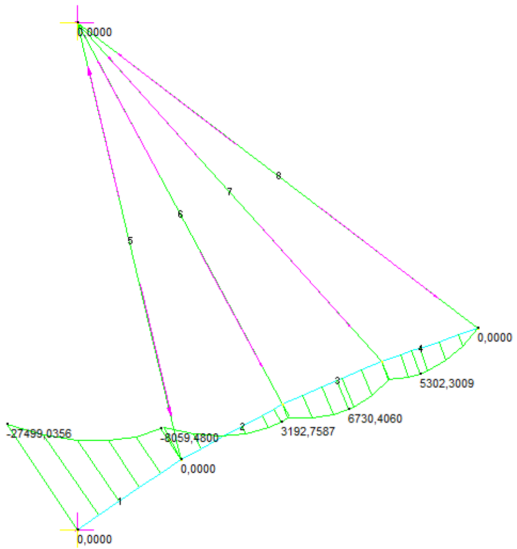

Figure 98: Section 5 Deleted in VD case $\alpha = 1, 2$

The tieback number T4 [Fig. 31] has been deleted in the Step 8:

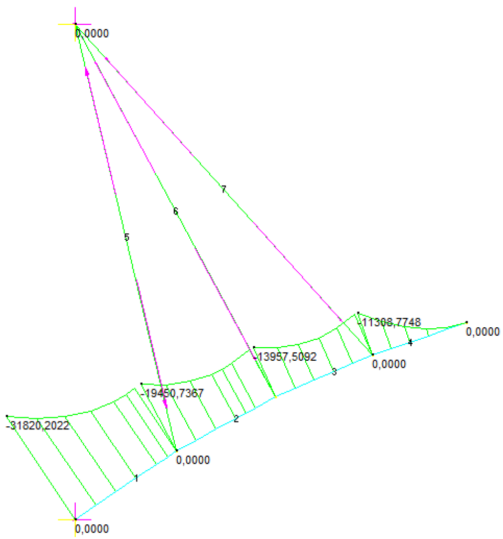

Figure 99: Tieback 4 Deleted in VD case $\alpha = 1,2$

The section number S4 [Fig. 31] has been deleted in the Step 9:

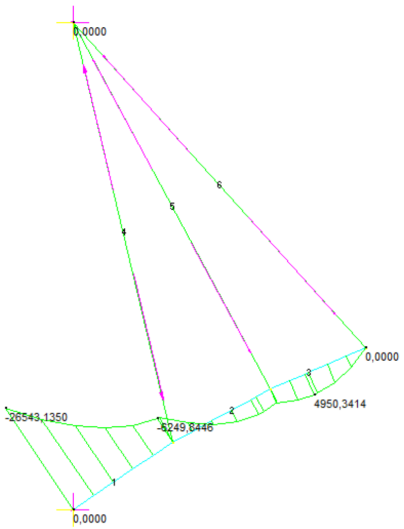

Figure 100: Section 4 Deleted in VD case $\alpha = 1, 2$

The tieback number T3 [Fig. 31] has been deleted in the Step 10:

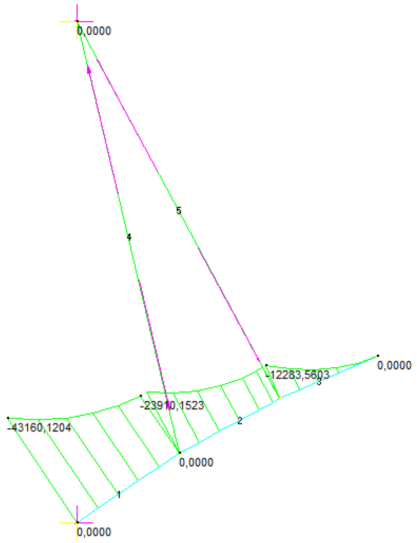

Figure 101: Tieback 3 Deleted in VD case $\alpha = 1,2$

The section number S3 [Fig. 31] has been deleted in the Step 11:

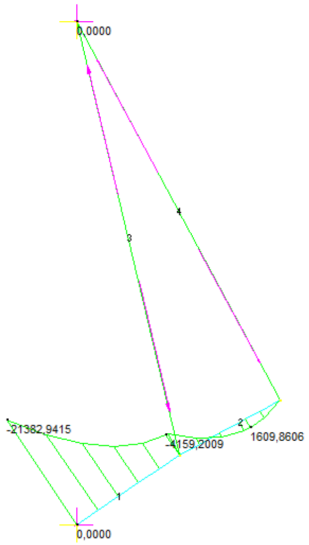

Figure 102: Section 3 Deleted in VD case $\alpha = 1, 2$

The tieback number T2 [Fig. 31] has been deleted in the Step 12:

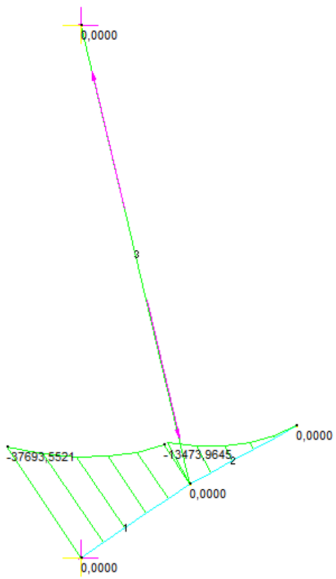

Figure 103: Tieback 2 Deleted in VD case $\alpha = 1,2$

The section number S2 [Fig. 31] has been deleted in the Step 13:

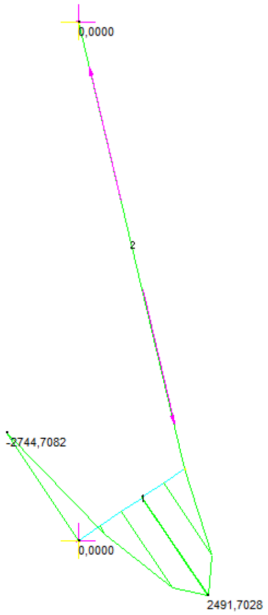

Figure 104: Section 2 Deleted in VD case $\alpha = 1, 2$

In all the process of back destruction the Maximum values of the Bending Moment are:

Step Number	M^+ $[kNm]$	M^- $[kNm]$
1	23699	-
10	-	-43160

Table 10: Maximum Moments Through the Back Destruction case $\alpha = 1, 2$

Case in which $\alpha = 1,5$ and N=8 The next case we are going to analyze is the one in which, $\alpha = 1,5$ and a number of segments N=8.

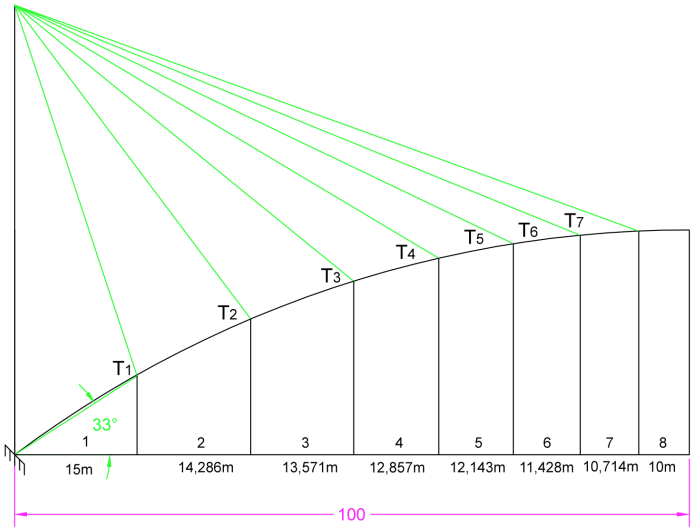

Figure 105: N=8 $\alpha = 1,5$

The last segment is:

$L' = \frac{2*100}{8(1+1,5)} = 10m$

The increment is:

$\Delta \text{Ł}' = \frac{10(1,5-1)}{8-1} = 0,714m$

In the picture 105 is showed the following configuration.

It is now useful apply the TOA and analyze the Bending Moment Diagram.

Now, appling the same procedure explained in the paragraph 6.2.1 is possible to evaluate the Bending Moment's Diagram:

Considering the equation 27 this is the matrix containing influence coefficents:

```
17.0650   34.1467   46.7094   54.4548   58.4632   61.4233   61.8874
 8.5325   25.1442   37.8719   46.0623   50.5307   53.8103   54.6274
      0   16.1417   29.0344   37.4548   42.5982   46.1973   47.3674
      0    8.0708   21.3083   30.4770   35.9059   39.8393   41.3703
      0         0   13.5822   23.2841   29.2137   33.4812   35.3733
      0         0    6.7911   17.0864   23.5413   28.1500   30.4047
      0         0         0   10.8888   17.8688   22.8187   25.4361
      0         0         0    5.4444   12.9554   18.2445   21.2187
      0         0         0         0    8.0420   13.6703   17.0013
      0         0         0         0    4.0210    9.9910   13.6766
      0         0         0         0         0    6.3117   10.3520
      0         0         0         0         0    3.1558    7.5386
      0         0         0         0         0         0    4.7253
      0         0         0         0         0         0    2.3626
```

Figure 106: Influence Coefficients' Matrix in VD case $\alpha = 1,5$

And finally, this is the contribution of the Self Weight Bending Moment products by the self weight:

```
1.0e+05 *

-6.9059
-5.8793
-4.9392
-4.1287
-3.3922
-2.7653
-2.2022
-1.7318
-1.3173
-0.9806
-0.6923
-0.4685
-0.2870
-0.1584
```

Figure 107: Self Weight Bending Moment' s Contribution in VD case $\alpha = 1,5$

Applying now the algorithm 34 is possible to calculate the values of optimized T expressed in the section 6.1.1:

```
1.0e+03 *

  0.8431
  0.8222
  1.1747
  0.8783
  2.0470
  0.7869
  6.0772
```

Figure 108: Optimized T in VD case $\alpha = 1,5$

And now, in the same way was made in the paragraph 6.2.1 pretensions N^o must be calculated.

In the following picture is showed the value of the matrix D:

```
  0.9282   -0.0924   -0.0632   -0.0322   -0.0112    0.0025    0.0117
 -0.0948    0.7830   -0.1956   -0.1234   -0.0642   -0.0222    0.0066
 -0.0607   -0.1832    0.7506   -0.2082   -0.1444   -0.0919   -0.0543
 -0.0277   -0.1036   -0.1866    0.7742   -0.2073   -0.1760   -0.1505
 -0.0085   -0.0476   -0.1144   -0.1832    0.7749   -0.2362   -0.2375
  0.0017   -0.0146   -0.0648   -0.1385   -0.2103    0.7333   -0.3014
  0.0071    0.0039   -0.0345   -0.1067   -0.1905   -0.2715    0.6627
```

Figure 109: Matrix D in VD case $\alpha = 1,5$

And this is the value of the static axial response in the cables:

N_i
$201,47$
$725,43$
$1397,90$
$2021,79$
$2441,68$
$2682,20$
$2774,04$

Table 11: Static Axial Forces in Tiebacks in VD case $\alpha = 1,5$

And this is the vector $T - N_g$:

```
1.0e+03 *

 0.6416
 0.0968
-0.2232
-1.1435
-0.3947
-1.8953
 3.3032
```

Figure 110: Vector T-Ng in VD case $\alpha = 1,5$

Appling the equation 6.1.2 is possible to deduce the values of pretensions N^o:

```
1.0e+03 *

 0.7798
 0.6318
 0.8839
 0.5496
 1.7257
 0.4881
 5.8029
```

Figure 111: Pretensions N^o in VD case $\alpha = 1,5$

Those values N^o must be applied to cables in the Straus7's Model, in this way is possible to let tiebacks' Axial Forces be the value desumed from the equation 34.

This is a table summarizing the values evaluated in this section.

Tieback Number	$T\ [kN]$	$N_g\ [kN]$	$T - N_g\ [kN]$	$N^o\ [kN]$
T1	$843,10$	$201,47$	$641,63$	$779,8$
T2	$822,20$	$725,43$	$96,77$	$631,8$
T3	$1174,70$	$1397,90$	$-223,20$	$883,9$
T4	$878,30$	$2021,79$	$-1143,50$	$549,6$
T5	$2047,00$	$2441,68$	$-394,68$	$1725,7$
T6	$786,90$	$2682,20$	$-1895,30$	$488,1$
T7	$6077,20$	$2774,04$	$3303,16$	$5802,9$

Table 12: Optimization Results' Summary in VD case $\alpha = 1,5$

Finally is possible to apply the values of the pretensions N_o to the model; the Bending Moment diagram produced is the optimized one (Picture **??**).

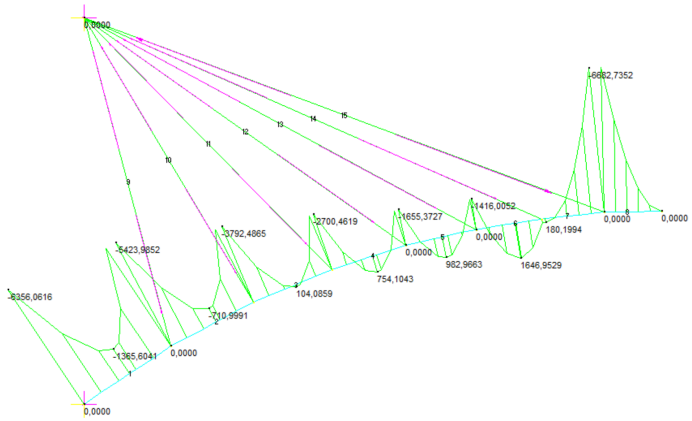

Figure 112: Closing Arch Configuration in VD case $\alpha = 1,5$

Comparing this Bending Moment diagram with the one in the picture 69 it's underline that the Maximum Moment in the Closing Arch Configuration has been reduced until become the middle of the one in the picture 69.

Precisely in this table are summerized the values of the Maximum Positive and Negative Bending Moment:

Configuration	M^+ $[kNm]$	M^- $[kNm]$
Standard Configuration	2638	-11977
AF $\alpha = 1,5$	1648	-6682,

Table 13: Maximum Moments in VD case $\alpha = 1,5$ Closing Arch Configuration

Back Destruction It is important now evaluate how is the Bending Moment distribution variating when step by step we proceed in back destruction in the same way has been done in the section 6.2.1.
The starter configuration is the one showed in the picture 112.

The section number S8 [Fig. 31] has been deleted in the Step 1:

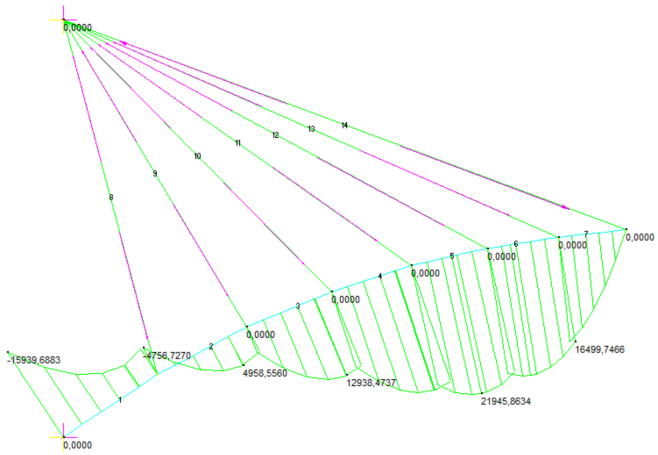

Figure 113: Section 8 Deleted in VD case $\alpha = 1,5$

The tieback number T7 [Fig. 31] has been deleted in the Step 2:

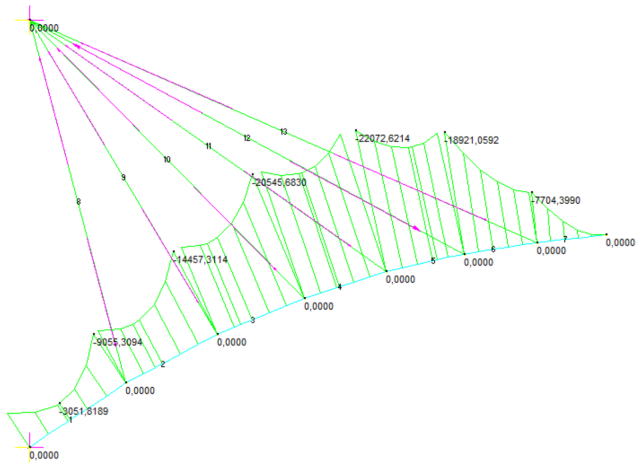

Figure 114: Tieback 7 Deleted in VD case $\alpha = 1,5$

The section number S7 [Fig. 31] has been deleted in the Step 3:

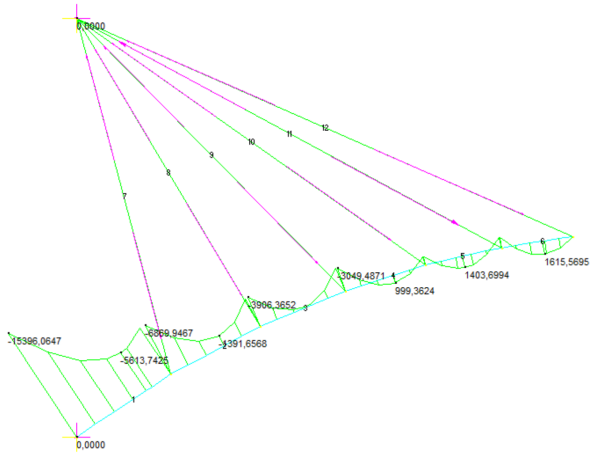

Figure 115: Section 7 Deleted in VD case $\alpha = 1,5$

The tieback number T6 [Fig. 31] has been deleted in the Step 4:

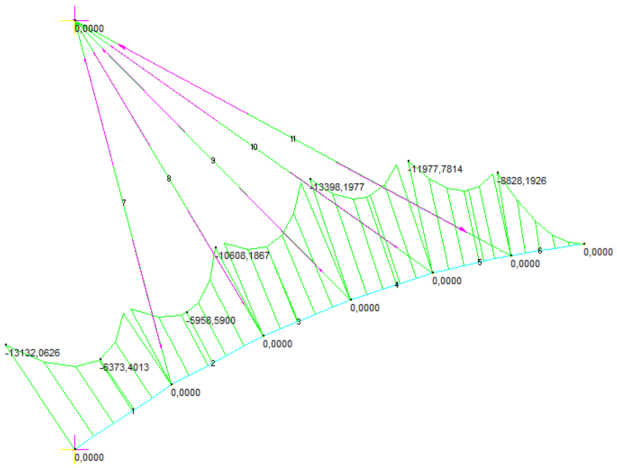

Figure 116: Tieback 6 Deleted in VD case $\alpha = 1,5$

The section number S6 [Fig. 31] has been deleted in the Step 5:

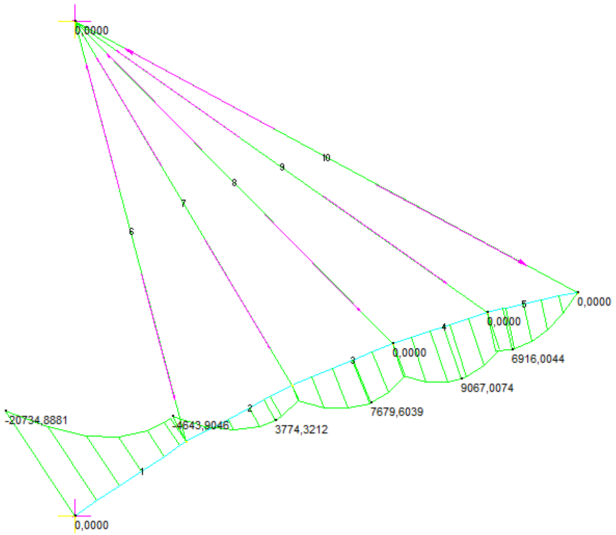

Figure 117: Section 6 Deleted in VD case $\alpha = 1,5$

The tieback number T5 [Fig. 31] has been deleted in the Step 6:

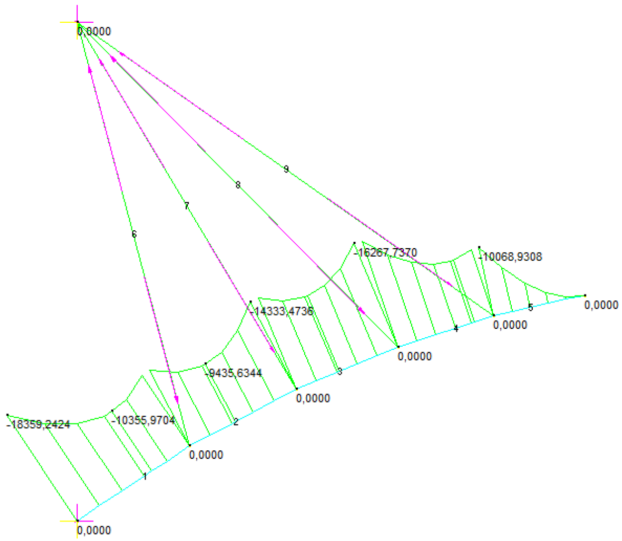

Figure 118: Tieback 5 Deleted in VD case $\alpha = 1,5$

The section number S5 [Fig. 31] has been deleted in the Step 7:

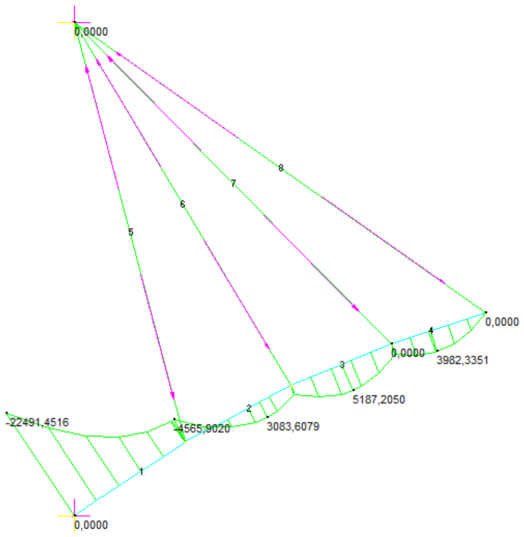

Figure 119: Section 5 Deleted in VD case $\alpha = 1,5$

The tieback number T4 [Fig. 31] has been deleted in the Step 8:

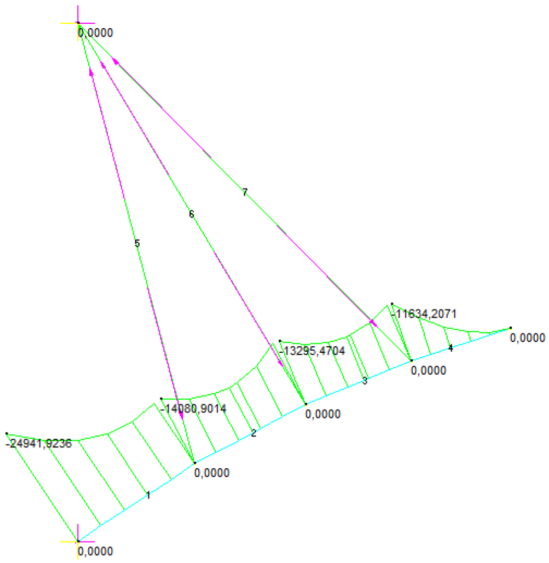

Figure 120: Tieback 4 Deleted in VD case $\alpha = 1,5$

The section number S4 [Fig. 31] has been deleted in the Step 9:

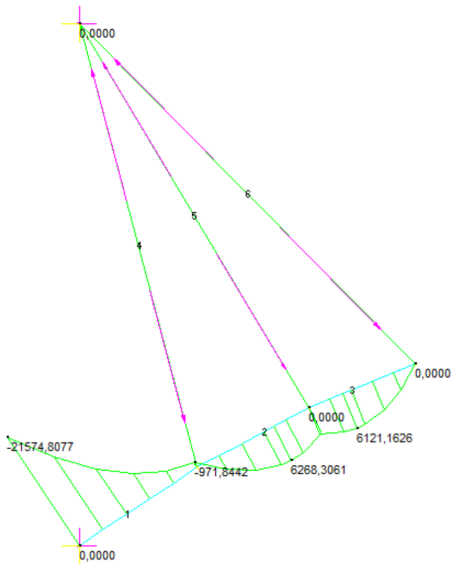

Figure 121: Section 4 Deleted in VD case $\alpha = 1,5$

The tieback number T3 [Fig. 31] has been deleted in the Step 10:

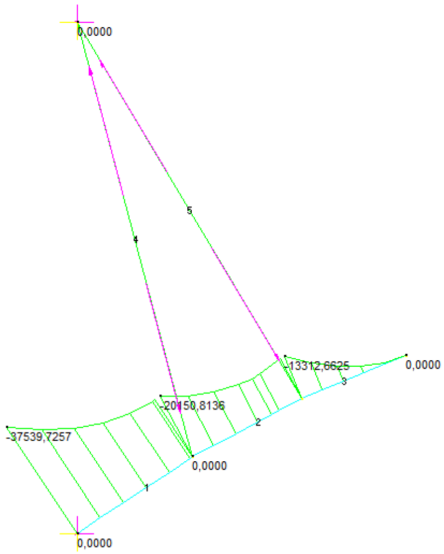

Figure 122: Tieback 3 Deleted in VD case $\alpha = 1,5$

The section number S3 [Fig. 31] has been deleted in the Step 11:

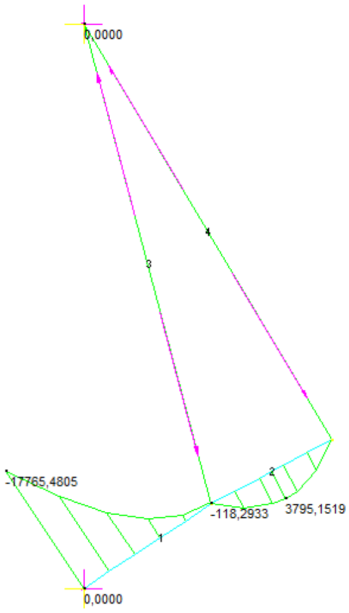

Figure 123: Section 3 Deleted in VD case $\alpha = 1,5$

The tieback number T2 [Fig. 31] has been deleted in the Step 12:

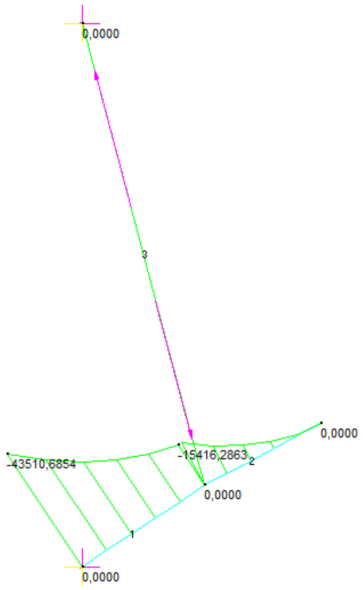

Figure 124: Tieback 2 Deleted in VD case $\alpha = 1,5$

The section number S2 [Fig. 31] has been deleted in the Step 13:

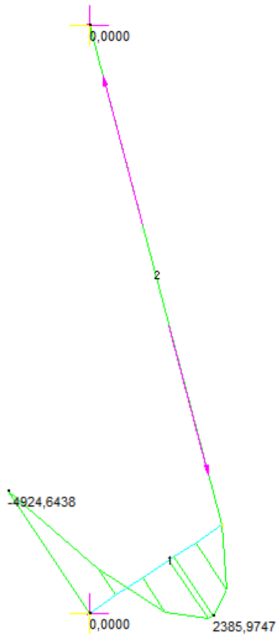

Figure 125: Section 2 Deleted in VD case $\alpha = 1,5$

In all the process of back destruction the Maximum values of the Bending Moment are:

Step Number	M^+ $[kNm]$	M^- $[kNm]$
1	21945	-
12	-	-43510

Table 14: Maximum Moments Through the Back Destruction

Case in which $\alpha = 1,8$ and N=8 The next case we are going to analyze is the one in which, $\alpha = 1,8$ and a number of segments N=8.

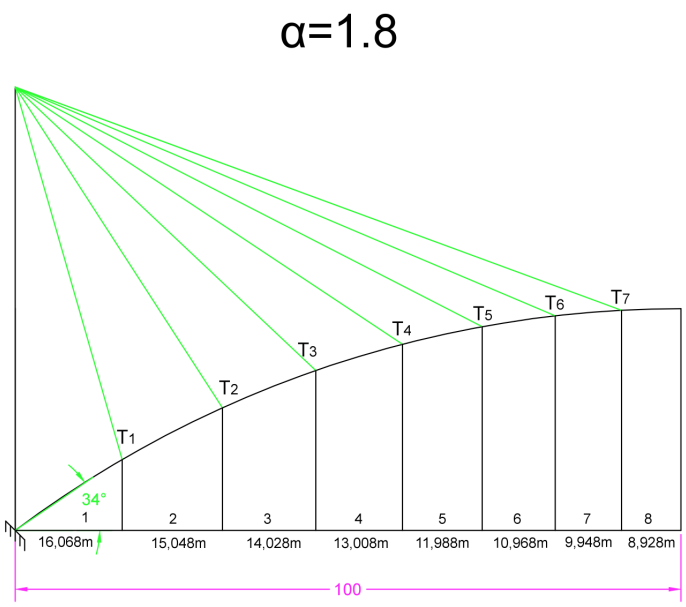

Figure 126: N=8 $\alpha = 1,8$

The last segment is:

$L' = \frac{2*100}{8(1+1,8)} = 8,928m$

The increment is:

$\Delta L' = \frac{10(1,8-1)}{8-1} = 1,02m$

In the picture 126 is showed the following configuration.

It is now useful apply the TOA and analyze the Bending Moment Diagram.

Now, appling the same procedure explained in the paragraph 6.2.1 is possible to evaluate the Bending Moment's Diagram:

Considering the equation 27 this is the matrix containing influence coefficents:

18.3970	36.1270	48.3630	55.7020	59.1230	61.2890	62.1910
9.1980	26.4840	38.9840	46.7910	50.7250	53.2520	54.4380
0	16.8420	29.6050	37.8790	42.3280	45.2140	46.6860
0	8.4210	21.6360	30.4540	35.4520	38.7080	40.4670
0	0	13.6660	23.0300	28.5770	32.2020	34.2480
0	0	6.8330	16.7850	22.8950	26.8870	29.2170
0	0	0	10.5390	17.2120	21.5720	24.1850
0	0	0	5.2700	12.5030	17.2220	20.1100
0	0	0	0	7.7939	12.8720	16.0340
0	0	0	0	3.8970	9.3200	12.7450
0	0	0	0	0	5.7690	9.4560
0	0	0	0	0	2.8840	6.8200
0	0	0	0	0	0	4.1830
0	0	0	0	0	0	2.0920

Figure 127: Influence Coefficients' Matrix in VD case $\alpha = 1,8$

And finally, this is the contribution of the Self Weight Bending Moment products by the self weight:

```
1.0e+05 *

-6.9049
-5.8078
-4.8102
-3.9715
-3.2144
-2.5866
-2.0267
-1.5723
-1.1746
-0.8618
-0.5962
-0.3977
-0.2381
-0.1298
```

Figure 128: Self Weight Bending Moment' s Contribution in VD case $\alpha = 1,8$

Applying now the algorithm 34 is possible to calculate the values of optimized T expressed in the section 6.1.1:

And now, in the same way was made in the paragraph 6.2.1 pretensions N^o must be calculated.

In the following picture is showed the value of the matrix D:

```
1.0e+03 *

 0.9078
 0.8872
 1.0930
 1.3152
 1.8699
 0.8309
 5.6703
```

Figure 129: Optimized T in VD case $\alpha = 1,8$

```
 0.9155   -0.1036   -0.0677   -0.0337   -0.0110    0.0033    0.0125
-0.1051    0.7670   -0.2032   -0.1270   -0.0656   -0.0240    0.0034
-0.0635   -0.1878    0.7500   -0.2078   -0.1455   -0.0968   -0.0635
-0.0281   -0.1044   -0.1847    0.7795   -0.2038   -0.1773   -0.1567
-0.0081   -0.0478   -0.1146   -0.1805    0.7781   -0.2349   -0.2387
 0.0022   -0.0156   -0.0682   -0.1405   -0.2102    0.7375   -0.2940
 0.0075    0.0020   -0.0406   -0.1127   -0.1939   -0.2669    0.6775
```

Figure 130: Matrix D in VD case $\alpha = 1,8$

And this is the value of the static axial response in the cables:

N_i
$243,297$
$831,715$
$1505,798$
$2049,884$
$2395,331$
$2564,199$
$2607,883$

Table 15: Static Axial Forces in Tiebacks in VD case $\alpha = 1,8$

And this is the vector $T - N_g$:

Appling the equation 6.1.2 is possible to deduce the values of pretensions N^o:

```
1.0e+03 *

 0.6645
 0.0555
-0.4128
-0.7347
-0.5254
-1.7333
 3.0624
```

Figure 131: Vector T-Ng in VD case $\alpha = 1,8$

```
1.0e+03 *

 0.7929
 0.5204
 0.5277
 0.6706
 1.2220
 0.2106
 5.0857
```

Figure 132: Pretensions N^o in VD case $\alpha = 1,8$

Those values N^o must be applied to cables in the Straus7's Model, in this way is possible to let tiebacks' Axial Forces be the value desumed from the equation 34.

This is a table summarizing the values evaluated in this section.

Tieback Number	$T\ [kN]$	$N_g\ [kN]$	$T - N_g\ [kN]$	$N^o\ [kN]$
T1	$907,80$	$243,297$	$664,50$	$792,9$
T2	$887,20$	$831,715$	$55,49$	$520,4$
T3	$1093,00$	$1505,798$	$-412,80$	$527,7$
T4	$1315,20$	$2049,884$	$-734,68$	$670,6$
T5	$1869,90$	$2395,331$	$-525,43$	$1222,0$
T6	$830,90$	$2564,199$	$-1733,30$	$210,6$
T7	$5670,30$	$2607,883$	$3062,42$	$5085,7$

Table 16: Optimization Results' Summary in VD case $\alpha = 1,8$

Finally is possible to apply the values of the pretensions N_o to the model; the Bending Moment diagram produced is the optimized one (Picture **??**).

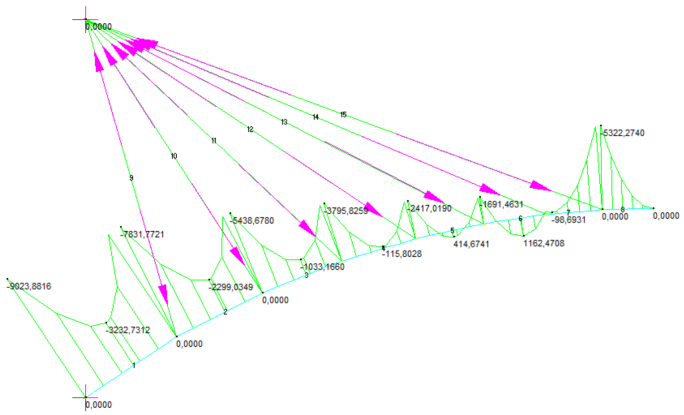

Figure 133: Closing Arch Configuration in VD case $\alpha = 1,8$

Comparing this Bending Moment diagram with the one in the picture 69 it's underline that the Maximum Moment in the Closing Arch Configuration has been reduced from the one in the picture 69.

Precisely in this table are summerized the values of the Maximum Positive and Negative Bending Moment:

Configuration	M^+ $[kNm]$	M^- $[kNm]$
Standard Configuration	2638	-11977
AF $\alpha = 1,8$	1162,47	-9023,88

Table 17: Maximum Moments in VD case $\alpha = 1,8$ Closing Arch Configuration

Back Destruction It is important now evaluate how is the Bending Moment distribution variating when step by step we proceed in back destruction in the same way has been done in the section 6.2.1.
The starter configuration is the one showed in the picture 112.

The section number S8 [Fig. 31] has been deleted in the Step 1:

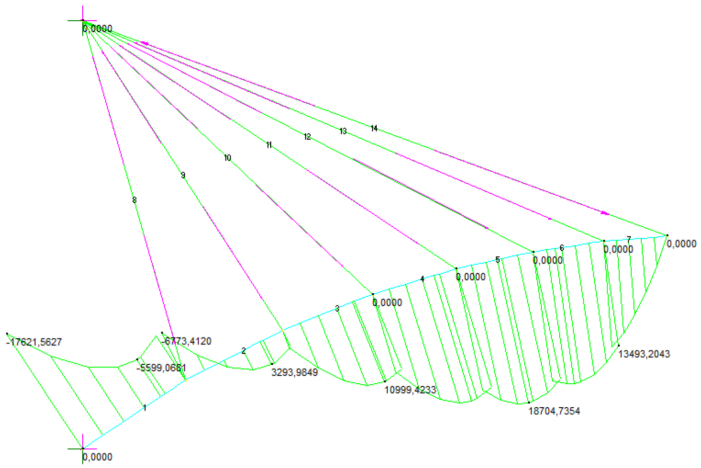

Figure 134: Section 8 Deleted in VD case $\alpha = 1,8$

The tieback number T7 [Fig. 31] has been deleted in the Step 2:

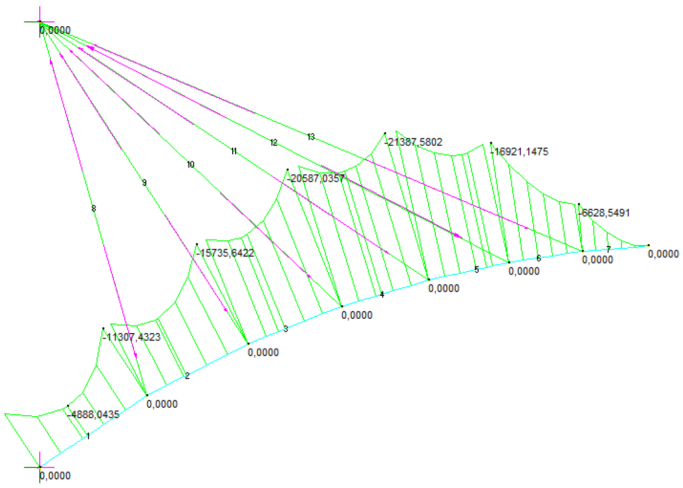

Figure 135: Tieback 7 Deleted in VD case $\alpha = 1,8$

The section number S7 [Fig. 31] has been deleted in the Step 3:

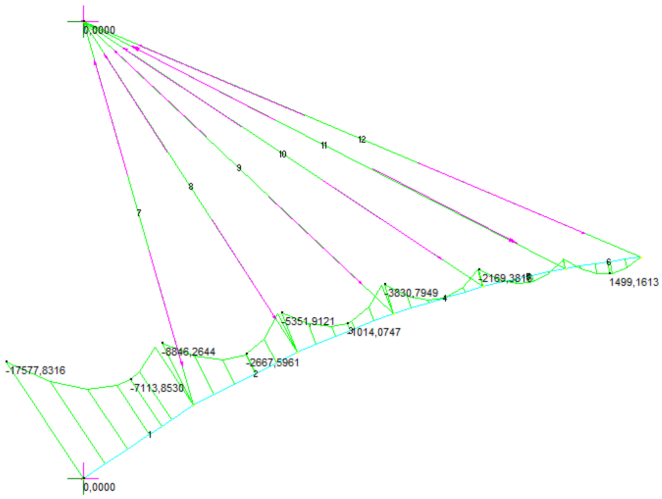

Figure 136: Section 7 Deleted in VD case $\alpha = 1,8$

The tieback number T6 [Fig. 31] has been deleted in the Step 4:

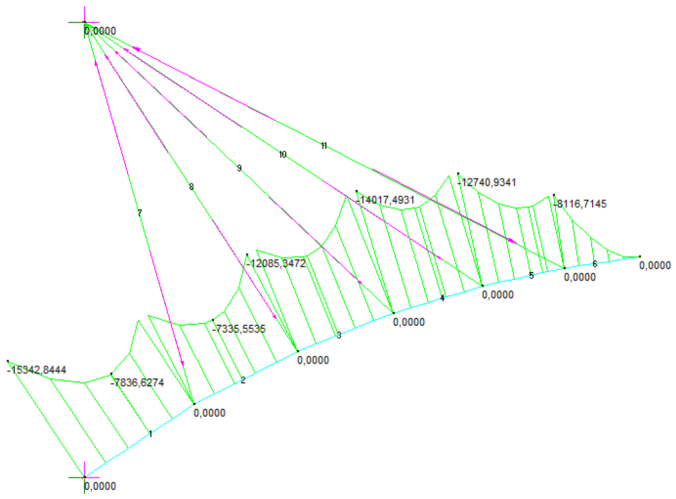

Figure 137: Tieback 6 Deleted in VD case $\alpha = 1,8$

The section number S6 [Fig. 31] has been deleted in the Step 5:

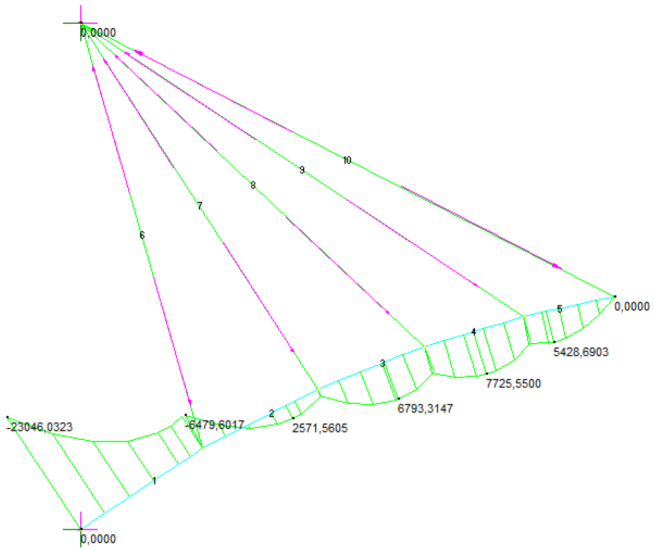

Figure 138: Section 6 Deleted in VD case $\alpha = 1,8$

The tieback number T5 [Fig. 31] has been deleted in the Step 6:

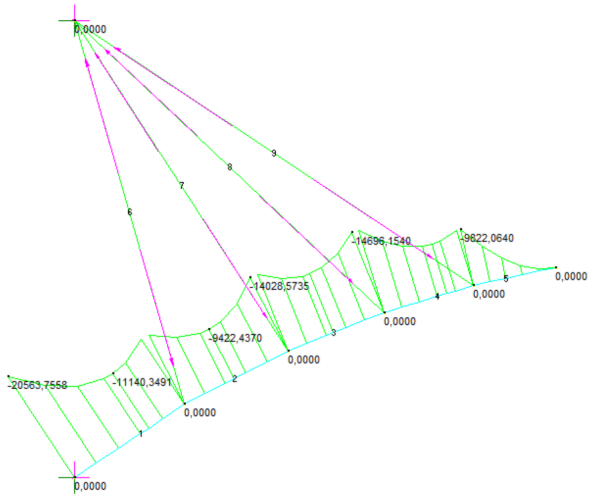

Figure 139: Tieback 5 Deleted in VD case $\alpha = 1,8$

The section number S5 [Fig. 31] has been deleted in the Step 7:

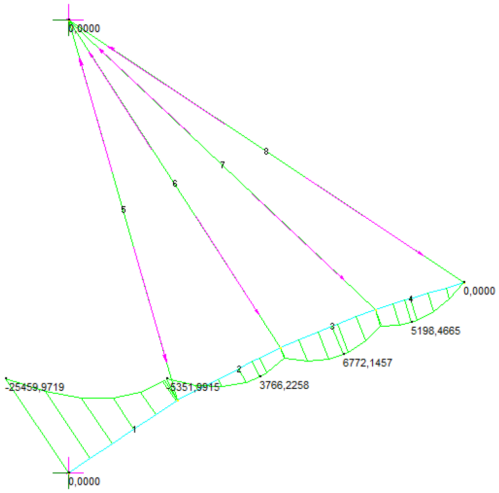

Figure 140: Section 5 Deleted in VD case $\alpha = 1,8$

The tieback number T4 [Fig. 31] has been deleted in the Step 8:

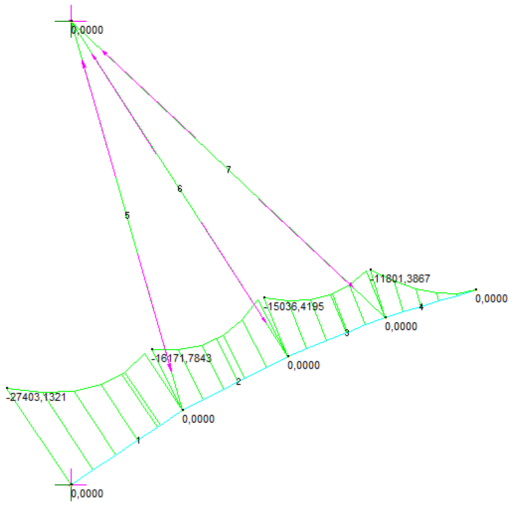

Figure 141: Tieback 4 Deleted in VD case $\alpha = 1,8$

The section number S4 [Fig. 31] has been deleted in the Step 9:

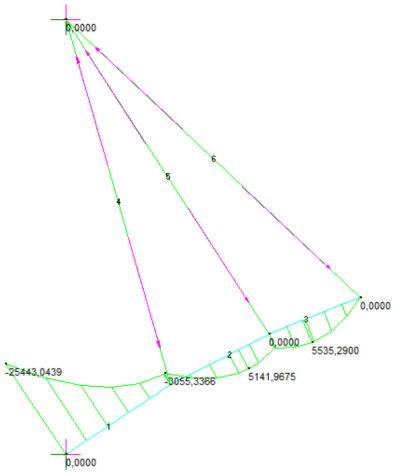

Figure 142: Section 4 Deleted in VD case $\alpha = 1,8$

The tieback number T3 [Fig. 31] has been deleted in the Step 10:

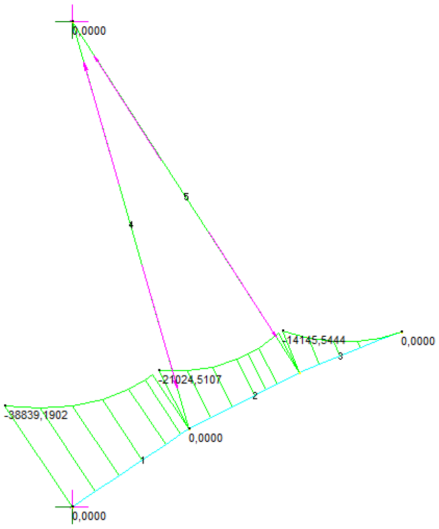

Figure 143: Tieback 3 Deleted in VD case $\alpha = 1,8$

The section number S3 [Fig. 31] has been deleted in the Step 11:

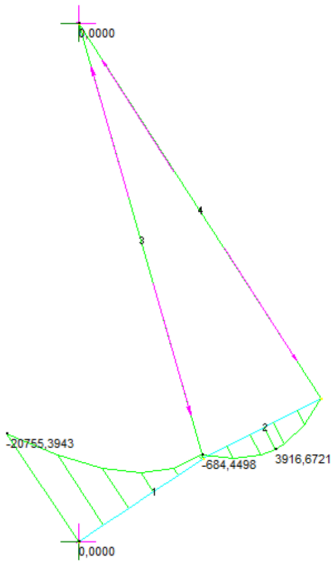

Figure 144: Section 3 Deleted in VD case $\alpha = 1,8$

The tieback number T2 [Fig. 31] has been deleted in the Step 12:

Figure 145: Tieback 2 Deleted in VD case $\alpha = 1,8$

The section number S2 [Fig. 31] has been deleted in the Step 13:

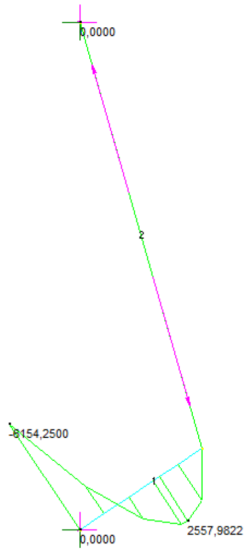

Figure 146: Section 2 Deleted in VD case $\alpha = 1,8$

In all the process of back destruction the Maximum values of the Bending Moment are:

Step Number	M^+ $[kNm]$	M^- $[kNm]$
1	18704,73	-
12	-	-47178,74

Table 18: Maximum Moments Through the Back Destruction case $\alpha = 1,8$

Comparison Among α Cases Analyzed In this table are summarized the maximum Bending Moments per each α.

α	M^+ $[kNm]$	M^- $[kNm]$
1,2	23699	-43160
1,5	21945	-43510
1,8	18704	-47178

Table 19: Comparison Among 3 different α in VD case

It is clear how the Variable Distribution is decreasing the bending moment, take in account an $\alpha = 1,2$ the minimum negative bending moment is obtained, otherwise what concern an $\alpha = 1,8$ the minimum positive bending moment is evaluated.

6.2.3 Moment's Redistribution

Once it is known the value T the value of the optimized tensions, and the back destruction have been perfomed, is possible to redistribuate the values of the bending moments along the emiarch.
The purpose is to deduce the number of tiebacks that redistribute the Bending Moment tensions.

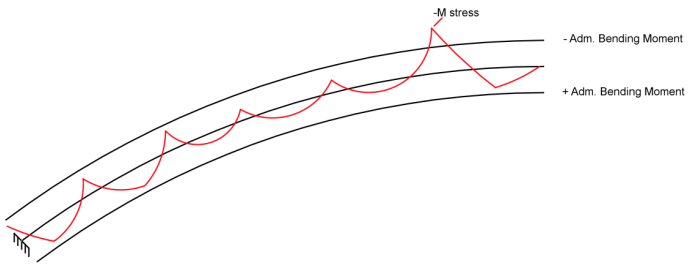

Figure 147: Sample of a Bending Moment Diagram in an Middlearch

Take in account the Bending Moment destribution in the picture 147 is simple to assert:

Defining η in the following way:

$$\eta = \frac{M_{stress}}{M_{adm}} \leq 1 \tag{43}$$

Where
M_{stress} is the Stress Bending Moment actually working into the arch,
M_{adm} is the Admissible Bending Moment from the section,
l' is the span we are proposing to reach,
l is the span we already evaluated in the section 6.2.1 (i.e. l=13,4m).

It is possible to write the relation

$$l'^2 = \eta l^2 \tag{44}$$

Consequentally it is possible to write

$$l' = \sqrt{\eta} l \tag{45}$$

And so

$$\frac{l'}{l} = \sqrt{\eta} \tag{46}$$

Remembering that N number of tiebacks analyzed in the paragraph 6.2.1 is inversely proportional to the span between two tiebacks l:

$$N \propto \frac{\alpha}{l} \tag{47}$$

So one can write recovering the equation 46 that:

$$\frac{N}{N'} = \sqrt{\eta} \tag{48}$$

And so remembering the equation 43

$$N' = N\sqrt{\frac{M_{stress}}{Madm}} \tag{49}$$

From the equation 49 is possible to evaluate the number of tiebacks can redistribute the Bending Moment M_{stress}.

Sample Case Recording the sample considered in the paragraph 6.2 let's calculate a new number of tiebacks N' that can redistribuate the Bending Moment M_{Stress}.

First of all we need to evaluate the Admissible Bending Moment M_{adm} taking into account the arch section analyzed in the paragraph 6.2 showed in the picture 148.

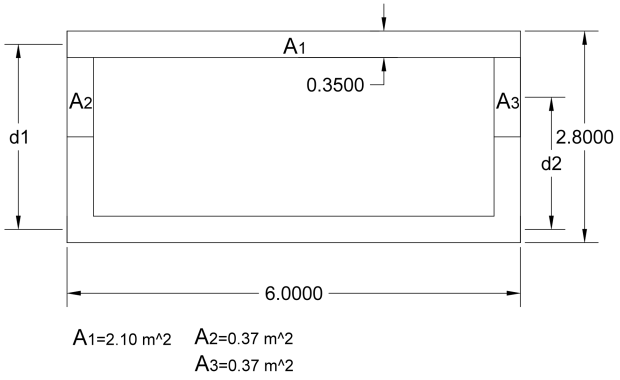

Figure 148: Arch's Section

The configuration from which we are going to start is the one showed in the picture 32.

The total Area interested in the calculus of the Admisible Bending Moment M_{adm} is equal to $A_{tot} = A_1 + A_2 + A_3$.

The Axial Forces interested are:

$$F_{c1} = \gamma_c f_{ck} A_1 \tag{50}$$

In this particular case $A_1 = 2450000mm^2$ and $A_2 = A_3 = 1750000mm^2$.

$$F_{c2} = F_{c3} = \gamma_c f_{ck} A_2 = \gamma_c f_{ck} A_3 \tag{51}$$

Where the safety factor is $\gamma_c = 0,85$ and the concrete $f_{ck} = 70MPa$.

The resultant of the Axial Concrete Force is:

$$F_c = F_{c1} + F_{c2} + F_{c3} = \gamma_c f_{ck} A_{tot} \tag{52}$$

And the Admisible Bending Moment is:

$$M_{adm} = F_{c1} d_1 + F_{c2} d_2 + F_{c3} d_2 \tag{53}$$

Where the values of the distance d_i is:
$d_1 = 2,45m$
$d_2 = 1,75m$

In this table are summarized all values concerning the previously calculus:

η	F_{c1} $[kN]$	F_{c2} $[kN]$	F_c $[kN]$	M_{adm} $[kNm]$	M_{stress} $[kNm]$
-	145775	208250	354025	721586	43383

Table 20: Moment's Redistribution Summary

6.3 Resultant Tieback

It is possible to calculate the horizontal forces and vertical forces into tiebacks. In this way it is possible if the inclination of the resultant's tieback is known it is possible to obtain the arm respect to the point 0, in fact the position of the resultant tieback is calculated.

$$\sum R_x = 10584,8kN \tag{54}$$

$$\sum R_y = 6185,0kN \tag{55}$$

The inclination of the resultant tieback will be:

$$\arctan \frac{\sum R_y}{\sum R_x} = 30,3^o \tag{56}$$

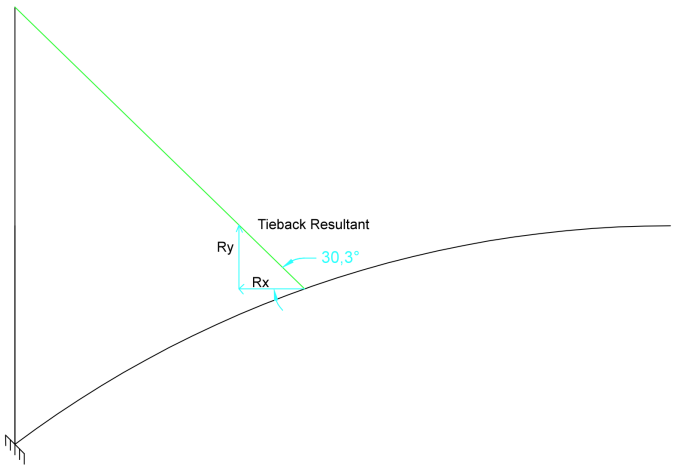

Figure 149: Tieback Resultant

6.4 Anchorage's Volume

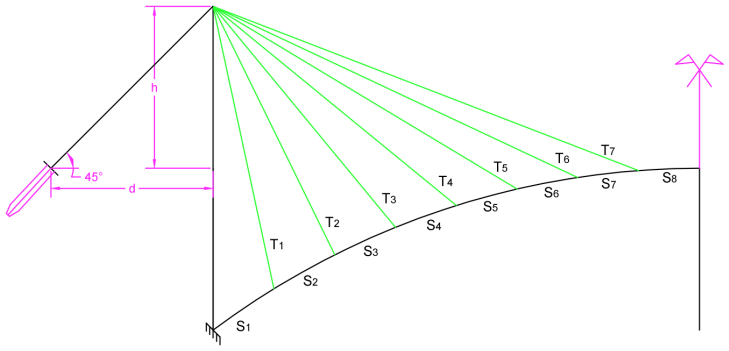

Figure 150: Anchorage System

The volumen of the anchorage is:

$$V = \frac{N}{fy}L \tag{57}$$

These quantities are showed in the picture (151), in details; N is the axial force into the cable, L is the lenght of the cable of anchorage, f_y is the stiffness of the steel.

Having $N = \frac{T_H}{cos\theta}$ e $cos\theta = \frac{d}{\sqrt{h^2+d^2}}$ the equation (57) become:

$$V = \frac{T_H L}{f_y cos\theta} = \frac{T_H\sqrt{h^2+d^2}}{f_y d}\sqrt{h^2+d^2} = \frac{T_H(h^2+d^2)}{d} \tag{58}$$

Deriving the function V

$$minV : \frac{2d * d - (h^2+d^2)1}{d^2} = 0 \tag{59}$$

Finally:

$$2d^2 - h^2 - d^2 = 0 -> h = d \tag{60}$$

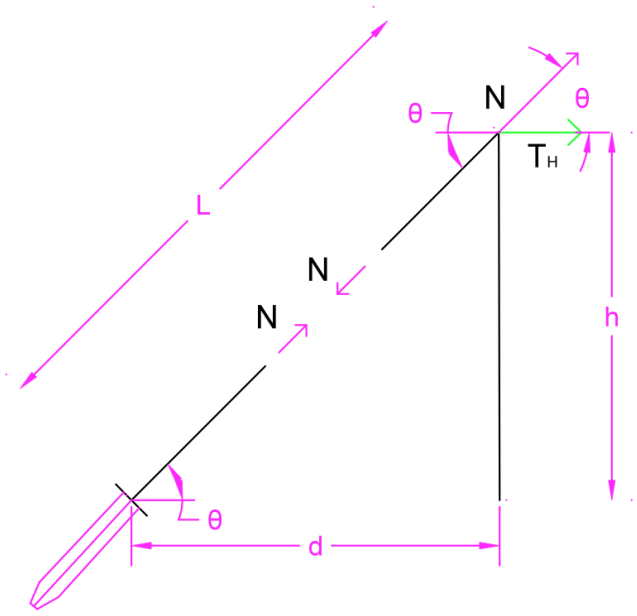

Figure 151: Anchorage's Optimum Slope

7 Conclusions and Future Developments

In this work various strategies of optimization have been adopted to better distribute the Bending Moment along the emiarch.

7.1 Variation Of The Height Of The Tower

It is possible to analyze all the configurations analyzed in this work with a different value of the height H of the provisional tower.

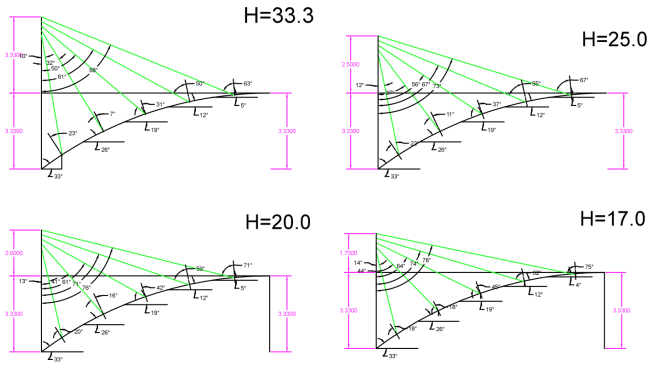

Figure 152: Variation Of The Height Of The Provisional Tower

7.2 Conclusions

Starting from what has been done in the article [10], in which, Au and Wang proposed a method of "two-stage" tensioning like one of the most practical we proposed ourselves the target to find a method of "one-stage" tensioning. The advantage is huge, once a pre-tension have been applied to a tieback there is no need to adapt the pre-tensions of the others tiebacks.

Applying the process analyzed in the section 6.2.1 is possible to evaluated the optimized tensions producing the best Bending Moment diagram per every arch bridge, actually what concerned this thesis is applicable not only to concrete arch bridge having the characteristics of the sample cases take into account in this thesis.

And then, applying the strategy analyzed in the section 6.2.2, especially checking the values of the Bending Moment through the back destruction, it is clear that inserting the tiebacks in appropriate position, depending to the value of α (look back section 6.2.2) it is possible to reduce further the maximum values of the Bending Moment along the entire process of construction.

Other manners to reduce the bending moment along the rib can be the Moment's Redistribution examined in the section 6.2.3, this method propose to deduce the number of tiebacks that can redistribute the Bending Moment defining a coefficient η relationship between M_{Stress} the Stress Bending Moment actually working into the arch and M_{adm} the Admissible Bending Moment from the section, finally getting N' the number of tiebacks we fixed like target.

References

[1] *Eurocode EN 1991-2*.

[2] *Probability, Statistics and Decision for Civil Engineers*. •, 1970, ch. •.

[3] del Valle Perez, J. A. Viaduct over the river ulla. *Hormigon y Acero* (2010).

[4] Kasarnowsky, S. The arches of the traneberg bridge in stockholm. *IABSE* (2013).

[5] Leonhardt, F., and Zellner, W. Comparative investigations between suspension bridges and cable-stayed bridges for spans exceeding 600 m.

[6] Liu, Z. Analytic model of long-span self-shored arch bridge. *JOURNAL OF BRIDGE ENGINEERING* (2002).

[7] Manterola, J. Railway arch bridge over the contreras reservoir in the madrid-levante high-speed railway line. In *Hormigon y Acero*.

[8] Millanes, F. Nuevo puente arco infante d. henrique sobre el rio duero en oporto. In *Hormigon y Acero*.

[9] Radic, J. Innovations in concrete arch bridge design. *ICE* (2006).

[10] Wang;, F. T. K. A. J., and Liu, G. Construction control of reinforced concrete arch bridges, 2003.